Adam Mickiewicz University in Poznań

The Faculty of Chemistry

DOCTORAL THESIS

mgr Jędrzej Mateusz Proch

Hyphenated systems based on detection by optical emission spectrometry in determination of metals and metalloids species

Układy łączone oparte na detekcji przy użyciu spektrometrii emisji optycznej w oznaczaniu form metali i metaloidów

In the form of a collection of published and thematically related scientific articles

Supervisor: prof. dr hab. Przemysław Niedzielski

Poznań 2021

Streszczenie pracy w j. polskim

Głównym celem rozprawy doktorskiej była konstrukcja i zastosowanie układów łączonych do oznaczenia form metali i metaloidów z wykorzystaniem Wielkokanałowego Systemu Wprowadzenia Próbki (MSIS) jako łącznika pomiędzy wysokosprawną chromatografią cieczową (HPLC), a technikami optycznej spektrometrii emisyjnej ze wzbudzeniem w plazmie zarówno indukcyjnie sprzężonej (ICP–OES) jak indukowanej mikrofalowo (MIP–OES). W części eksperymentalnej rozprawy zaprojektowano trzy układy łączone, w oparciu o trzy tryby pracy komory MSIS: (1) generowania wodorków, (2) konwencjonalnej nebulizacji oraz (3) trybu podwójnego (dual-mode). W części aplikacyjnej pracy przedstawiono zastosowanie opracowanych metod do analizy specjacyjnej i pierwiastkowej 58 próbek yerba mate (*Ilex paraguariensis).*

W pierwszej pracy, wchodzącej w skład podstawowych osiągnięć naukowych, zastosowano MSIS w trybie generowania wodorków jako łącznik anionowymiennej HPLC i ICP-OES w oznaczeniu As(III), As(V) i DMA. Zoptymalizowano szczegółowo proces generowania wodorków w komorze MSIS. Aplikacyjność metody zademonstrowano na próbkach środowiskowych (gleby, części roślin) oraz żywności (yerba mate). Uzyskane wyniki zostały wykorzystane w opracowaniu kolejnego osiągniecia podstawowego.

W drugiej pracy, wchodzącej w skład podstawowych osiągnięć naukowych, zastosowano MSIS w trybie nebulizacji (jako konwencjonalna komora mgielna). Równolegle połączono i optymalizowano dwa połączenia kationowymiennej HPLC z różnymi detektorami, MIP-OES oraz ICP-OES. Opracowane metody zastosowano do oznaczenia Fe(II) i Fe(III) w pięciu grupach próbek rzeczywistych (np. ceramika archeologiczna, yerba mate, próbki geologiczne). Uzyskane wyniki posłużyły do porównania właściwości obu detektorów oraz zostały wykorzystane w opracowaniu kolejnego osiągniecia podstawowego.

W trzeciej pracy, wchodzącej w skład podstawowych osiągnięć naukowych, zastosowano MSIS w połączeniu opisanych wyżej trybów (tryb dual) i obu systemów chromatograficznych w pojedynczym układzie łączonym, 2 HPLC-MSIS-ICP-OES, służącym równoczesnemu oznaczeniu 18 form 15 pierwiastków, występujących zarówno jako kationy i aniony. Aplikacyjność metody została również przedstawiona na pięciu grupach próbek. O potencjale techniki świadczyło wykrycie wielu niezidentyfikowanych form Cu, Fe, Mn i Zn, których identyfikacja jakościowa i ilościowa stanowić będzie przedmiot kolejnych badań naukowych.

W czwartej pracy wchodzącej w skład podstawowych osiągnięć naukowych, zaprezentowano oznaczanie form arsenu i żelaza w 58 próbkach yerba mate (*Ilex paraguariensis)* przy użyciu opracowanych wcześniej technik łączonych. Uzyskane wyniki oceniono również w kontekście całkowitej zawartości pierwiastków.

Podsumowując, zbiór czterech artykułów naukowych, stanowiących osiągniecia podstawowe, bazuje na nowatorskich układach łączonych do oznaczania form metali i niemetali.

Table of Contents:

1. General goals of the thesis

The main goal of the doctoral thesis was the construction and application of hyphenated systems to determine speciation forms of metals and metalloids using the Multi-mode Sample Introduction System (MSIS) as an interface between high performance liquid chromatography (HPLC) and optical emission spectrometry techniques, both inductively coupled plasma (ICP-OES) as well as microwave-induced (MIP-OES). In the experimental part of the thesis, three hyphenated techniques were designed, based on three work modes of the MSIS chamber: (1) hydride generation, (2) conventional nebulization and (3) dual-mode. The application of the developed methods were presented for speciation and elemental analysis of 58 yerba mate *(Ilex paraguariensis)* samples.

2. Specific goals of particular core of achievements

In the first work, which is part of the core scientific achievements, MSIS was used in the hydride generation mode as an interface of anion-exchange HPLC and ICP-OES in the determination of As (III), As (V) and DMA. The hydride generation process in the MSIS chamber has been optimized in detail. The applicability of the method was demonstrated on environmental (soils, parts of plants) and food samples (yerba mate). The obtained results were used in the development of the next core achievement.

In the second work, which is part of the core scientific achievements, MSIS was used in the nebulization mode (as a conventional spray chamber). Two combinations of cation-exchange HPLC with different detectors were combined and optimized in parallel, MIP-OES and ICP-OES. The developed methods was used to determine Fe(II) and Fe(III) in five groups of real samples (e.g. archaeological pottery, yerba mate, geological samples). The obtained results were used to compare the properties of both detectors and were used in the development of the next core achievement.

In the third work, which is part of the core scientific achievements, MSIS was used in the combination of the above-described modes (dual-mode) and both chromatographic systems in single hyphenated technique, 2 HPLC-MSIS-ICP-OES, used for the simultaneous determination of 18 speciation forms of 15 elements occurring both as cations and anions. The applicability of the method was also demonstrated on five groups of samples. The potential of the technique was evidenced by the detection of many unidentified speciation forms of Cu, Fe, Mn and Zn, the qualitative and quantitative identification of which will be the subject of further scientific research.

In the fourth paper, which is part of the core scientific achievements, the determination of the speciation forms of arsenic and iron in 58 samples of yerba mate *(Ilex paraguariensis)*, using previously developed hyphenated techniques, was presented. The obtained results were also assessed in the context of the total content of elements.

Summarizing the above, the collection of four scientific articles, which are the core scientific achievements, is based on novel hyphenated systems for the determination of metals and metalloids species.

3. Scientific achievements

CORE SCIENTIFIC ACHIEVEMENTS:

[D1] **J. Proch**, P. Niedzielski (2020). In–spray chamber hydride generation by multi–mode sample introduction system (MSIS) as an interface in the hyphenated system of high performance liquid chromatography and inductivity coupled plasma optical emission spectrometry (HPLC/HG–ICP–OES) in arsenic species determination. *Talanta*, *208*, 120395. doi: 10.1016/j.talanta.2019.120395
IF (2020) = 6.057 **CiteScore (Scopus) = 9.4** **Centyl (Scopus) = 91** **MEiN = 100 pkt.**

[D2] **J. Proch**, P. Niedzielski (2021). Multi–mode Sample Introduction System (MSIS) as an interface in the hyphenated system 2 HPLC–MSIS–ICP–OES in simultaneous determination of metals and metalloids species. *Analytica Chimica Acta*, *1147*, 1–14. doi: 10.1016/j.aca.2020.12.047
IF (2020) = 6.558 **CiteScore (Scopus) = 9.3** **Centyl (Scopus) = 95** **MEiN = 100 pkt.**

[D3] **J. Proch**, P. Niedzielski (2021). Iron species determination by high performance liquid chromatography with plasma based optical emission detectors: HPLC–MIP OES and HPLC–ICP OES. *Talanta, 231*, 122403. doi: 10.1016/j.talanta.2021.122403
IF (2020) = 6.057 **CiteScore (Scopus) = 9.4** **Centyl (Scopus) = 91** **MEiN = 100 pkt.**

[D4] **J. Proch**, A. Orłowska, P. Niedzielski (2021). Elemental and Speciation Analyses of Different Brands of Yerba Mate (*Ilex paraguariensis*). *Foods*, *10*(12), 2925. doi: 10.3390/foods10122925
IF (2020) = 4.350 **CiteScore (Scopus) = 3.0** **Centyl (Scopus) = 93** **MEiN = 100 pkt.**

NON–CORE SCIENTIFIC ACHIEVEMENTS:

[5] M. Krueger, U. Wicenciak, Z. Kowarska, P. Niedzielski, L. Kozak, M. Krueger, K. Jakubowski, **J. Proch**, M. Mleczek, A. Waśkiewicz (2018). First results of organic residue analysis on ceramic vessels (Jiyeh and ChhÎm, Lebanon) by high perfomance liquid chromatography with tandem mass spectrometry. *Mediterranean Archaeology and Archaeometry, 18*(1), 209–220. doi: 10.5281/zenodo.1165358
IF (2020) = 0.591 **CiteScore (Scopus) = 1.2** **Centyl (Scopus) = 91** **MEiN = 70 pkt.**

[6] P. Rzymski, J. Budzulak, P. Niedzielski, P. Klimaszyk, **J. Proch**, L. Kozak, B. Poniedziałek (2018). Essential and toxic elements in commercial microalgal food supplements. *Journal of Applied Phycology*, *31*(6), 3567–3579. doi: 10.1007/s10811–018–1681–1
IF (2020)= 3.215 **CiteScore (Scopus) = 5.0** **Centyl (Scopus) = 91** **MEiN = 70 pkt.**

[7] C. Grochowski, E. Blicharska, J. Bogucki, **J. Proch**, A. Mierzwińska, J. Baj, J. Litak, A. Podkowiński, J. Flieger, G. Teresiński, R. Maciejewski, P. Niedzielski, P. Rzymski (2019). Increased Aluminum Content in Certain Brain Structures is Correlated with Higher Silicon Concentration in Alcoholic Use Disorder. *Molecules*, *24*(9), 1721. doi: 10.3390/molecules24091721
IF (2020) = 4.411 **CiteScore (Scopus) = 4.7** **Centyl (Scopus) = 74** **MEiN = 140 pkt.**

[8] J. Dolar–Szczasny, J. Święch, J. Flieger, M. Tatarczak–Michalewska, P. Niedzielski, **J. Proch**, D. Majerek, J. Kawka, J. Mackiewicz (2019). Levels of Trace Elements in the Aqueous Humor of Cataract Patients Measured by the Inductively Coupled Plasma Optical Emission Spectrometry. *Molecules*, *24*(22), 4127. doi: 10.3390/molecules24224127
IF (2020) = 4.411 **CiteScore (Scopus) = 4.7** **Centyl (Scopus) = 74** **MEiN = 140 pkt.**

[9] B. Poniedziałek, M. Siwulski, A. Wiater, I. Komaniecka, A. Komosa, M. Gąsecka, Z. Magdziak, M. Mleczek, P. Niedzielski, **J. Proch**, M. Ropacka–Lesiak, M. Lesiak, E. Henao, P. Rzymski (2019). The Effect of Mushroom Extracts on Human Platelet and Blood Coagulation: In vitro Screening of Eight Edible Species. *Nutrients, 11*(12), 3040. doi: 10.3390/nu11123040
IF (2020) = 5.717 CiteScore (Scopus) = 6.4 Centyl (Scopus) = 87 MEiN = 140 pkt.

[10] C. Grochowski, M. Szukała, J. Litak, A. Budny, **J. Proch**, D. Majerek, E. Blicharska, P. Niedzielski (2020). Correlations Between Trace Elements in Selected Locations of the Human Brain in Individuals with Alcohol Use Disorder. *Molecules, 25*(2), 359. doi: 10.3390/molecules25020359
IF (2020) = 4.411 CiteScore (Scopus) = 4.7 Centyl (Scopus) = 74 MEiN = 140 pkt.

[11] M. Mleczek, A. Budka, M. Siwulski, P. Mleczek, M. Gąsecka, A. Jasińska, P. Kalač, K. Sobieralski, P. Niedzielski, **J. Proch**, P. Rzymski (2020). Investigation of differentiation of metal contents of Agaricus bisporus, Lentinula edodes and Pleurotus ostreatus sold commercially in Poland between 2009 and 2017. *Journal of Food Composition and Analysis, 90*, 103488. doi: 10.1016/j.jfca.2020.103488
IF (2020) = 4.556 CiteScore (Scopus) = 6.4 Centyl (Scopus) = 87 MEiN = 100 pkt.

[12] G. Orłowski, P. Niedzielski, J. Karg, **J. Proch** (2020). Colour–assisted variation in elytral ICP–OES–based ionomics in an aposematic beetle. *Scientific Reports, 10*(1). doi: 10.1038/s41598–020–79329–4
IF (2020) = 4.379 CiteScore (Scopus) = 7.1 Centyl (Scopus) = 93 MEiN = 140 pkt.

[13] G. Orłowski, P. Niedzielski, D. Merta, P. Pokorny, **J. Proch** (2020). Quantifying the functional disparity in pigment spot–background egg colour ICP–OES–based eggshell ionome at two extremes of avian embryonic development. *Scientific Reports, 10*(1). doi: 10.1038/s41598–020–79040–4
IF (2020) = 4.379 CiteScore (Scopus) = 7.1 Centyl (Scopus) = 93 MEiN = 140 pkt.

[14] M. Mleczek, A. Budka, M. Siwulski, P. Mleczek, S. Budzyńska, **J. Proch**, M. Gąsecka, P. Niedzielski, P. Rzymski (2021). A comparison of toxic and essential elements in edible wild and cultivated mushroom species. *European Food Research and Technology, 247*(5), 1249–1262. doi: 10.1007/s00217–021–03706–0
IF (2020) = 2.998 CiteScore (Scopus) = 4.4 Centyl (Scopus) = 77 MEiN = 70 pkt.

[15] L. Kozak, J. Souza, A. Nawrot, **J. Proch**, M. Kaźmierski, A. Zawieja, P. Niedzielski (2021). Handheld ED–XRF spectrometers in geochemical investigation:Comparative studies for glacial deposits from Spitsbergen, *Polish Polar Research, 42*(3), 163–172. doi: 10.24425/ppr.2021.137141
IF (2020) = 1.308 CiteScore (Scopus) = 2.7 Centyl (Scopus) = 60 MEiN = 70 pkt.

[16] M. Zubaidi, **J. Proch,** P. Konieczny, Ł. Tomczyk (2021). Toxicity Testing by the Microbial Assay for Risk Assessment (MARA) in Relation to Trace Elements Content in King Bolete (Boletus edulis) Collected in Several Sites of Poland. *Applied Sciences (Switzerland), 11*(9), 4166. doi: 10.3390/app11094166
IF (2020) = 2.679 CiteScore (Scopus) = 3.0 Centyl (Scopus) = 71 MEiN = 100 pkt.

[17] J. Flieger, J. Dolar–Szczasny, R. Rejdak, D. Majerek, M. Tatarczak–Michalewska, **J. Proch**, E. Blicharska, W. Flieger, J. Baj, P. Niedzielski (2021). The Multi–Elemental Composition of the Aqueous Humor of Patients Undergoing Cataract Surgery, Suffering from Coexisting Diabetes, Hypertension, or Diabetic Retinopathy. *International Journal of Molecular Sciences, 22*(17), 9413. doi: 10.3390/ijms22179413
IF (2020) = 5.923 CiteScore (Scopus) = 6.0 Centyl (Scopus) = 83 MEiN = 140 pkt.

[18] L. Kozak, A. Michałowski, **J. Proch**, M. Krueger, O. Munteanu, P. Niedzielski (2021). Iron Forms Fe(II) and Fe(III) Determination in Pre–Roman Iron Age Archaeological Pottery as a New Tool in Archaeometry. *Molecules*, *26*(18), 5617. doi: 10.3390/molecules26185617
IF (2020) = 4.411 CiteScore (Scopus) = 4.7 Centyl (Scopus) = 74 MEiN = 140 pkt.

BIBLIOMETRIC DATA:

Total IF = 76.41 (2020), Citations: 78 (Scopus) H–index = 6 Total MEiN = 2000 pkt.

Other scientific achievements:

EMPLOYMENT:

1.11.2021 – now	**Lecturer** (for a replacement, 1/2 time job) in General and Analytical Chemistry Teaching Laboratory, Faculty of Chemistry, Adam Mickiewicz University in Poznań.

INTERNSHIP:

5.10.2020 – 28.10.2020 (shortened due to the COVID–19 pandemic)	**Laboratory of Atomic Spectrochemistry, Faculty of Science, Masaryk University, Brno, Czech Republic** Learning to work and conducting research using laser–induced breakdown spectroscopy (LIBS) and comparative research using previously known instrumental techniques, under the supervision of doc. Karel Novotný, Ph.D

PARTICIPATION IN CONFERENCES:

Ecology & Safety, 30th International Conference, 2021, Burgas, Bulgaria	**J. Proch,** P. Niedzielski, "Hyphenated techniques as tools to finding markers of processes occurring in the environment" **– poster presentation**
9th International Conference on Radiation in Various Fields of Research, 2021, Herceg Novi, Montenegro	**J. Proch,** P. Niedzielski, "Multi–mode Sample Introduction System (MSIS) as an interface between high performance liquid chromatography (HPLC) and inductively coupled plasma optical emission spectrometry (ICP OES) in arsenic speciation analysis" **– poster presentation**
47th International Conference of the Slovak Society of Chemical Engineering, 2021, Bratislava, Slovakia	**J. Proch**, P. Niedzielski, "High performance liquid chromatography with plasma based optical emission detectors: HPLC–MIP OES and HPLC–ICP OES in iron speciation analysis" **– poster presentation**
3rd International Conference on Virtual Archaeology, 2018, Sankt Petersburg, Russia	A. Michałowski, P. Niedzielski, K. Jakubowski, **J. Proch**, M. Teska, M. Krueger, "The archaeological pottery XRF mapping and visualisation of the concentrations of selected elements" **– oral presentation**
Pottery – the main source of knowledge for cultural change in the Central European, 2017, Poznań, Poland	M. Krueger, **J. Proch,** "Non–destructive analyses – in search of similarities and differences of archaeological finds" **– oral presentation**
XXV Poznań Analytical Conversatory, Poznań University of Technology, 2016, Poznań, Poland	**J. Proch,** P. Niedzielski, K. Jakubowski, M. Bartkowiak, M. Krueger, "Research remains of organic matter (food, cosmetics) in archaeological ceramics – sample preparation" **– poster presentation**

PARTICIPATION IN ORGANIZING THE CONFERENCES:

Pottery – the main source of knowledge for cultural change in the Central European, 2017, Poznań, Poland	International archaeology workshops
Settlements Pottery of the pre–Roman Iron Age in Central European Barbaricum – new research perspectives, 2015, Poznań, Poland	International archaeology workshops

4. Scientific resume

After finishing education at the 5th High School in Poznań, (06.2012), I started the first degree studies at Faculty of Chemistry, Adam Mickiewicz University in Poznań on the cosmetics chemistry (10.2012). At the beginning of summer term of the second years, I met Prof. Przemysław Niedzielski as the lecturer of the subject entitled: "Biologically active materials and its analysis". After a few lectures, I was sure that I would like to carry out my undergraduate research under his supervision. I started the actual work in the Research Group of Speciation Analytics and Hyphenated Techniques in the Department of Analytical Chemistry in 10.2014.

I was very impressed with the multitude of samples that passed through the laboratory and I took advantage of the opportunities offered by voluntary work. Since then, I started my research together with the Faculty of Archeology, firstly in sample preparation. I completed my bachelor thesis entitled "Research remains of organic matter (food, cosmetics) in archaeological ceramics - sample preparation" at the Department of Analytical Chemistry under the supervision of Prof. Przemysław Niedzielski on 29.06.2015. Then, I started my II degree studies of Cosmetics Chemistry at Faculty of Chemistry, Adam Mickiewicz University in Poznań in 10.2015. I also continued my research and the voluntary work, gaining new experience, also in caring for younger students. In the meantime, I was an instructor at an international archaeological workshop (in 2015 and 2017) on the preparation of ceramics samples for destructive and non-destructive analyzes. I completed later my master's thesis entitled "Archaeometric studies of archaeological pottery with X-ray fluorescence (XRF)" and I became Master of Science on 22.06.2017. Meanwhile, I was chosen by my supervisor to be a new PhD student in his research group.

After the PhD interview in 07.2021, I officially started my PhD studies in 10.2021 in the international and interdisciplinary program of PhD studies "ChemInter", implemented under the project POWR.03.02.00-00-I026/1610.2021, at the Faculty of Chemistry at the University of Adam Mickiewicz in Poznań. From the beginning of my work as a PhD candidate, I undertook the organization of our laboratory work, becoming an effective intermediary between students and Prof. Niedzielski. At the same time, I was acquiring knowledge about new types of analytical techniques, independently performing about 5000-6000 analyzes per year (excluding the COVID-19 pandemic). I also co-supervised and performed analyzes for every master and bachelor students from our research group (8-10 students per year) and every students supervised by Prof. Tadeusz Sobczyński (from 2017 until now).

In the period from 5.10.2020 to 4.01.2021, I planned to be an intern at Faculty of Science, Masaryk University, Brno, the Czech Republic to learn how to work and conduct a research using laser–induced breakdown spectroscopy (LIBS) and to carry out comparative research using previously known instrumental techniques under the supervision of doc. Karel Novotný, Ph.D in the Laboratory of Atomic Spectrochemistry. Unfortunately, I was forced to shorten the internship due to the COVID-19 pandemic

and I came back to Poland on 28.10.2020. Nevertheless, my work was highly evaluated by my internship mentor.

During my short scientific carrier, I have often been involved in many research topics, which broaden my scientific horizons. The visible part of many co-operations are publications from non-core scientific achievements (15 articles). Virtually every experiment I have participated in, has been interdisciplinary. The full list of research groups and scientists with whom I have worked, is very long. As permanent collaborators, I could list Life Science University in Poznań (especially Faculty of Forestry and Wood Technology), Medical Universiity of Lublin, Medical University of Karol Marcinkowski in Poznań, and several faculties of Adam Mickiewicz University, e.g. Archaeology, Geology, Geography and Biology.

Since 02.2021, I am a member of the Interdisciplinary Research Group Archaeometry, which was established in cooperation with two faculties of the University of Adam Mickiewicz in Poznań: Faculty of Archaeology and Faculty of Chemistry. In 2021, I conducted my first experiments without active participation of my supervisor in cooperation with scientists from Life Science University of Poznań.

During my doctoral studies (10.2017 – 10.2021), I taught on the laboratory classes in 3 subjects (300h): Biologically active materials and its analysis (150h), Speciation analysis in environmental studies (120h), Analysis of water and soil pollutions (30h). My work was always rated very highly by the students (average mark from the questionnaires = 4.94). Partly because of this, I have started working as a lecturer (for a replacement, 1/2 time job) in General and Analytical Chemistry Teaching Laboratory, Faculty of Chemistry, Adam Mickiewicz University in Poznań since 1.11.2021. Now I am conducting the laboratory classes entitled “Physico-chemical basis of life” (100h) and I will also conduct “The base of instrumental analysis” (45h) in the next term.

I am systematic in my activities and consequently pursues the set goal. I am also a hardworking and ambitious person, willing to expand and share his knowledge. My sentence is “nothing stands in the way”, which help me to fight against any adversity. Every day I am able to overcome new limits, just like following the science path I have chosen in my career.

5. Introduction

Although more than fifty years have passed since the first usage [1], chemical vapor generation (CVG) is being developed as an efficient way of sample introduction. Originally, hydride generation (HG) was combined with atomic absorption spectrometry (AAS) to avoid atomization difficulties of arsenic in a flame burner. The idea was to use a reducing agent with an acidic medium directly prior to measurements. Arsine (AsH_3) was generated by the reaction of zinc (Zn) with hydrochloric acid (HCl), in a liquid nitrogen trap. The trap was heated, then collected AsH_3 was carried by a nitrogen steam into air–acetylene flame of AAS. This method was named "gas–sampling technique" [2].

Other procedures generating volatile hydrides were also carried out and sodium borohydride ($NaBH_4$) was applied for the first time as a reductant solution by Braman et al. in 1972 [3]. The main advantage of using $NaBH_4$ was the possibility of simple dosing and automating the entire process. In comparison to the metal–acid medium, the reduction of an element using $NaBH_4$–acid (usually HCl) was much faster and more efficient as well as reduced the blank [4]. The general model of CVG/HG reaction was recently reviewed by D'Ulivo (2019) and the formation of the volatile hydrides in the $NaBH_4$–acid mixture is the result of two competitive reactions. (**Figure 1**) [5].

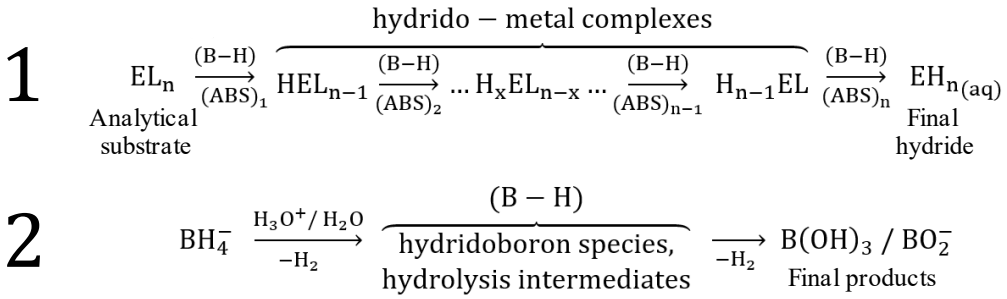

Fig. 1. Competitive reaction pathways during CVG/HG: (1) analytical derivatization pathway and (2) hydrolysis pathway of BH_4^-. Captions: (E) volatile species forming element; (L) ligand; (ABS) analyte–borane complex intermediates; (B–H) borane species with at least one B–H bond and hydridoboron species, $[L_{3-n}BH_n]^z$ (n = 1, 2, 3, and z = 0, ±1), which are the hydrolysis products of BH_4^-The figure based on ref. [5].

The first pathway (1) involves reactions of the analytical substrate (EL_n) with borane species containing at least one B–H bond (e.g. borohydride anions and/or the hydridoboron intermediates), which are formed during the hydrolysis of BH_4^- (Pathway 2). Analyte–boron complexes (ABC) are then formed as intermediates. Subsequently, H atoms are transferred stepwise from boranes to EL_n with the formation of series of hydrido–metal complexes. As the result of the derivatization reaction (Pathway 1), the final hydride is formed in the liquid phase ($EH_{n(aq)}$). If EH_n has a sufficient thermal stability (as in the case of e.g. AsH_3, SeH_3, SbH_3), it is transferred to the gas phase [5]. The above mentioned mechanism is the theoretical basis of the HG reaction. In the case of some metal, e.g. Hg(II) and Cd(II),

EH_n can be also partially or completely decomposed to free atoms (E^0). This mechanism is the basis of the CVG reaction.

The efficiency of the CVG/HG reaction in the liquid phase (Figure 1) is related to the following factors: (1) oxidation state of the element, (2) type and concentration of reductant solution, (3) type and concentration of acidic medium, (4) pH of the solution, (5) sample matrix type, (6) presence and concentration of interfering elements, (7) reactivity of hydride–forming elements, and (8) CVG/HG technique [4]. In addition, the optimal CVG/HG technique should ensure the efficient transport of volatile compounds to enable the stable and volatile hydrides undergo the thermal decomposition upon reaching the atomization/excitation source. Therefore, different modes in CVG/HG process have been explored e.g. continuous flow (CF) and flow injection (FI). In the CF modes, all reagents (sample, acid and reducing agent) are provided separately by a peristaltic pump to a reaction cell where they are mixed and formed to volatile hydrides [6, 7]. In the FI modes, the sample is injected by a valve with a loop into a carrier solution, which is continuously pumped [8]. Recently, the coupling of CVG/HG techniques with solid phase extraction (SPE) has also been gaining popularity [9, 10].

Regardless of the CVG/HG technique, there is a need for the continuous development of modern and more efficient generators that are able to meet the key challenges of analytical chemistry and environmental monitoring. Nevertheless, the most reasonable choice are the CF modes when designing the CVG/HG method as simple and repeatable, ensuring the shortest possible time of a single analysis simultaneously. Nowadays (2021), the most of CF-CVG/HG systems are based on modified spray chambers [11-12], pneumatic [13] or modified nebulizers (e.g. direct hydride generation nebulizer, DHGN [14], *Flow Blurring*® Multi Nebulizer, FBMN [15] and micro–flow ultrasonic nebulizer with quadruple–mode micro capillary system, μ–USN/QSC [16]) and external accessories (which are both laboratory-made [17] and commercially available [18]).

Due to its simple design and commercialization, Multi–mode Introduction System (MSIS, formerly Marathon Scientific, Canada, now Agilent, USA) has attracted special attention in recent years. MSIS is a modified spray chamber and its advantage, over other types of generators, is the ability to work in three work modes (Figure 2): hydride generation (HG), nebulization (Neb) and the combination of the above two modes (Dual).

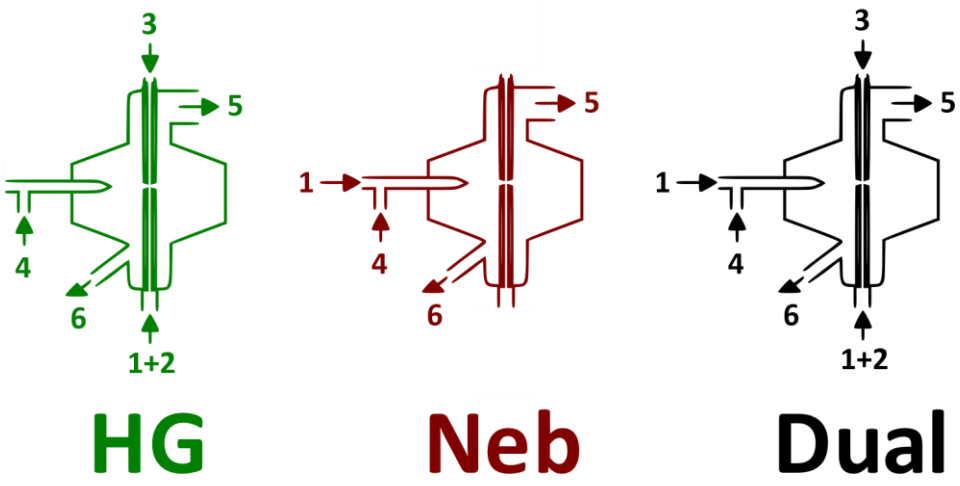

Fig. 2. Three work modes of Multi–mode Sample Introduction System: (HG) hydride generation, (Neb) nebulization, and (Dual) the combination of HG and Neb (dual–mode). Captions: (1) sample, (2) acidic medium, (3) reductant solution, (4) carrier gas, (5) plasma, (6) drain.

The first evaluation of MSIS and its modes was performed in 2002 [19]. Since this time, MSIS has been coupled with various types of spectrometers, e.g. inductively coupled plasma mass spectrometry (ICP-MS)[20], inductively coupled plasma optical emission spectrometry (ICP-OES)[21], microwave induced plasma optical emission spectrometry (MIP-OES)[22] and AAS [23]. At the same time, three modes of operation were also investigated to obtain optimal conditions for the simultaneous determination of non-hydride forming and volatile hydride forming elements. Cross-comparing of three modes of MSIS, it was reported that some elements (e.g. Be, Co, Cr, Mn), which previously could be determined in the Neb mode only, were also detected using HG mode [24].

The desire to develop methods based on more economical detectors than ICP-MS, has made that MSIS and other CVG/HG techniques are frequently coupled with MIP-OES and ICP-OES. The first application of continuous flow HG–ICP-OES was presented in late 1970s when HG was used to efficiently introduce some elements, e.g. As, Bi, Sb, Se and Te [25] into the plasma torch using $NaBH_4$ as a reductant solution. In the following years, more successful CVG/HG applications with plasma based OES were presented, including those with MSIS as a hydride generator. The main advantage of this combination is that optical emission spectrometry is more resistant to extremely low pH and high concentrations than ICP-MS. Ensuring the efficient analyte transport combined with reduced plasma solvent load using MSIS (as a hydride generator), a competitive method could be obtain with ICP-OES.

Although new MSIS-based methods allowed to determine more and more elements (including noble metals [26]), most of them were focused on the determination of total element contents. The methods, determining any element species by CVG/HG with plasma-based OES, were undertaken rarely and they were usually non-chromatographic, based on additional sample pretreatment (e.g. prereduction) [27, 28]. These systems, which are able to separate species of elements (on-line, using

liquid chromatography) prior to their detection in spectrometer, are called hyphenated techniques. Only two MSIS-based hyphenated techniques with detection by OES were presented previously. Al–Assaf et al. reported the first usage of MSIS in its HG mode as an interface between high performance liquid chromatography and ICP-OES to determine four arsenic species in soils [29]. In turn, Barrientos et al. introduced HPLC–MSIS–MIP OES (with N_2 as working gas) to determine Se(IV) and selenomethionine (SeMet) in biofortified yeasts [30]. The following shortcomings or compilations of above mentioned systems were noticed: (1) long-time procedure of sample preparation (24h), (2) gradient flow of HPLC, (3) the applicability was only performed on spiked samples, (4) specified to contaminated soils [29], (4) additional reaction coil between HPLC and MSIS, (5) post-column reagents for pre-oxidation step, and (6) the method was specified to selenium-enriched yeast [30].

Summarizing the above, there was a lack of new hyphenated technique using MSIS (in HG mode) as an interface between HPLC and ICP-OES to determine some element species, without any post-column reagents and additional reaction coils. Moreover, the applicability had to be wide (performed on several groups of real samples), preceded by a simple and short-time procedure of sample preparation. Therefore, the successful application of HPLC-HG-ICP-OES to determine of arsenic species in environmental and food samples led to the publication listed as the first core scientific achievement **[D1].**

On one hand, dual-mode and HG mode of MSIS give some advantages over conventional nebulization, therefore they are more frequently applied than Neb mode. On the other hand, dual-mode cannot be successfully applied without the optimization of its operating conditions in Neb mode. In addition, the successful combination of HPLC and ICP-OES through MSIS, prompted an attempt to directly connect the output of the column to the nebulizer sample channel. In this way, another new hyphenated technique could be designed. Due to that most of elements occur in the solution as cations (e.g. iron), the column type was changed to cation-exchange.

The most interesting element that occurs in several speciation forms as a cation, was iron (Fe), which is kinetically reactive and thermodynamically stable in two main species, Fe(II) and Fe(III). Moreover, iron is the fourth most abundant element in the Earth's crust and iron cycling was observed in living organisms as well as the environment [31]. According to this, iron speciation analysis seemed to be one of the major challenges in analytical or environmental chemistry. However, a lack of new methods (especially based on HPLC–ICP MS) for fast simultaneous determination of Fe species is surprising in comparison to metalloids (e.g. As, Sb, Se) and other metals (e.g. Al, Cr, Hg) [32].

Obtaining the optimal conditions to separate iron species, the composition of mobile phase is crucial. In 1995, pyridine–2,6–dicarboxylic acid (PDCA) was described as a component of mobile phase for a separation of transition metals, including Fe(II) and Fe(III) [33]. In the following years, the most popular composition of PDCA-based eluent was a mixture of PDCA, potassium sulfate (K_2SO_4), potassium hydroxide (KOH) and formic acid (HCOOH), which was applied for the first time by Cardellicchio et al. [34] and commercialized later. Surprisingly, this eluent has only been used with

HPLC-UV [35-36]. On one hand, the most desirable way is to transfer the advantages of commercialized PDCA eluent from HPLC-UV to HPLC-ICP-OES, whose limits of detection (LODs) are significantly better. On the other hand, several problems as excitation interferences, plasma instability, plasma extinction, nebulizer clogging and torch damage, may be caused by the higher salt load on ICP. The solution was substitution of ICP-OES with MIP-OES as a detector in the hyphenated methods.

For first time, MIPs with emission spectrometry were applied in 1965 [37], however there has been no commercial available MIP-OES until 2011. Its main advantage over ICP-OES is that it enable to generate nitrogen (N_2) directly from atmospheric air by an external generator (lower cost of a single analysis). The shortcomings are monochromator–based system, which detects analytical signal sequentially and lower temperature of plasma (ca. 5000 K), which generates more signal interferences in comparison to ICP-OES. Nevertheless, the instrument became competitive and attractive. In the last years, MSIS was frequently coupled with MIP-OES to enhance its LODs in determination of volatile hydride forming elements (rarely non-hydride forming elements). However, no iron speciation studies have been reported using MIP-OES while presenting satisfactory results to determine its total content.

In the literature, only two hyphenated systems were used to simultaneously determine of Fe(II) and Fe(III) on real samples [38, 39]. However, the applicability of both methods, HPLC-ICP-OES [38] and HPLC-ICP-MS [39], was performed on specified materials only, rat brain tissues and cerebrospinal fluid respectively, which contain much less iron than soils, sediments etc. In this case, ICP-MS is an overly demanding detector (requiring thousand-fold dilution). According to this, HPLC-MIP-OES became the method which was optimized and applied parallel with HPLC-ICP-OES. Comparing their features, the evaluation of the MSIS working in Neb mode was performed and presented in the second core scientific achievement [**D2**].

In the literature, there were also significant application of MSIS in dual-mode for simultaneous determination of non-hydride forming and volatile hydride forming elements [20-22, 24]. However, this mode has never been used in the determination of element species. Although multi-elemental speciation analysis was performed for 9 oxyanion species of 6 elements [40], it has never been performed for elements occurring as cation and anions. The combination of modes (Neb and HG in dual-mode) in speciation analysis should not be significantly different from the total analysis. After the first and second achievement [**D1**-**D2**], it was possible to adopt easily the conditions designing a new hyphenated system. The main advantage is the simultaneous separation by two different HPLC columns of anions (e.g. three arsenic species) and cations (e.g. two iron species) in one run. Introducing the analytes in two different modes of MSIS, i.e. Neb mode for non-hydride forming elements and HG mode for volatile hydride forming elements, minimalized the inferences. Moreover, it was assumed that detection of any unknown species is possible by performing the method applicability on real samples. Noticing the huge potential in the described system, MSIS working in dual mode was performed as interface between two HPLC and ICP-OES and presented in the third core scientific achievement [**D3**].

The implementation of the method into regular laboratory work should be the next stage in the development of any system, including hyphenated technique. By developing three systems as part of core scientific achievements [**D1-D3**], yerba mate (*Ilex paraguariensis)* was chosen as the suitable material to perform the applicability of the methods from the following factors: (1) its consumption has extended [41], (2) it was successfully applied in the method development [41], and (3) no speciation analysis has been reported yet. It is more practical to demonstrate two fair methods than the excellent one. Therefore the speciation analysis was performed with two single-elemental methods [**D1-D2**] instead of the multi-elemental [**D3**]. The methodology was the first elemental and speciation analysis of yerba mate *(Ilex paraguariensis)* and the first application on large sample series using both HPLC-HG-ICP-OES and HPLC-ICP-OES. Noticing this potential, the work is presented in the fourth core scientific achievement as the application part of the doctoral thesis [**D4**].

6. Materials and methods

The materials and methods can be divided into two groups: fixed and variable parameters during the studies. Firstly, those fixed to all hyphenated techniques are listed. High–pure deionized water (≥18 MΩ cm resistivity), obtained from Milli–Q Direct 3 Water Purification System (Merck–Millipore, Germany) was used in all experiments. High–pure argon (Ar, N–5.0, 99.999% purity), obtained from Linde Gas (Poland) was applied as a working gas in each hyphenated technique, based on the ICP–OES detection. In turn, on–line nitrogen generator ZEFIRO MP (CINEL S.r.l. Gas Generators Technology) produced pure nitrogen (N_2, purity >99.5%), applied as a working gas in HPLC–MIP OES **[D2]**. A reductant solution was prepared daily by dissolving powdered sodium tetrahydroborate ($NaBH_4$, obtained from Sigma–Aldrich) in 0.1% (w/v) NaOH (Merck). An acidic medium was prepared by dilution of 30% HCl (Suprapur®, Merck). HG reagents had identical flow rate in every system, 1.0 ml min^{-1}.

All described HPLC systems were built from the same pump, Shimadzu LC–10AT (Shimadzu, Japan) and sample loop (injection volume 200 μL). Regardless of the applied mobile phase, the flow was isocratic. The Agilent 5110 ICP–OES (Agilent, USA) was used as a detector. Main features of the spectrometer are dichroic spectral combiner (DSC), which enables simultaneous measurements in radial and axial view (synchronous vertical dual view, SVDV), Echelle grading fixed optics (thermostated at 35°C) and VistaChip II with CCD detector, which is cooled to –40°C using triple Peltier system. Nebulizer gas and auxiliary gas flow rates were fixed, 0.7 and 1.0 L min^{-1}. Five–channel peristaltic pump was used to supply reagents and drain the waste. The Agilent MP–AES 4200 (Agilent, USA), applying N_2 as a working gas, was additionally used [**D2**]. Main features of the spectrometer are air-cooled magnetron operating at 2450 MHz, Czerny–Turner monochromator with 600 mm focal length, holographic diffraction grating, and CCD detector (directly cooled to 0°C using a thermoelectric Peltier

system). Auxiliary and plasma gas flows were fixed at 1.5 and 20 L min^{-1} respectively. Other investigated parameters were listed according to the core achievements and summarized in Table 1.

As a main procedure of sample preparation, ultrasound–assisted extraction in diluted phosphoric acid (H_3PO_4) was used. The following procedure was applied in every work **[D1–D4]**. 0.50–1.00 (±0.01) g of a dry sample was accurately weighted and placed in polyethylene test tube. Then 8.0 ml of 1 mol L^{-1} phosphoric acid, prepared from 85% H_3PO_4 (POCh, Poland), was added. The ultrasound–assisted extraction was conducted in an ultrasonic bath for 30 min at ambient temperature. After this step, the sample was filtered through a paper filter (previously rinsed with 200 ml of high–pure deionized water and 20 ml of phosphate buffer). Finally, extracts were neutralized with a few drops of 15 mol L^{-1} NaOH (up to pH 6.0–6.5) and filled up to 10 ml with deionized water (or phosphate buffer **[D2]**). As an alternative procedure of sample preparation, was hydrochloric acid leaching, used to determine Fe(II) and Fe(III) in post–glacial sediments and archaeological pottery **[D2]**. 1.00±0.01 g of a dry sample was accurately weighted and placed in a conical flask. Then 20 ml of 2 mol L^{-1} HCl was added and the flask with the reflux condenser was heated up to approx. 80°C. The temperature was then held for 30 min. After extraction and cooling, the sample was filtered through a paper filter (previously rinsed with 200 mL of high–pure deionized water) and filled up to 50 ml with deionized water.

Multi–Mode Sample Introduction System as a hydride generator

Referred in [D1]: J. Proch, P. Niedzielski (2020). *Talanta*, *208*, 120395. doi: 10.1016/j.talanta.2019.120395

Stock standard solutions (1000 mg As L^{-1}) of As(III), DMA and As(V) were prepared from sodium arsenite ($NaAsO_2$), dimethylarsinic acid ($C_2H_7AsO_2$) and disodium hydroarsenate heptahydrate ($Na_2HAsO_4 \cdot 7H_2O$), obtained from Sigma–Aldrich (USA). By dilution and mixing of three arsenic forms in a single solution, the working standard solutions were prepared daily. An anion–exchange column, Supelco LC–SAX–1, 250 x 4.6 mm, id. resin particles 5 µm (Merck, Germany) was used in chromatographic system. Phosphate buffer was prepared by mixing of disodium hydrophosphate (Na_2HPO_4) and potassium dihydrophosphate (KH_2PO_4 x 2 H_2O) (both obtained from Merck), and applied as a mobile phase. The outlet of column (PEEK tubing) was connected by Tygon sleeve and T–connector with a tube supplying the acidic medium and the eluent–acid mixture was introduced by the lower channel of MSIS. The upper channel of MSIS was used to supply the reductant solution. MSIS worked as a hydride generator (HG mode), therefore a sample channel of nebulizer (OneNeb, Agilent, USA) stayed blocked. Other investigated parameters were listed in Table 1.

Multi–Mode Sample Introduction System as a spray chamber with pneumatic nebulizer

Referred in [D2]: J. Proch, P. Niedzielski (2021). *Talanta*, *231*, 122403. doi: 10.1016/j.talanta.2021.122403

Stock standard solutions (1000 mg Fe L^{-1}) of Fe(II) and Fe(III) were prepared from ferrous ammonium sulfate hexahydrate and ferric ammonium sulfate dodecahydrate respectively (both obtained from Acros Organics, USA). By dilution and mixing of two iron forms in a single solution, the working standard solutions were prepared daily. A cation–exchange column, Dionex IonPac CS5A, 250 x 4.0 mm, id. resin particles 5 μm (Thermo Fisher Scientific, USA) was used in chromatographic system. A PDCA–based eluent was prepared by mixing reagents obtained from Merck: pyridine–2,6–dicarboxylic acid (PDCA), potassium hydroxide (KOH), potassium sulfate (K_2SO_4) and formic acid (HCOOH). The outlet of HPLC column (PEEK tubing) was directly connected with a sample channel of a pneumatic nebulizer. MSIS worked as a conventional spray chamber (Neb mode), therefore HG channels (supplying $NaBH_4$ and HCl in HG mode) stayed blocked. 0.1 mol L^{-1} sodium sulfite, prepared from powdered Na_2SO_3 (Merck), was periodically used for the column conditioning.

Multi–mode Sample Introduction System (MSIS) as an interface in the hyphenated system 2 HPLC–MSIS–ICP–OES in simultaneous determination of metals and metalloids species

Referred in [D3]: J. Proch, P. Niedzielski (2021). *Analytica Chimica Acta*, *1147*, 1–14. doi: 10.1016/j.aca.2020.12.047

Commercial standards were obtained from Romil (UK). All speciation standards and HG reagents as well as anion– and cation– exchange chromatographic systems were repeated in accordance with the first and second core scientific achievements **[D1–2]**. MSIS worked in its dual–mode, therefore simultaneous introduction and determination of non–hydride forming (Neb mode) and volatile hydride forming analytes (HG mode) was obtained. The outlet of anion–exchange column (PEEK tubing) was connected by Tygon sleeve and T–connector with a tube supplying the acidic medium. In turn, the outlet of cation–exchange column (PEEK tubing) was directly connected with a sample channel of a pneumatic nebulizer. Other investigated parameters were listed in Table 1.

Table 1. Investigated conditions during the optimization of described hyphenated techniques. Optimized parameters are underlined.

	HPLC–HG–ICP–OES	**HPLC–ICP–OES**	**HPLC–MIP–OES**	**2 HPLC–MSIS–ICP–OES**	
Column type	Anion–exchange (Supelco LC–SAX–1)	Cation–exchange (Dionex IonPac CS5A)		Anion–exchange (Supelco LC–SAX–1)	Cation–exchange (Dionex IonPac CS5A)
Eluent type (pH)	phosphate buffer, (6.0±0.2)	PDCA eluent, (4.2±0.2)		phosphate buffer, (6.0±0.2)	PDCA eluent, pH (4.2±0.2)
Composition [mmol L^{-1}]	KH_2PO_4 (12.5, <u>25</u>, 50) and Na_2HPO_4 (1.25, <u>2.5</u>, 5.0)	PDCA (7.0), KOH (66), K_2SO_4 (5.6) and HCOOH (74)		KH_2PO_4 (25) and Na_2HPO_4 (2.5)	PDCA (7.0), KOH (66), K_2SO_4 (5.6) and HCOOH (74)
Eluent flow [ml min^{-1}]	2.0	0.5, 1.0, 1.5, <u>2.0</u>		1.0	1.0
MSIS (work mode)	HG	Neb		Dual	
				HG	Neb
$NaBH_4$ [%, w/v]	0.10, 0.25, 0.50, 0.75, <u>1.00</u>, 1.25, 1.50	N/A		1.00	N/A
HCl [mol L^{-1}]	0.10, 0.25, 0.50, 1.00, 2.50, <u>5.00</u>	N/A		5.00	N/A
RF power [kW]	1.45	1.20	1.00	1.20	
Plasma gas flow [L min^{-1}]	<u>12</u>, 15, 18	12	20	12	
Torch view	<u>axial</u>	SVDV	axial	SVDV	
Analytical wavelengths [nm]	As 188.980, As 193.696, As 197.198, <u>As 228.812</u>, As 232.984	Fe 234.350, <u>Fe 238.204</u>, Fe 259.940, Fe 261.382	Fe 259.940, <u>Fe 371.993</u>	As 228.812, Cd 214.439, Co 238.892, Cu 327.395, Fe 234.350, Ge 209.426, Mn 257.610, Ni 231.604, Pb 220.353, Ru 240.272, Se 196.026, Sr 460.733, Tl 190.794, V 292.401, Zn 213.857	

<u>Elemental and speciation analyses of different brands of yerba mate (Ilex paraguariensis)</u>

<u>Referred in [D4]</u>: J. Proch, A. Orłowska, P. Niedzielski (2021). *Foods*, *10*(12), 2925. doi: 10.3390/foods10122925

This study was the application of the methods (described in details in Chapter 7), therefore all conditions were repeated in accordance with the previous core scientific achievements **[D1–D3]**. Additionally, total content of 16 elements were determined using ICP-OES analysis after two samples preparation procedures: ultrasound-assisted extraction (repeated after **[D1-D3]**) and microwave-assisted digestion in which a sample (0.50±0.01 g) was digested in 5.0 ml of 65% HNO_3 (Merck) using microwave digestion system, MARS 6 (CEM, USA). The conditions of ICP-OES in total analysis was identical with our previous studies [**D2-D3**].

7. Core achievements commentaries

Multi–Mode Sample Introduction System as a hydride generator

Referred in [D1]: J. Proch, P. Niedzielski (2020). *Talanta*, *208*, 120395. doi: 10.1016/j.talanta.2019.120395

The aim of this work was to evaluate and apply Multi–mode Sample Introduction System (MSIS, Agilent, USA), in its hydride generation (HG) mode, as an interface between anion–exchange HPLC and ICP–OES. The assumed advantages of the method (HPLC–HG–ICP–OES), compared to the systems described previously, were: a repeatable design (the system was only based on parts commercially available), avoidance of post–column reagents, simple sample preparation procedure, and short analysis time. The system was used to determine three arsenic species, arsenites [As(III)], arsenates [As(V)], and dimethylarsinic acid (DMA) in environmental and food samples. My role in this study was conceptualization, methodology, investigation, writing – original draft, review and editing (equally contributed with my supervisor), data curation and validation.

The study consisted of design, optimization, validation and application of the method. The general scheme of described system is presented in **Figure 3**. The part was faded out to highlight the aim of the core achievements following one by one.

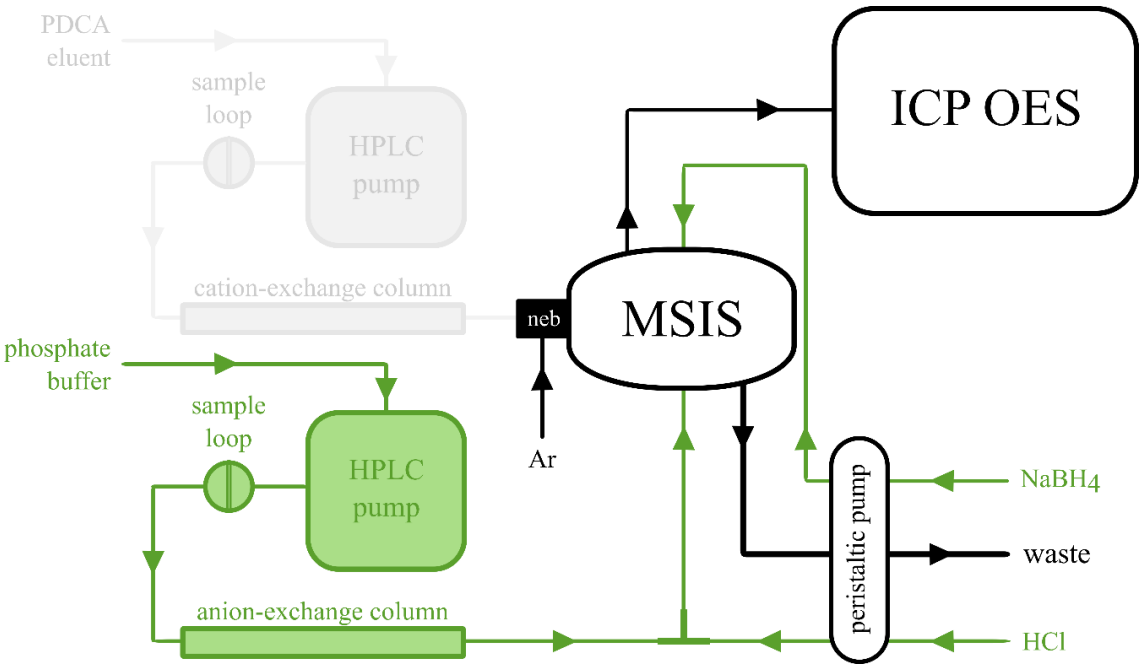

Fig. 3. General scheme of HPLC–HG–ICP–OES with MSIS, working in its HG mode, as an interface between HPLC and ICP–OES.

Firstly, the composite optimization of the hydride generator (MSIS) was conducted with HG–ICP–OES (prior to the HPLC connection) and investigated parameters were: analytical wavelength, plasma

gas flow, $NaBH_4$ and HCl concentration. After this stage, HPLC was coupled with HG–ICP–OES and mobile phase concentration was also optimized. All operating parameters were summarized in Materials and Methods (Section 5, **Table 1**). Under optimal conditions, the peak resolution was satisfactory in the whole investigated range (LOD–1000 μg L^{-1}) and retention times (RTs) were 100–355 s. Precision (2.7–5.7%) was calculated as relative standard deviation (RSD%) of the standard measurement containing 100 μg L^{-1} of each As species in single solution. Limits of detection (LODs, 2.08–6.97 μg L^{-1}) were calculated as 3 standard deviation (SD) of the blank measurements (n=10). Obtained method allowed to determine three arsenic species. Due to the lack of Certified Reference Materials (CRMs), containing certified values of As(III), As(V) and DMA extractable by phosphoric acid, the recovery (95–106%) was evaluated using the standard addition method.

The applicability was performed with three groups of real samples: (1) soil located in the proximity of industry wastes disposal site, (2) parts of 2 years old common oaks *(Quercus robus)* growing in the solution enriched with arsenic species, and (3) yerba mate (*Ilex paraguariensis)*, available on the Polish market. The first group (n=3) was highly contaminated with inorganic arsenic species. The substantial domination of As(V) was observed (4960–5920 mg kg^{-1}), also evidenced by high As(V)/As(III) ratio (450–713). However, DMA was determined <LOD in all sample. The second group (n=6) was the most diverse in terms of the content of arsenic forms. As(III) and DMA were only found in two samples, 27–44 μg kg^{-1} and 266–750 μg kg^{-1} respectively. As(V) was detected above LOD in one sample (197 μg kg^{-1}). The third group (n=6) contained arsenic species at very low levels.

The usage of MSIS as a hydride generator and an interface between HPLC and ICP–OES allowed to design novel hyphenated technique, which was based only on commercial available parts avoiding the post–column reagents. Three arsenic speciation forms could be determined in relatively short time (up to 400 s) with considerably low LODs and high precision. Results were comparable with other CVG/HG technique coupled to plasma–based OES. Summarizing the above, the study became the first step in the evaluation of MSIS as an interface in hyphenated techniques.

Multi–Mode Sample Introduction System as a spray chamber with a pneumatic nebulizer

Referred in [D2]: J. Proch, P. Niedzielski (2021). *Talanta*, *231*, 122403. doi: 10.1016/j.talanta.2021.122403

The aim of this work was to evaluate and apply MSIS, working as a conventional spray chamber in its nebulization (Neb) mode, as an interface in the hyphenated techniques. In this case, the same chromatographic system (based on a cation–exchange column) was coupled with two different detectors, MIP–OES and ICP–OES. For the first time, the parallel optimization of two hyphenated systems, HPLC–ICP–OES and HPLC–MIP–OES, was conducted. Both systems were used to determine two iron species, Fe(II) and Fe(III) in five types of real samples. The assumed advantages of the method were: a repeatable design (both systems were only based on parts commercially available), avoidance of post–column reagents, simple procedure of sample preparation, and short analysis time. Moreover, the

advantages and shortcomings of the both detectors were assessed in iron speciation studies. My role in this study was conceptualization, methodology, investigation, writing – original draft, review and editing (equally contributed with my supervisor), data curation and validation.

The study consisted of design, optimization, validation and application of the method. The general scheme of described system is presented in **Figure 4**. The part, which was investigated previously, was faded out.

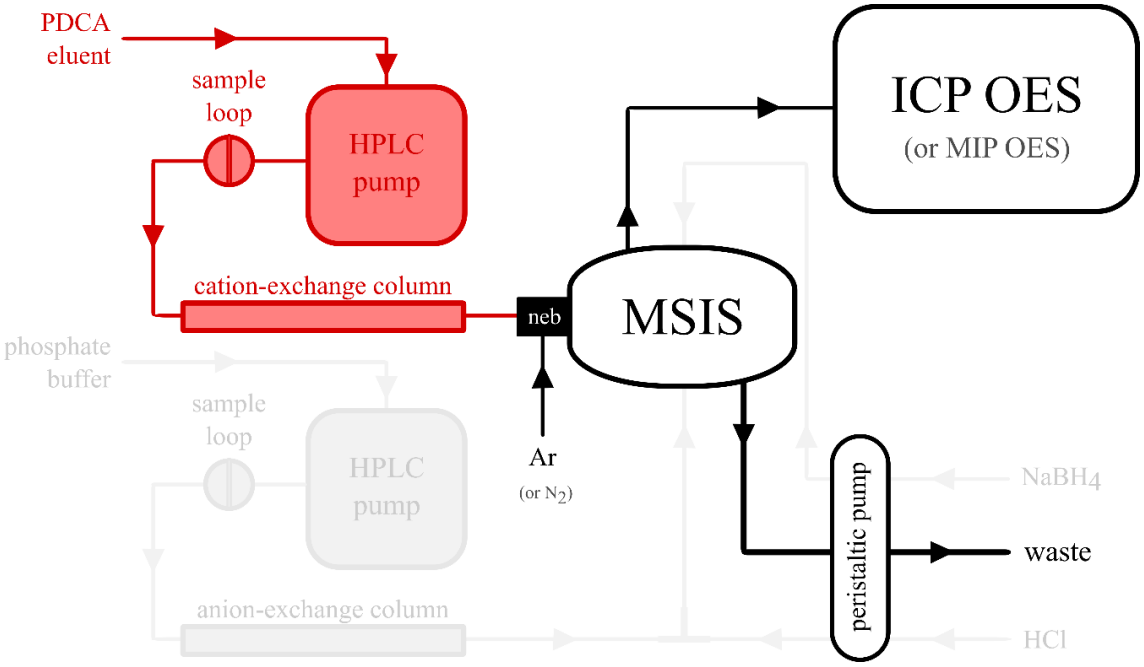

Fig. 4. General scheme of HPLC–ICP–OES or HPLC–MIP–OES with MSIS, working in its Neb mode, as an interface between HPLC and plasma–based optical emission spectrometry.

Firstly, the parallel optimization of HPLC–ICP–OES and HPLC–MIP–OES was conducted and investigated parameters were: plasma ignition, plasma gas flow, nebulization flow, analytical wavelength, mobile phase composition and chromatographic run. Most of these parameters were adopted from the previous studies. All operating parameters were also summarized in Materials and Methods (Section 5, **Table 1**). Under optimal conditions, the peak resolution was satisfactory in the whole investigated range. RTs were 103–242 s. Moreover, the RT ratio was calculated [as Fe(II)/Fe(III)], which was equal to 2.36±0.09 s. This value was in accordance with the literature (data obtained with the same column and the eluent). For the optimal analytical wavelengths, precision was slightly better for MIP–OES (2.1–2.8%) than ICP–OES (3.6–4.1%). However, significantly lower LODs were obtained with ICP–OES,16.2–18.9 μg L^{-1}, than MIP–OES, 281–324 μg L^{-1}. Regardless of the detector, lower LODs and RSD were calculated for Fe(III) than Fe(II), 2.8–4.1%. Due to the lack of Certified Reference Materials (CRMs), containing certified values of Fe(II) and Fe(III), the recovery

was evaluated using the standard addition method. More consistent recoveries were obtained from ICP–OES (97–113%) in comparison to MIP–OES (94–115%).

The applicability was performed with five groups of real samples: (1) post–glacial sediments (Spitsbergen, Svalbard), (2) archaeological pottery, (3) soil located in the proximity of industry wastes disposal site, (4) river sediments (Mekong, Vietnam), and (5) yerba mate (*Ilex paraguariensis)*, available on the Polish market. Additionally, two procedures of sample preparation were used: hydrochloric acid leaching (1–2) and ultrasound–assisted extraction (3–5). It is worth to mention that these extractants are less effective for inorganic sample due to some iron fractions are built in silicates.

In comparison of the systems, a limiting factor of HPLC–MIP–OES was Fe(II), which was found below LOD in 3 samples more than HPLC–ICP–OES. Nevertheless, the accuracy, calculated as ratio of HPLC–MIP–OES and HPLC–ICP–OES results, was in acceptable range (80–120%) with an exception (77%) for post–glacial sediments. Moreover, the following observations were noted: (1) both methods were equally applicable whether the ratio was 25 or lower, (2) MIP–OES was recommended when high concentration is expected (total Fe > 10 g kg^{-1}), (3) ICP–OES was recommended when the ratio was 32 and higher.

The usage of MSIS as a spray chamber with pneumatic nebulization and as an interface between HPLC and ICP–OES allowed to design parallel two novel hyphenated techniques. Both methods were based only on commercial available parts avoiding the post–column reagents. Two iron speciation forms could be determined in significantly short time (up to 300 s) with considerably low LODs and high precision. The crucial parameters in the method evaluation were: (1) mutual ratio of Fe(II) and Fe(III) as well as (2) assumed total Fe concentration in material. Results were comparable with HPLC–based techniques coupled with various detectors, however MIP–OES was complementary (not alternative) detector in the hyphenated systems. Summarizing the above, the study became the second step in the evaluation of MSIS as an interface in hyphenated techniques.

Multi–mode Sample Introduction System in dual–mode as an interface

Referred in [D3]: J. Proch, P. Niedzielski (2021). *Analytica Chimica Acta*, *1147*, 1–14. doi: 10.1016/j.aca.2020.12.047

The aim of this work was to combine the achievements obtained in previous studies [**D1–D2**] and apply MSIS working in dual–mode as an interface between two different chromatographic systems and ICP–OES. An anion–exchange column (HG mode) was used to separate 5 speciation forms while a cation–exchange column (Neb mode) was used to separate 13 speciation forms. In this way, 18 speciation forms of 15 elements were simultaneously determined by ICP–OES. For the first time, the hyphenated system based on detection in optical emission spectrometry, was applied to simultaneously determine elements occurring as two cations (iron) and three anions (arsenic). The main advantages of the first and second core scientific achievement were kept: a repeatable design (both system was only based on parts commercially available), avoidance of post–column reagents, simple procedure of sample

preparation, and relative short analysis time. My role in this study was conceptualization, methodology, investigation, writing – original draft, review and editing (equally contributed with my supervisor), data curation and validation.

The study consisted of design, optimization, validation and application of the method. The general scheme of described system is presented in **Figure 5.**

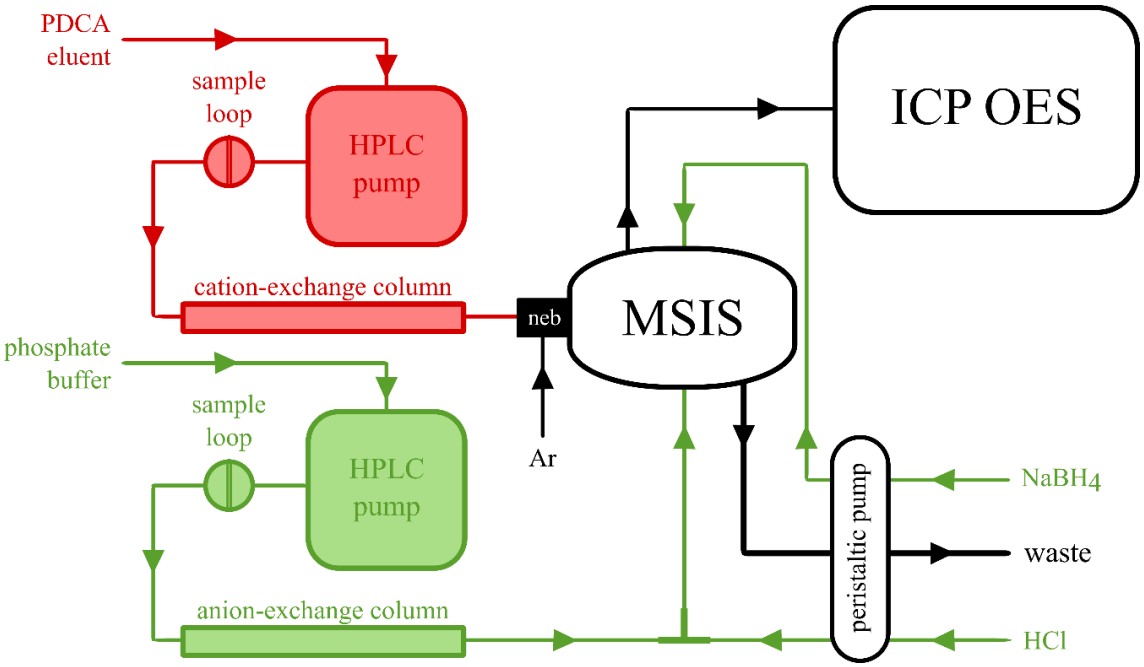

Fig. 5. General scheme of 2 HPLC–MSIS–ICP–OES using its dual–mode an interface between two HPLC system (anion– and cation–exchange) and ICP–OES.

After short optimization, lower eluent flow was chosen (1 ml min^{-1}), therefore RTs increased in comparison to previously studies [**D1–D2**]. Other parameters were adopted. All operating parameters were also summarized in Materials and Methods (Section 5, **Table 1**). After the preliminary study (not published data), 18 species of 15 elements were chosen to further investigations. Typical chromatograms, obtained with standard solutions, were shown in **Figure 6**.

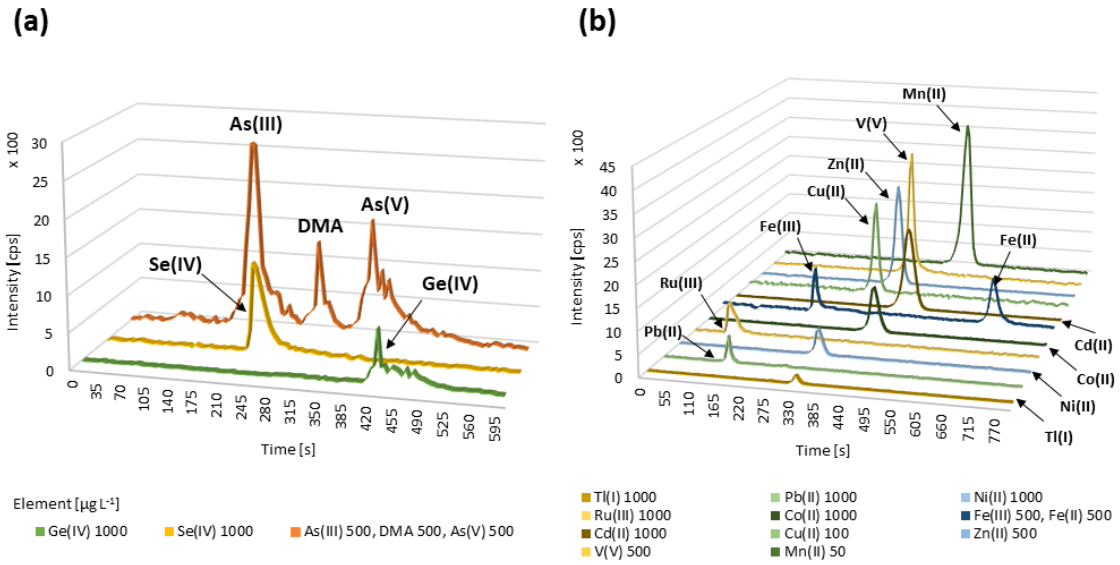

Fig. 6. Typical chromatograms of standard solutions obtained by 2 HPLC–MSIS–ICP–OES with (a) anion–exchange column and (b) cation–exchange column under experimental conditions.

Under optimal conditions, the peak resolution was satisfactory in the whole investigated range. Relative short RTs were 80–635 s. For the optimal analytical wavelengths, the sufficient precision was obtained (RSD<20%), with Sr(II) as an exception (26%). LODs were generally below 20 µg L^{-1}, however slight higher LODs were for Ru(III), Tl(I), Pb(II) and Sr(II). Due to the lack of Certified Reference Materials (CRMs), the recovery was evaluated using the standard addition method (81–120%).

The applicability was performed with five groups of real samples: (1) post–glacial sediments (Spitsbergen, Svalbard), (2) archaeological pottery, (3) soil located in the proximity of industry wastes disposal site, (4) river sediments (Mekong, Vietnam), and (5) yerba mate (*Ilex paraguariensis)*. It is worth to mention that the extractant (1 mol L^{-1} H_3PO_4) is less effective for inorganic sample matrix (1–4) due to some element fractions are built in silicates. According to this, element content was depended from sample matrix type, however a domination of Fe(III) and As(V) was observed over Fe(II) and As(III) regardless of the investigated group. Obtained results were in accordance with the literature data.

The usage of MSIS in dual–mode, as an interface between two HPLC and ICP–OES allowed to design a novel hyphenated technique, which has no counterpart. The method is still based only on commercial available parts avoiding the post–column reagents. In relative short time (up to 700 s of a single analysis), 18 speciation forms of 15 elements could be determined quantitively. However, the observation of several undefined species of Cu, Fe, Mn and Zn in real sample was the most significant in this core scientific achievements. According to this, its results and conclusions will be discussed in the Summary and Perspective (Section 9) as being a perspective of further research. In turn, the applicability will be discussed in the Application part of the doctoral thesis (Section 8).

8. Application

Elemental and speciation analyses of different brands of yerba mate (Ilex paraguariensis)

Referred in [D4]: J. Proch, A. Orłowska, P. Niedzielski (2021). *Foods*, *10*(12), 2925. doi: 10.3390/foods10122925

The aim of the application of hyphenated techniques previously developed, HPLC–HG–ICP–OES [**D1]** and HPLC–ICP–OES **[D2]** is speciation analyses of different brands of yerba mate (Ilex paraguariensis). Additionally, 16 elements (including As and Fe) were determined by ICP–OES to evaluate content of As(III), As(V), DMA, Fe(II) and Fe(III) in context of their total contents. The speciation analysis of yerba mate were performed for the first time as well as such a big collection i.e. 58 samples (49 products of 13 brands) were analyzed by hyphenated techniques for the first time. My role in this study was conceptualization, methodology (equally contributed with my supervisor), investigation and writing – original draft (contributed with Aleksandra Orłowska), data curation and validation.

The application of the method consisted of sample preparation, instrumental analysis and statistical analysis. All reagents and parameters, which were adopted after previous core scientific achievements [**D1–D3]**, were also summarized in Materials and Methods (Section 5). After sample homogenization, 58 samples were prepared parallel in two procedures, microwave–assisted digestion and ultrasound assisted extraction. The digests were used to determine total content of 16 elements by ICP–OES while extracts were analyzed triple to determine: (1) As(III), As(V) and DMA by HPLC–HG–ICP–OES [D1], (2) Fe(II) and Fe(III) by HPLC–ICP–OES [D2], and (3) 16 elements in their H_3PO_4 extractable contents by ICP–OES. In the case of Cr extractable content, the results were significantly higher than its total content. According to this, only 15 elements were determined in H_3PO_4 extracts. After the analysis, undefined extractable forms were calculated as the difference between the extractable content (determined by ICP–OES) and the sum of speciation forms (arsenic or iron, determined by HPLC–HG–ICP–OES or HPLC–ICP–OES respectively). In turn, non–extractable fraction was calculated as a difference of total content and extractable content (both determined by ICP–OES).

Method limits of quantitation (MQLs), which include a sample preparation, were in the following ranges: 0.062–0.210 mg kg^{-1} and 0.360–0.300 mg kg^{-1} for As and Fe species respectively. As(III) was found in two samples while As(V) and DMA were detected above MQL in four samples. Total and extractable contents of arsenic were found above MQL in 20 and 8 samples respectively. The median percentage (n=8) of As extractable content was 29%. In turn, total and extractable content of iron were found in all samples (n=58), while Fe(II) and Fe(III) were only found in 26 and 31 samples respectively. The results were surprising, as it was expected that ionic Fe(II) and Fe(III) in yerba mate are widespread. The median percentage (n=58) of Fe extractable content was 8% (the lowest value of all elements). The contents of other detected elements were generally in accordance to the literature. According to this, results of total content were also subjected to statistical analysis (using e.g. principle components

analysis, PCA), however any relationship between samples of the same origin, type, composition and brand, were hardly to indicate.

Summarizing the above, the methods developed as a part in the core scientific achievements [D1–D2] were successfully applied for the determination of arsenic and iron species in yerba mate. The results showed that most of elements were built into the plant tissues during the growth stage. Therefore the determination of speciation forms of any element must be evaluated in the context of the total content. Iron is an example, where non–extractable content predominated (92% as median). These results changed the view on elemental and speciation composition of yerba mate. The occasional occurrence of selected species in yerba mate or their high total content, were accidental rather than related to investigated factors, i.e. kind, composition, country of origin, brand or packing. Nevertheless, it is a pioneering application in speciation studies of yerba mate.

9. Summary and perspectives

The conclusion of the first and second core scientific achievements [**D1–D2**], was directly used to design the method, described in the third core scientific achievements [**D3**] as well as they were applied to determine arsenic and iron species in yerba mate samples [**D4**]. Nevertheless, the significant results were obtained in qualitive speciation analysis, which were performed in the third core scientific achievements [**D3**].

During the method application, there were detected several undefined species of transition metals. The chromatograms were showed in **Figure 7**.

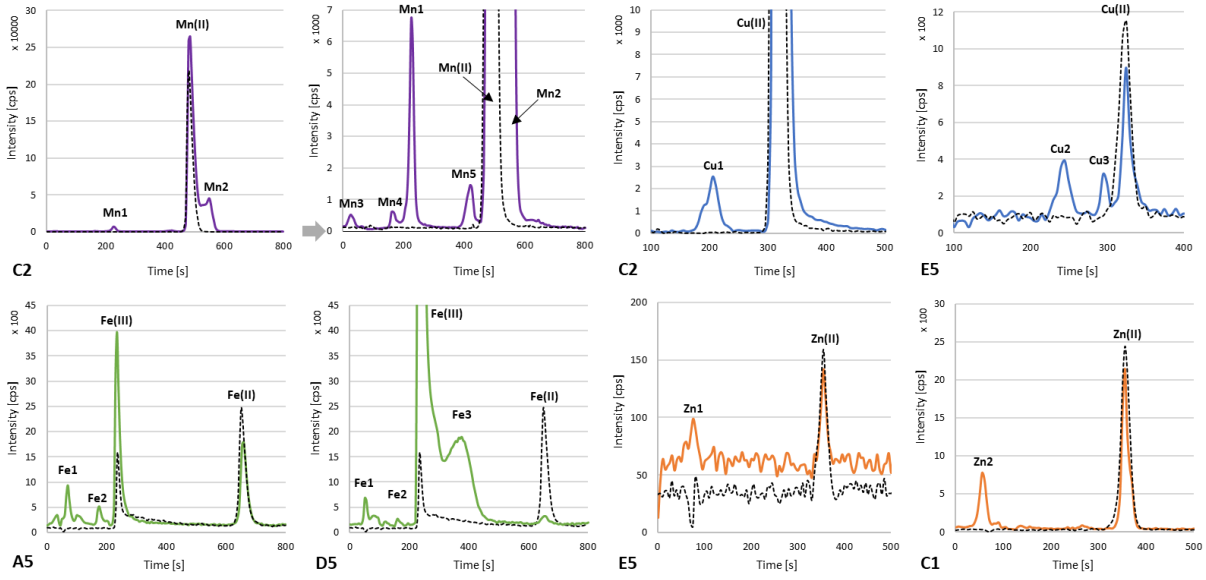

Fig. 7. Undefined species of Cu (Cu1–Cu3), Fe (Fe1–3), Mn (Mn1–5) and Zn(1–2), found in real samples (A – post–glacial sediment, C – soil located in the proximity of industry wastes disposal site, D – river sediments (Mekong, Vietnam), and E – yerba mate) and compared with the standard solutions.

Several undefined forms of Mn (Mn1–5) were found in sample C2 (soil located in the proximity of industry wastes disposal site). Undefined Cu species (Cu1–Cu3) were detected both in yerba mate (E5) and soil located in the proximity of industry wastes disposal site (C2). In turn, undefined Fe species (Fe1–3) were found only in sediments, both post-glacial (A5) and river (D5). Undefined species of Zn (Zn1–2) were detected in soil located in the proximity of industry wastes disposal site (C1) and yerba mate (E5). Only the chromatograms of standards, i.e. Cu(II), Fe(II), Fe(III), Mn(II) and Zn(II) is easy to identify (**Figure 7**).

The study attempted to identify other undefined forms on the basis of literature data, however, these are insufficient. In the case of Mn, one of five peaks could be Mn(III), while Cu(I) could be one peak from Cu1–Cu3. There is a surprising lack of the hyphenated technique for determination of Cu, Fe and Mn. The method presented unexplored potential in identification forms, then quantification, validation and application. Each element, detected in common conditions from the third core scientific achievements [**D3**], may require slight different condition to obtain the optimal separation of undefined forms without losing the parameters of detector. Therefore, new sample preparation methods, which will be dedicated for single- and multi-elemental speciation analysis, are crucial. Other important part of the further investigation could be specific sample matrix, which contains the desired species. By investigating all of mentioned factors, even more than one doctoral thesis could be reported.

Summarizing all above, there is many parameters of single-elemental methods which will be re-use in regular laboratory work [D1, D2] as well as many new questions and variables obtained with the multi-elemental method. Every mentioned parameter is a new separated scientific journey, which I would like to continue.

10. References

[1] Brandenberger, H., & Bader, H. (1967). Determination of nano¬gram amounts of mercury in solution by a flameless atomic absorption method. *Helvetica Chimica Acta*, *50*(5), 1409–1415. doi: 10.1002/hlca.19670500522

[2] Holak, W. (1969). Gas–sampling technique for arsenic determination by atomic absorption spectrophotometry. *Analytical Chemistry*, *41*(12), 1712–1713. doi: 10.1021/ac60281a025

[3] Braman, R., Justen, L., & Foreback, C. (1972). Direct volatilization–spectral emission type detection system for nanogram amounts of arsenic and antimony. *Analytical Chemistry*, *44*(13), 2195–2199. doi: 10.1021/ac60321a011

[4] Ślachciński, M. (2014). Recent Achievements in Sample Introduction Systems for Use in Chemical Vapor Generation Plasma Optical Emission and Mass Spectrometry: From Macro– to Microanalytics. *Applied Spectroscopy Reviews*, *49*(4), 271–321. doi: 10.1080/05704928.2013.823547

[5] D'Ulivo, A. (2019). The contribution of chemical vapor generation coupled with atomic or mass spectrometry to the comprehension of the chemistry of aqueous boranes. *Journal of Analytical Atomic Spectrometry*, *34*(5), 823–847. doi: 10.1039/c9ja00039a

[6] García, M., Aguirre, M., & Canals, A. (2017). Determination of As, Se, and Hg in fuel samples by in–chamber chemical vapor generation ICP OES using a Flow Blurring® multinebulizer. *Analytical and Bioanalytical Chemistry*, *409*(23), 5481–5490. doi: 10.1007/s00216–017–0484–6

[7] Lima, A., Da Costa, M., Ferreira, D., Richter, E., & Munoz, R. (2015). Fast ultrasound–assisted treatment of inorganic fertilizers for mercury determination by atomic absorption spectrometry and microwave–induced plasma spectrometry with the aid of the cold–vapor technique. *Microchemical Journal*, *118*, 40–44. doi: 10.1016/j.microc.2014.07.012

[8] Escudero, L., Pacheco, P., Gasquez, J., & Salonia, J. (2015). Development of a FI–HG–ICP–OES solid phase preconcentration system for inorganic selenium speciation in Argentinean beverages. *Food Chemistry*, *169*, 73–79. doi: 10.1016/j.foodchem.2014.07.127

[9] Calvo Fornieles, A., García de Torres, A., Vereda Alonso, E., & Cano Pavón, J. (2016). Simultaneous determination of traces of Pt, Pd, and Ir by SPE–ICP–OES. Test for chemical vapor generation. *Microchemical Journal*, *124*, 82–89. doi: 10.1016/j.microc.2015.07.024

[10] Tyburska, A., & Jankowski, K. (2013). Determination of selenium in dietary supplements by optical emission spectrometry after alkaline dissolution and subsequent headspace solid phase microextraction. *Journal of Pharmaceutical and Biomedical Analysis*, *74*, 268–272. doi: 10.1016/j.jpba.2012.11.011

[11] Fujihara, J., & Nishimoto, N. (2020). Total antimony analysis by hydride generation–microwave plasma–atomic emission spectroscopy with applications. *Microchemical Journal*, *157*, 104992. doi: 10.1016/j.microc.2020.104992

[12] Welna, M., & Szymczycha–Madeja, A. (2014). Effect of sample preparation procedure for the determination of As, Sb and Se in fruit juices by HG–ICP OES. *Food Chemistry*, *159*, 414–419. doi: 10.1016/j.foodchem.2014.03.046

[13] Jankowski, K., Giersz, J., & Paprocka, M. (2014). Improved determination of iodine by sequential (photo)chemical vapor generation and pneumatic nebulization in the programmable temperature spray chamber and inductively coupled plasma optical emission spectrometry. *Microchemical Journal*, *113*, 17–22. doi: 10.1016/j.microc.2013.11.006

[14] Rojas, I., Murillo, M., Carrión, N., & Chirinos, J. (2003). Investigation of the direct hydride generation nebulizer for the determination of arsenic, antimony and selenium in inductively coupled plasma optical emission spectrometry. *Analytical and Bioanalytical Chemistry*, *376*(1), 110–117. doi: 10.1007/s00216–003–1856–7

[15] Pereira, C., Aguirre, M., Nóbrega, J., Hidalgo, M., & Canals, A. (2014). Aerosol generation of As and Se hydrides using a new Flow Blurring® multiple nebulizer for sample introduction in inductively coupled plasma optical emission spectrometry. *Microchemical Journal*, *112*, 82–86. doi: 10.1016/j.microc.2013.09.006

[16] Matusiewicz, H., & Ślachciński, M. (2017). Simultaneous determination of As, Bi, Sb, Se and Sn by microwave induced plasma spectrometry using a quadruple–mode microflow ultrasonic nebulizer for in situ hydride generation with internal standardization. *Microchemical Journal*, *131*, 70–78. doi: 10.1016/j.microc.2016.11.017

[17] Welna, M., Szymczycha–Madeja, A., & Pohl, P. (2017). Improvement in the single and simultaneous generation of As, Bi, Sb and Se hydrides using a vapor generation accessory (VGA) coupled to axially viewed inductively coupled plasma optical emission spectrometry (ICP OES). *Analytical Methods*, *9*(5), 871–880. doi: 10.1039/c6ay02932a

[18] Deng, B., Xu, X., Xiao, Y., Zhu, P., & Wang, Y. (2015). Understanding the effects of potassium ferricyanide on lead hydride formation in tetrahydroborate system and its application for determination of lead in milk using hydride generation inductively coupled plasma optical emission spectrometry. *Analytica Chimica Acta*, *853*, 179–186. doi: 10.1016/j.aca.2014.10.034

[19] McLaughlin, R., & Brindle, I. (2002). A new sample introduction system for atomic spectrometry combining vapour generation and nebulization capacities. *Journal of Analytical Atomic Spectrometry*, *17*(11), 1540–1548. doi: 10.1039/b208011g

[20] Asfaw, A., & Wibetoe, G. (2006). Dual mode sample introduction for multi–element determination by ICP–MS: the optimization and use of a method based on simultaneous introduction of vapor formed by $NaBH_4$ reaction and aerosol from the nebulizer. *Journal of Analytical Atomic Spectrometry*, *21*(10), 1027. doi: 10.1039/b604116g

[21] Asfaw, A., & Wibetoe, G. (2005). Simultaneous determination of hydride (Se) and non–hydride–forming (Ca, Mg, K, P, S and Zn) elements in various beverages (beer, coffee, and milk), with minimum sample preparation, by ICP–AES and use of a dual–mode sample–introduction system. *Analytical and Bioanalytical Chemistry*, *382*(1), 173–179. doi: 10.1007/s00216–005–3188–2

[22] Matusiewicz, H., & Ślachciński, M. (2007). Simultaneous determination of hydride forming (As, Bi, Ge, Sb, Se, Sn) and Hg and non–hydride forming (Ca, Fe, Mg, Mn, Zn) elements in sonicate slurries of analytical samples by microwave induced plasma optical emission spectrometry with dual–mode sample introduction system. *Microchemical Journal*, *86*(1), 102–111. doi: 10.1016/j.microc.2006.12.002

[23] Ritschdorff, E., Fitzgerald, N., Mclaughlin, R., & Brindle, I. (2005). The use of a modified Multimode Sample Introduction System for the simple and rapid determination of cadmium by chemical vapour generation atomic absorption spectrometry. *Spectrochimica Acta Part B: Atomic Spectroscopy*, *60*(1), 139–143. doi: 10.1016/j.sab.2004.10.006

[24] Anderlini, T. K., & Beauchemin, D. (2018). Improvements to the analytical performance of inductively coupled plasma optical emission spectrometry by coupling a multi–mode sample introduction system to an infrared heated preevaporation tube. *Journal of Analytical Atomic Spectrometry*, *33*, 1068. doi: 10.1039/C8JA00051D

[25] Thompson, M., Pahlavanpour, B., Walton, S., & Kirkbright, G. (1978). Simultaneous determination of trace concentrations of arsenic, antimony, bismuth, selenium and tellurium in aqueous solution by introduction of the gaseous hydrides into an inductively coupled plasma source for emission spectrometry. Part I. Preliminary studies. *The Analyst*, *103*(1227), 568. doi: 10.1039/an9780300568

[26] Guerrero, M., Alonso, E., Pavón, J., Cordero, M., & García de Torres, A. (2016). Simultaneous determination of chemical vapour generation forming elements (As, Bi, Sb, Se, Sn, Cd, Pt, Pd, Hg) and non–chemical vapour forming elements (Cu, Cr, Mn, Zn, Co) by ICP–OES. *Journal of Analytical Atomic Spectrometry*, *31*(4), 975–984. doi: 10.1039/c5ja00471c

[27] Tanabe, C., Hopfer, H., Gilleland, G., Liba, A., Ebeler, S., & Nelson, J. (2016). Total arsenic analysis in Californian wines with hydride generation – microwave plasma – atomic emission spectroscopy (HG–MP–AES). *Journal of Analytical Atomic Spectrometry*, *31*(6), 1223–1227. doi: 10.1039/c6ja00051g

[28] Welna, M., Pohl, P., & Szymczycha–Madeja, A. (2019). Non–chromatographic Speciation of Inorganic Arsenic in Rice by Hydride Generation Inductively Coupled Plasma Optical Emission Spectrometry. *Food Analytical Methods*, *12*(2), 581–594. doi: 10.1007/s12161–018–1388–6

[29] Al–Assaf, K., Tyson, J., & Uden, P. (2009). Determination of four arsenic species in soil by sequential extraction and high performance liquid chromatography with post–column hydride generation and inductively coupled plasma optical emission spectrometry detection. *Journal of Analytical Atomic Spectrometry*, *24*(4), 376. doi: 10.1039/b820300h

[30] Barrientos, E., Wrobel, K., Torres Guzman, J., Corrales Escobosa, A., & Wrobel, K. (2016). Determination of SeMet and Se(iv) in biofortified yeast by ion–pair reversed phase liquid chromatography–hydride generation–microwave induced nitrogen plasma atomic emission spectrometry (HPLC–HG–MP–AES). *Journal of Analytical Atomic Spectrometry*, *31*(1), 203–211. doi: 10.1039/c5ja00276a

[31] Sánchez, M., Sabio, L., Gálvez, N., Capdevila, M., & Dominguez-Vera, J. (2017). Iron chemistry at the service of life. *IUBMB Life*, *69*(6), 382–388. doi: 10.1002/iub.1602

[32] Grotti, M., Terol, A., & Todolí, J. (2014). Speciation analysis by small–bore HPLC coupled to ICP–MS. *Trac Trends in Analytical Chemistry*, *61*, 92–106. doi: 10.1016/j.trac.2014.06.009

[33] Janvion, P., Motellier, S., & Pitsch, H. (1995). Ion–exchange mechanisms of some transition metals on a mixed–bed resin with a complexing eluent. *Journal of Chromatography A*, *715*(1), 105–115. doi: 10.1016/0021–9673(95)00576–9

[34] Cardellicchio, N., Ragone, P., Cavalli, S., & Riviello, J. (1997). Use of ion chromatography for the determination of transition metals in the control of sewage–treatment–plant and related waters. *Journal of Chromatography A*, *770*(1–2), 185–193. doi: 10.1016/s0021–9673(97)00086–1

[35] Kaasalainen, H., Stefánsson, A., & Druschel, G. (2016). Determination of Fe(II), Fe(III) and Fe total in thermal water by ion chromatography spectrophotometry (IC–Vis). *International Journal of Environmental Analytical Chemistry*, *96*(11), 1074–1090. doi: 10.1080/03067319.2016.1232717

[36] Ashworth, C., Weller, C., & Frisch, G. (2019). Quantifying indium with ion chromatography in hydro- and biohydrometallurgical leaching solutions. *Journal of Separation Science*, *42*(15), 2517–2522. doi: 10.1002/jssc.201900295

[37] McCormack, A., Tong, S., & Cooke, W. (1965). Sensitive Selective Gas Chromatography Detector Based on Emission Spectrometry of Organic Compounds. *Analytical Chemistry*, *37*(12), 1470–1476. doi: 10.1021/ac60231a007

[38] Fernsebner, K., Zorn, J., Kanawati, B., Walker, A., & Michalke, B. (2014). Manganese leads to an increase in markers of oxidative stress as well as to a shift in the ratio of Fe(II)/(III) in rat brain tissue. *Metallomics*, *6*(4), 921. doi: 10.1039/c4mt00022f

[39] Solovyev, N., Vinceti, M., Grill, P., Mandrioli, J., & Michalke, B. (2017). Redox speciation of iron, manganese, and copper in cerebrospinal fluid by strong cation exchange chromatography – sector field inductively coupled plasma mass spectrometry. *Analytica Chimica Acta*, *973*, 25–33. doi: 10.1016/j.aca.2017.03.040

[40] Mulugeta, M., Wibetoe, G., Engelsen, C., & Lund, W. (2010). Optimization of an anion-exchange high performance liquid chromatography-inductively coupled plasma-mass spectrometric method for the speciation analysis of oxyanion-forming metals and metalloids in leachates from cement-based materials. *Journal of Chromatography A*, *1217*(40), 6186-6194. doi: 10.1016/j.chroma.2010.07.082

[41] Cardozo Junior, E., & Morand, C. (2016). Interest of mate (Ilex paraguariensis A. St.–Hil.) as a new natural functional food to preserve human cardiovascular health – A review. *Journal of Functional Foods*, *21*, 440–454. doi: 10.1016/j.jff.2015.12.010

[42] Pardinho, R., Dalla Vecchia, P., Mendes, A., Bizzi, C., Mello, P., Duarte, F., & Flores, E. (2018). Determination of toxic elements in yerba mate by ICP–MS after diluted acid digestion under O2 pressure. *Food Chemistry*, *263*, 37–41. doi: 10.1016/j.foodchem.2018.04.112

Talanta 208 (2020) 120395

Contents lists available at ScienceDirect

Talanta

journal homepage: www.elsevier.com/locate/talanta

In–spray chamber hydride generation by multi–mode sample introduction system (MSIS) as an interface in the hyphenated system of high performance liquid chromatography and inductivity coupled plasma optical emission spectrometry (HPLC/HG–ICP–OES) in arsenic species determination

Jędrzej Proch, Przemysław Niedzielski*

Adam Mickiewicz University, Faculty of Chemistry, Department of Analytical Chemistry, Uniwersytetu Poznańskiego 8, 61–614, Poznań, Poland

ARTICLE INFO

Keywords:
Hyphenated systems
ICP-OES
MSIS
Arsenic speciation

ABSTRACT

The paper presents a new usage of a commercial in–spray chamber hydride generator, Multi–mode Sample Introduction System (MSIS) as a connector of high pressure liquid chromatography and inductivity coupled plasma optical emission spectrometry (HPLC/HG–ICP–OES). This hyphenated technique was applied in a determination of inorganic and organic arsenic species. The optimization of a hydride generation process in MSIS and a chromatographic separation (using anion–exchange HPLC column with phosphate buffer as a mobile phase) were carried out compositely. The method allowed to determine three arsenic forms, As(III), As(V) and dimethylarsinate (DMA) within 400s of a single analysis. The obtained limits of detection (LODs) were 2.08 $\mu g\,L^{-1}$ for As(III); 6.97 $\mu g\,L^{-1}$ for As(V); 6.15 $\mu g\,L^{-1}$ for DMA and precision 2.7%, 4.8%, and 5.7%, respectively, for 100 $\mu g\,L^{-1}$. The described method was used for environmental and food samples analyses.

1. Introduction

Hydride generation technique (HG), as a part of chemical vapor generation technique (CVG), was applied first time with atomic absorption spectrometry (AAS) in the determination of arsenic (As) [1] and a new method was called “gas–sampling technique”. This research was a succession of the determination of mercury (Hg) with chemical vapor generation (CVG) technique [2] and this method was described as “flameless”. Both studies were the origin of a new way of sample introduction technique and it has used since this time.

According to Long et al., 2012, HG technique is the most widely–used of all CVG techniques [3]. It is successfully used with different type of spectrometry, both atomic absorption (AA) and atomic emission (AE) [4]. Additionally, HG techniques found an application in spectrometry with inductively couple plasma (ICP), both mass spectrometry (MS) [5] and optical emission spectrometry (OES) [6,7]. Moreover, HG technique was coupled with microwave inducted plasma optical emission spectrometer (MIP–OES) and applications of HG–MIP–OES with helium (He) [8] and argon–helium mixture (Ar–He) as a plasma gas were reported [9]. Since MIP–OES with nitrogen (N_2), as a plasma gas, was commercialized, HG–MIP–OES technique became popular [10,11]. This flexibility in the HG technique combining with various type of spectrometer is the main advantage. What is more, the method separates all hydride–forming elements e.g. selenium (Se), antimony (Sb), germanium (Ge), bismuth (Bi) from the sample matrix. It increases the method sensitivity and even small amounts of these elements can be determined successfully. Limits of detections (LODs) for HG with OES can be close to results obtained by graphite furnace atomic absorption spectrometry (GFAAS) [12], although obtaining such results requires long–term application tests.

The main difficulty with a usage of HG technique is a choice of optimal parameters for hydrides forming. According to published papers, there are no plain optimal HG parameters [13,14]. Due to this, HG parameters have to be established experimentally before an application of the method. The base of the technique is a choice of concentrations of acidic medium i.e. hydrochloric acid (HCl) and sodium (or potassium) borohydride ($NaBH_4$ or KBH_4), which are required to effective generation of volatile hydride–forming. In addition, the flow rates of these reagents are equally important. According to this, some authors acidify their samples firstly to avoid adding HCl directly [12,14]. On the other hand, it increases the time of sample preparation and low pH values of HCl concentration in hydride generation step caused a decrease of the obtained analytical signal, especially for MMA and DMA [15]. The last difficulty is related to an equipment. Although the optimal HG

* Corresponding author.
E-mail address: pnied@amu.edu.pl (P. Niedzielski).

https://doi.org/10.1016/j.talanta.2019.120395
Received 6 June 2019; Received in revised form 20 September 2019; Accepted 26 September 2019
Available online 30 September 2019
0039-9140/

parameters were set up, additional reaction loops and/or gas–liquid separators is required to introduce samples and mix all reagents. It forced a development of commercial systems including sample introduction with a hydride generator. A commercial system (VGA–77P (Varian, Austria)), used previously with HG–AAS [16,17] was applied for HG–ICP–OES successful [13]. Some authors made original devices with similar abilities for their research needs [18–20].

Multi–mode Sample Introduction System (MSIS) is modified cyclonic spray chamber developed by Marathon Scientific (Ontario, Canada). MSIS, along with different commercial available systems as Flow Blurring® multinebulizer (FBMN) [20,21] or direct hydride generation nebulizer (DHGN) [6] is a way to generate volatile hydride–forming elements in spray chamber directly. MSIS is able to work in two single modes: a conventional spray chamber with pneumatic nebulizer or a hydride generator, where nebulizer flow rate is block. Moreover, MSIS allows to determine volatile hydride–forming and non–hydride–forming elements simultaneously in conjunction with third mode, a connection of two single modes (dual–mode). Additionally, MSIS is a system which can be applied in various spectrometry techniques i.e. MIP–OES, ICP–OES, ICP–MS.

Recently, the most popular OES technique coupled with MSIS is MIP–OES. Tanabe et al., 2016 determined As species in Californian wines using HG–MIP–OES technique with nitrogen–based plasma and the MSIS [10]. Authors decided about a usage of a reducing agent to reduce all As species to As(III). What is more, MSIS was used in the HG mode only. On the other hand, this research has increased the interest in the technique possibilities and Machado et al., 2017 used the same system in multielemental determination of As, Bi, Ge, Sb, Sn in various food samples e.g. powdered milk, bovine liver, rice [12]. Although this study avoided species analyses, author presented significant results for elements except Sn. This examples shows a gap which can be filled by a usage of hyphenated techniques in optical system i.e. a connection of chromatography and optical emission spectrometry.

Possibilities of MSIS was reported previously by Barrientos et al., 2016. Authors were first who presented MSIS as a connector of ion–pair reversed phase high pressure liquid chromatography (HPLC) and MIP–OES for determination of Se(IV) and Se(Met) in biofortified yeast [22]. Although MSIS was used as a connector, the system was expanded by additional post–column reaction loop was required to oxidize organic selenium compounds. So far, there has not been published studies presented a simultaneous determination of inorganic and organic element species without reducing or oxidizing agents. Moreover, MSIS has not been used as a connector of HPLC and ICP–OES.

In this work, a new hyphenated system with the MSIS as an interface between HPLC and ICP-OES was performed. The system was only built from commercial available devices to be repeated easily by further researchers. HG process was conducted in spray chamber directly and the quantitate determination of three arsenic species: As(III), As(V) and dimethylarsinic acid (DMA) was conducted in HG work mode. The determination of MMA was rejected, according to Cava-Montesinos et al., 2002 [15] who reported that MMA is not detectable at pH 4. What is more, no additional reducing and oxidizing agent were used and arsenic species were determined post–column directly. HG reagents concentration, separation conditions and instrumental parameters were optimized to obtain satisfying LODs and an accuracy. The secondary aim was to perform a system which is able to be a profitable alternative of commercial available devices (less apparatus costs, lower reagents consumption, less interferences etc.). The method was applied for various environmental and food samples analysis i.e. soil samples located in the proximity of industry wastes disposal site, 2 years-old common oaks (Quercus robur) growing in hydroponic experiments with Knop solution enriched with arsenic forms and yerba mate (Ilex paraguariensis).

2. Experimental

2.1. Gases and reagents

High–pure argon (N–5.0, purity 99.999%), obtained from Linde (Poland), was employed as a plasma gas. All reagents were diluted by high–pure deionized water (≥18 MΩ cm resistivity) obtained from a Milli–Q water purification system (Millipore, USA).

Stock standard solutions (1000 mg As L^{-1} in a single solution) of As (III), As(V), DMA were prepared by dissolving appropriate amounts of sodium arsenite ($NaAsO_2$), disodium hydroarsenate ($Na_2HAsO_4{\cdot}7H_2O$) and cacodylic acid ($C_2H_7AsO_2$) respectively, obtained from Sigma–Aldrich (USA). Stock standard solutions were stored in glass bottles at 4 °C in darkness. Less concentrated standard solutions were obtained by a dilution of the stock solutions were prepared daily.

Sodium tetrahydroborate ($NaBH_4$) solutions were prepared daily, by dissolving appropriate amounts of powdered $NaBH_4$ (Sigma–Aldrich) in water and stabilized with 0.1% (w/v) NaOH (Merck). HCl solutions were prepared from 30% HCl (Suprapur®, Merck). The mobile phase, a phosphate buffer, was prepared by mixing of disodium hydrophosphate (Na_2HPO_4) and potassium dihydrophosphate ($KH_2PO_4{\cdot}2H_2O$) obtained from Merck. Appropriate amounts of powder reagents were dissolved and mixed to obtained the stock mobile phase solution, 50 mmol L^{-1} $KH_2PO_4{\cdot}2H_2O$ and 5 mmol L^{-1} Na_2HPO_4.

2.2. Instrumentation

The hyphened technique, HPLC–HG–ICP–OES with MSIS as an interface is shown in Fig. 1. The HPLC system was constructed from a HPLC pump, Shimadzu LC–10AT (Shimadzu, Japan) and an anion–exchange HPLC column, Supelco LC–SAX1, 250 mm × 4.6 mm i.d, resin particle size 5 μm (Supelco, Germany). Mobile phase flow rate was isocratic at 2 mL min^{-1} and an injection volume (sample loop volume) was 200 μL. PEEK tubing was used to transfer the LC column eluent from the MSIS unit was inserted into a Tygon sleeve. In the next stage of the investigation, the outlet of the HPLC column was connected with the tube which supply HCl using T–shape connecter and reagents were introduced both to vertical–placed inlet of the MSIS unit. Cohesion of the introduced phase (eluent from the column) and the applied flow rates of HG reagents allowed a direct eluent introduction (peristaltic pump avoiding) to the MSIS unit.

The MSIS unit (Marathon Scientific, Canada) was a hydride generation system and an interface between HLPC and ICP–OES. The hydride generation process is possible due to inlets located vertically in the center of this unit. HG reagents were delivered to the chamber, mixed at the tops of the inlets and volatile hydrides were formed and carried with gas (argon) from the MSIS unit to ICP torch. The upper inlet of the unit was used to provide $NaBH_4$ solution. The lower inlet provided HCl solution and post column reagents (an eluent with sample solution). Additionally, the MSIS unit had a function of gas–liquid separator and due to this, the excess liquid was carry from the chamber using a peristaltic pump. The waste liquid flow rate was proportional to the sum of HG reagents flow rates.

The inductively coupled plasma optical emission spectrometer, Agilent 5110 ICP–OES (Agilent Technologies, USA), was used as a detector of the hyphenated system. The synchronous vertical dual view (SVDV) of the plasma were accomplished in the spectrometer and allows the axial and radial view analysis simultaneously. However, only axial torch view were used in this work. The usage of the Cooled Cone Interface (CCI) technology minimize interferences and recombination removing the cool plasma tail from the axial optical path. Even small amounts of free hydrogen are able to destabilized plasma and turn it off. According to this, RF power was set up at maximum value i.e. 1450 W. Nebulizer and auxiliary argon flow rates were 0.7 L min^{-1} and 1.0 L min^{-1} responsibly. A nebulizer sample channel stayed blocked in HG work mode. HG reagents were pumped continuously to the MSIS unit

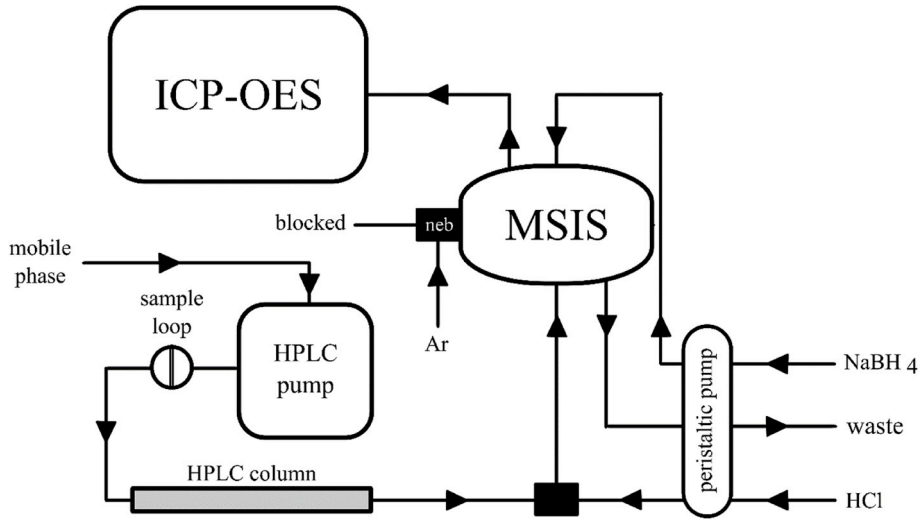

Fig. 1. General scheme of described technique, HPLC/HG–ICP–OES with MSIS as an interface.

Table 1
Optimized instrumental parameters for HPLC/HG–ICP–OES.

HPLC conditions	
Pump	Shimadzu LC–10AT
Column	Supelco LC–SAX 1, (250 mm × 4.6 mm i.d., 5 μm)
Mobile phase	Phosphate buffer, 2.5 mmol L^{-1} disodium hydrophosphate (Na_2HPO_4) + 25 mmol L^{-1} potassium dihydrophosphate ($KH_2PO_4 \times 2H_2O$)
Mobile phase flow rate [mL min^{-1}]	2
Injection volume [μL]	200
Hydride generation parameters	
$NaBH_4$ concentration [%, w/v]	1.00
NaOH concentration [%, v/v]	0.10
HCl concentration [mol L^{-1}]	5.00
$NaBH_4$ flow rate [mL min^{-1}]	1
HCl flow rate [mL min^{-1}]	1
ICP–OES conditions	
Spectrometer	ICP 5110 Dual–View
RF generator [MHz]	27
RF power [W]	1450
Nebulizer gas flow rate [L min^{-1}]	0.7
Plasma gas flow rate [L min^{-1}]	12
Auxiliary gas flow rate [L min^{-1}]	1.0
Peristaltic pump speed [rpm]	12
Nebulizer/spray chamber type	pneumatic/MSIS
Torch view	axial
Analytical wavelengths [nm]	188.980, 193.696, 197.198, 228.812, 232.984

with flow rates established at 1 mL min^{-1} and the peristaltic pump speed set at 12 rpm. Echelle grading fixed optic was thermostated at 35 °C and a detector, VistaChip II with the Charge Coupled Device (CCD) was cooled to −40 °C using triple Peltier system. The analytical signal response (intensity) [cps] was read every 5s, according to the time of analysis. At the beginning of studies, five arsenic analytical wavelengths were chosen based on the literature research and spectrometer software, 188.980 nm, 193.696 nm, 197.198 nm, 228.812 nm, 232.984 nm, respectively. The above parameters were constant and these influences were not investigated. All instrumental parameters for HPLC/HG–ICP–OES are shown in Table 1.

2.3. Sample preparation

Sample preparation procedure was repeated after Niedzielski et al., 2013 [23]. Accurately weighted 1.00 (± 0.01) g of a dry sample was placed in polyethylene test tube. 8 mL of 1 mol L^{-1} orthophosphate acid (H_3PO_4) was added to each sample and the ultrasound assisted extraction was conducted by 30 min at ambient temperate. In the next step, samples were filtered using a paper filter, which had been washed by 200 mL of high–pure deionized water and 20 mL of phosphate buffer. Sample solutions were neutralized with a few drops of 15 mol L^{-1} NaOH to obtain pH value in the range from 6.0 to 6.5 and filled up to the final volume of 10 mL. Samples were determined rapidly after preparation.

3. Results and discussion

3.1. Argon plasma flow rates optimization

Composite optimization was carried out to achieve the best results for As species determination by HPLC–HG–ICP–OES. The MSIS unit was coupled to ICP–OES to optimize spectrometer parameters and establish concentrations of HG reagents. In the first row, plasma gas flow rate was investigated in the range from 12 to 18 L min^{-1}. For the parameter optimization, others parameter were established at constant values. According to this, 1.00% $NaBH_4$ (w/v) in 0.10% NaOH (v/v) and 1.00 mol L^{-1} HCl were chosen as center values of the range of tested concentrations. Results for two analytical wavelengths, 197.198 nm and 232.984 nm were rejected due to high values (≥20%) of relative standard deviation (RSD) for results in the entire concentration range, irrespective of plasma flow rates. In the investigated range, a decrease in the analytical signal response was observed for the same analytical line wavelengths as the plasma gas flow rate increased. What is more, the highest intensity was noted for 228.812 nm in the whole range. In the literature, the best analytical signal responses for arsenic are observed for different wavelengths, 188.980 nm or 193.696 nm. According to the literature, obtained results are novel and the optimal analytical line wavelength was set up at 228.812 nm. The optimization of plasma gas flow rate was repeated during the investigation of $NaBH_4$ concentration. The influence of plasma gas flow rate on the analytical signal response is presented in Fig. 2.

3.2. HG reagents optimization

In the next step, the influence of $NaBH_4$ concentration was investigated in the following range, 0.10–1.50% (w/v). Each $NaBH_4$ solution were stabilized in 0.10% NaOH (v/v). HCl concentration was constant, 1.00 mol L^{-1}. Intensity counts were carried out for chosen

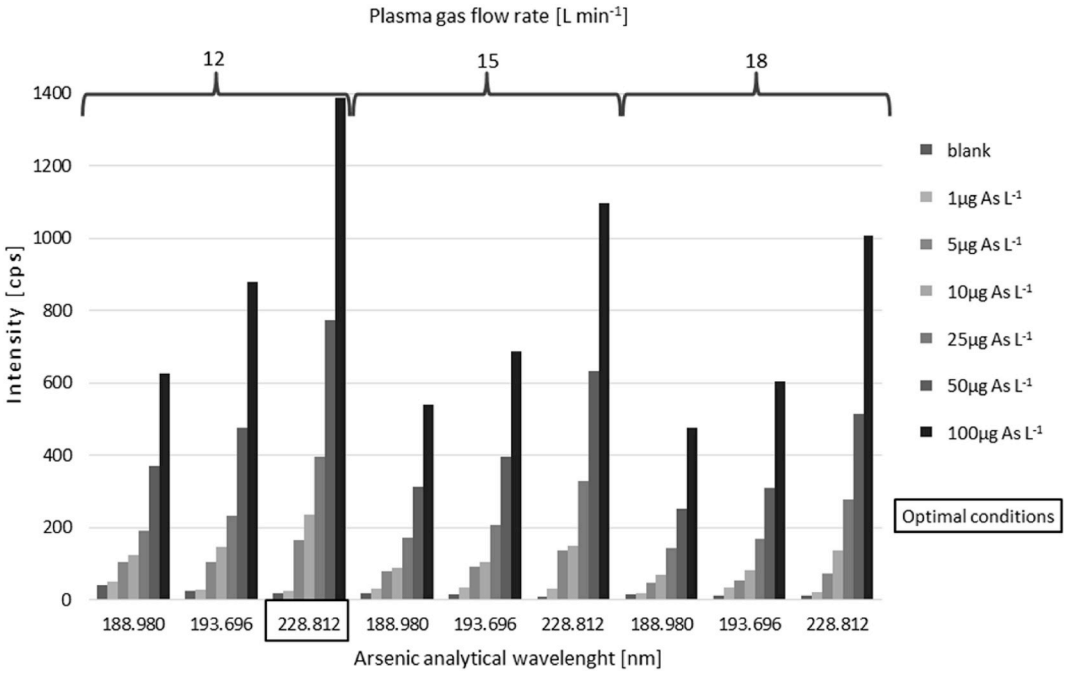

Fig. 2. The influence of plasma gas flow rate [L min^{-1}] on the analytical signal response (intensity) [cps] for HG (MSIS)–ICP–OES, 1.00% $NaBH_4$ (w/v), 1.00 mol L^{-1} HCl (optimal conditions in the frame).

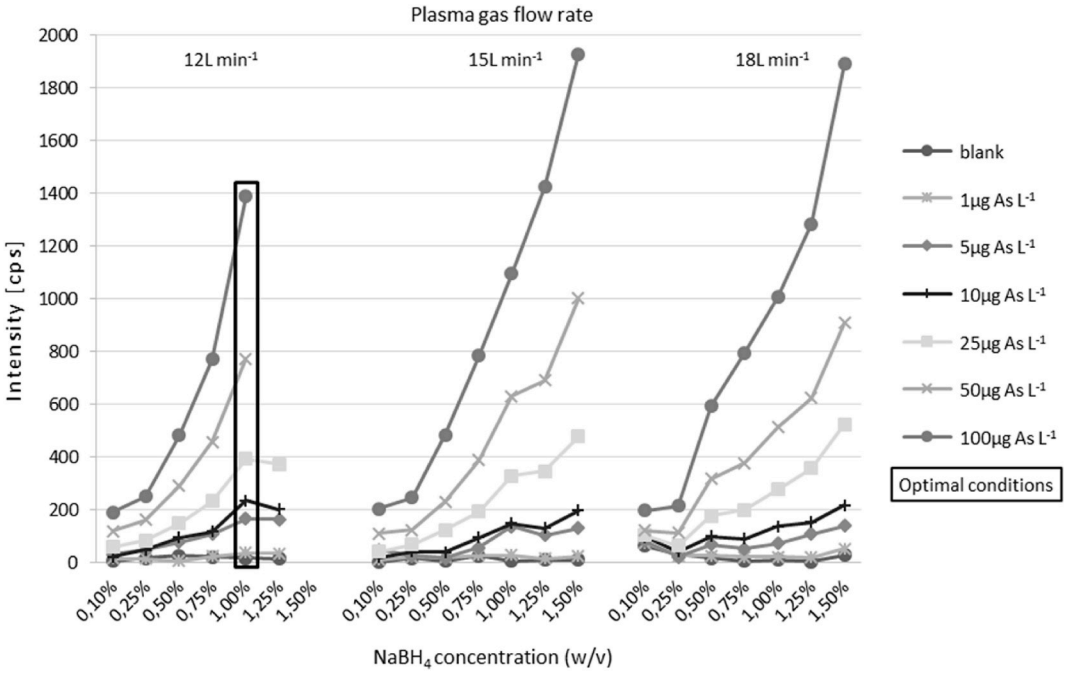

Fig. 3. The influence of $NaBH_4$ concentration [% w/v] and plasma gas flow rate [L min^{-1}] on the analytical signal response (intensity) [cps] for HG(MSIS)–ICP–OES, As I 228.812 nm and 1.00 mol L^{-1} HCl (optimal conditions in the frame).

analytical line wavelength, 228.812 nm. In the tested range, an increase of the analytical signal response was observed with the increase of the $NaBH_4$ concentration and the plasma gas flow rate. However, a decrease in the analytical signal response was noted for identical $NaBH_4$ concentrations as the plasma gas flow rate increased. Moreover, when the plasma gas flow rate were established at 12 L min^{-1}, the higher $NaBH_4$ concentrations, 1.25–1.50% (w/v), destabilized plasma due to a significant amount of free hydrogen in ICP torch. Due to this, these conditions were not carried out anymore and data were rejected According to above observations, the optimal $NaBH_4$ concentration was established at 1.00% (w/v). What is more, results of plasma flow rate optimization was confirmed and established at 12 L min^{-1}. Even 1.50% $NaBH_4$ with plasma gas flow rate set up at 15 L min^{-1} allowed to obtain better results, the selection of optimal conditions was dictated by a significant lower consumption of plasma gas. Complete results of the $NaBH_4$ concentration optimization are presented in Fig. 3.

In the last step, the influence of HCl concentration on analytical signal response was carried out in the range from 0.10 to 5.00 mol L^{-1}. Other parameters stayed constant and established due to previous observations, 1.00% $NaBH_4$ (w/v), 12 L min^{-1} of plasma gas flow rate and

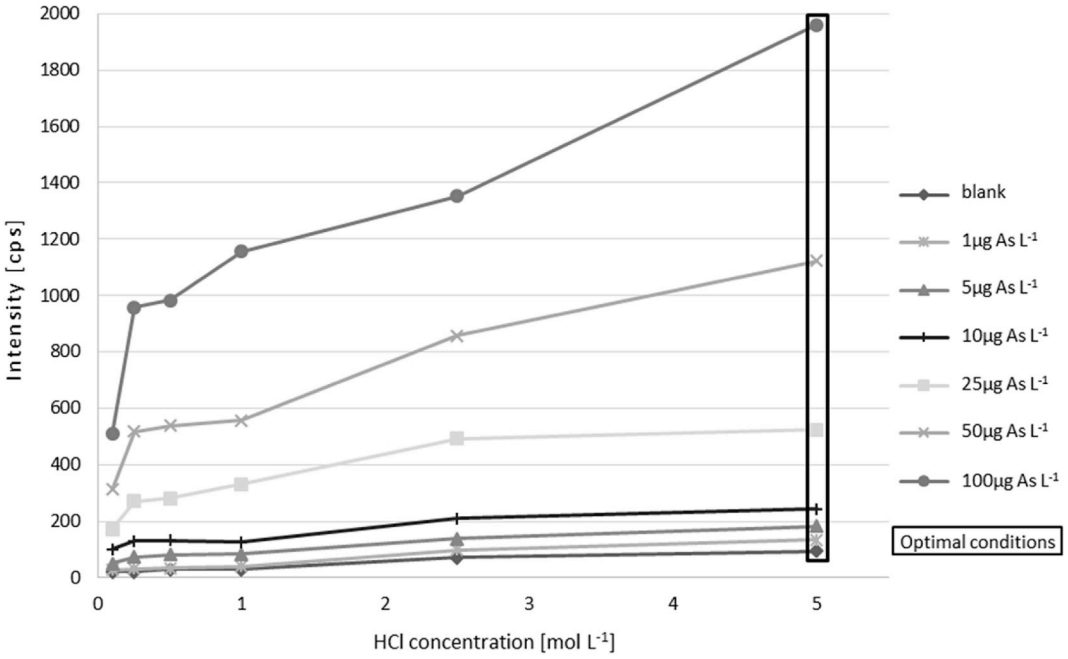

Fig. 4. The influence of HCl concentration [mol L^{-1}] on the analytical signal response (intensity) [cps] for HG(MSIS)–ICP–OES, As I 228.812 nm, 1.00% $NaBH_4$ (w/v) and plasma gas flow rate 12 L min^{-1} (optimal conditions in the frame).

analytical line wavelength, 228.812 nm. The continuous increase was observed in the whole investigated range. In the range from 1.00 to 10.0 µg L^{-1}, the slight increase of analytical signal response was noted as HCl concentration increased. In the range from 25.0 to 100 µg L⁻1, this increase of analytical signal response was more proportional to HCl concentration. Due to this observation and to achieve as low LOD as possible, 5.00 mol L^{-1} HCl was chosen as the optimal parameter (Fig. 4, in frame). The influence of HCl concentration on the analytical signal response is shown in Fig. 4.

3.3. HPLC optimization

The procedure of HPLC optimization was the same as Niedzielski 2005. Standard solutions contained 1000 µg L^{-1} of As(III), As(V) or DMA were carried out separately to define retention time [s] of each form, irrespective of investigated HPLC parameters.

Various authors have observed the influence of eluent concentration (sodium or potassium phosphates [19–21,24,25] on the retention time of arsenic species). In this work, the optimization of mobile phase concentration was performed: (as mmol L^{-1} phosphates (PO_4)) represented by a phosphate buffer. The mutual relation of disodium hydrophosphate and potassium dihydrophosphate were constant and fixed in the ratio of 1:10. Due to results obtained by Niedzielski 2005, the pH influence on retention time was not investigated and set at 6.0. The investigation was carried in the range of 11.0–55.0 mmol L^{-1} PO_4. Results were shown in Fig. 5, and the influence of mobile phase concentration was observed. The variability of retention time of As(III), DMA and As(V) was in the ranges, 100–120s, 175–200s, 260–355s, respectively. The highest variability of retention time was noted for As (V) form, approx. 55s.

The slight decrease of retention time of As(III), from 120s to 100s, was observed for 26.5 mmol L^{-1} PO_4. On the other hand, a different course of the curve showing retention time dependence on the eluent concentration was observed in case of As(V) and DMA. In the range 11.0–26.5 mmol L^{-1} PO_4, the significant increase of retention time from 260s to 355s was observed for As(V). On the other hand, the increase of retention time was noted in the range 26.5–55.0 mmol L^{-1} PO_4 (from 355s to 325s). In the case of DMA, changes of retention time are much smaller than As(V) and in the range 11.0–26.5 mmol L^{-1} PO_4, the slight increase was observed (from 190s to 200s). In the range 26.5–55.0 mmol L^{-1} PO_4, the slight decrease of retention time from 200s to 175s was observed and it is similar to As(V).

Investigated speciation forms of As(III), As(V) and DMA within mobile phase concentration values of 11.0–55.0 mmol L^{-1} PO_4 occurred separately in the eluent from the analytical column and did not overlay each other. In case of 11.0 mmol L^{-1} PO_4, peak areas of each arsenic species occurred close and the risk of overlay was high. Due to above observations, results for buffer concentrations below 11.0 mmol L^{-1} PO4 were rejected and further optimization of mobile phase were cancelled. In the case of 55.0 mmol L^{-1} PO_4, retention time differences were acceptable between As(V) and DMA but not acceptable between As(III) and DMA. Due to this, the optimal mobile phase concentration (Fig. 5, in the frame) was established at 26.5 mmol L^{-1} PO_4. In the case, retention time differences between arsenic species were at the maximum value, the risk of peaks area overlay was the least and peak areas had optimal shapes. Optimal experimental conditions ensured good peaks separation of three arsenic forms by considerably short analysis time, not exceeding 400s in case of determinations of environmental samples were accepted for a further analytical work. According to Niedzielski 2005, chromatographic column temperature changes in the range 10–80 °C entailed no significant retention time changes of the determined arsenic species [16]. And the investigation of the temperature influence were rejected.

The changes of retention time within longer time intervals (longer than a month) were observed during an analytical work. According to this, periodic controls were conducted with a single As form standard solutions to confirm respective retention times.

3.4. Analytical merit of figures

Retention time of As(III), As(V) and DMA species, was found at 100s, 355s and 200s respectively and it was determined depending on the optimal conditions of chromatographic separation and hydride generation (Table 1). Peak areas were proportional to the height in the whole investigated range. However, response of As(III) was three times more intensive than signals of As(V) and DMA at the same standard

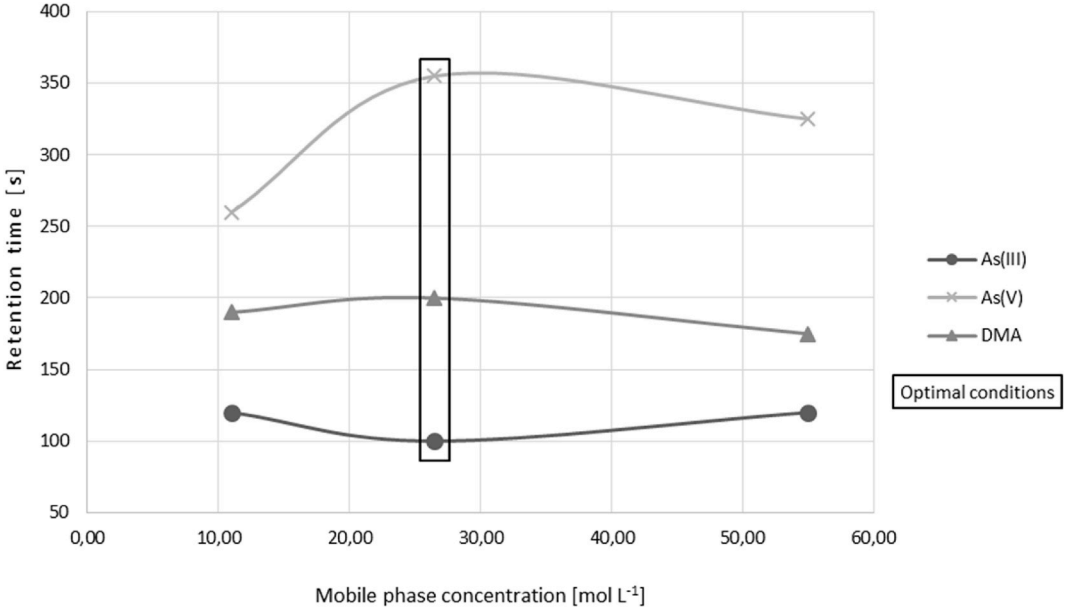

Fig. 5. The influence of mobile phase (phosphate buffer) concentration [mol L^{-1}] on retention time [s] of As(III), As(V) and DMA for HPLC/HG(MSIS)–ICP–OES, (optimal conditions in the frame).

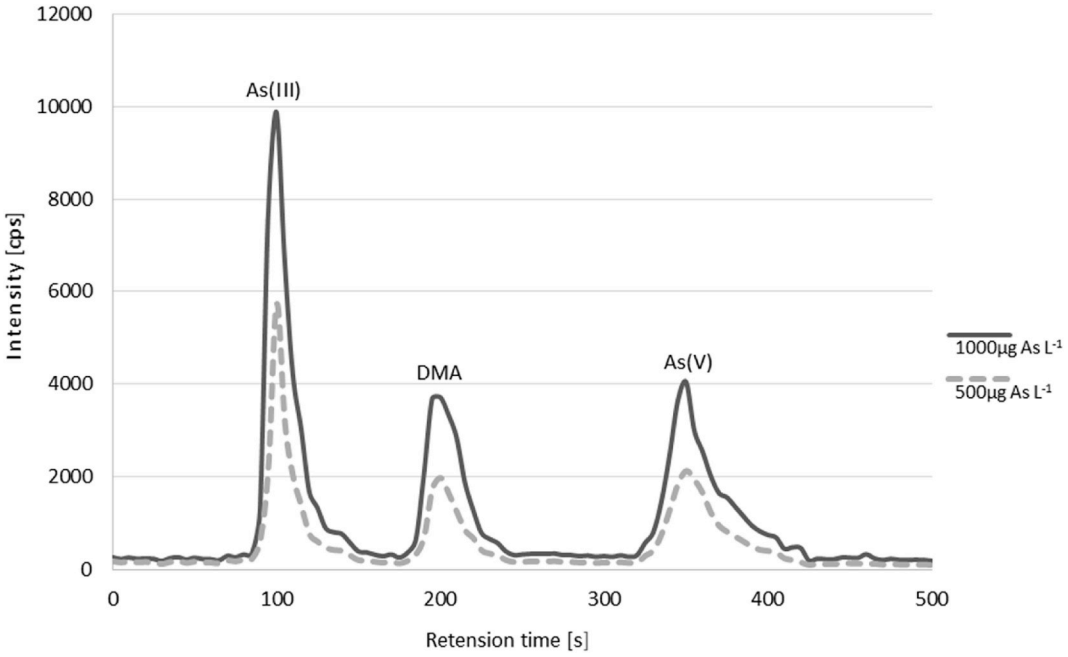

Fig. 6. Typical chromatograms presenting the separation of As species standard solutions obtained by HPLC/HG(MSIS)–ICP–OES in optimized conditions.

Table 2
Analytical figures of merit (n = 3, peak area).

	As(III)	As(V)	DMA
Retention time [s]	100	355	200
LOD (as 3σ) [µg L^{-1}]	2.08	6.97	6.15
LOQ (as 3 LOD) [µg L^{-1}]	6.23	20.9	18.5
Linear range of calibration curve [µg L^{-1}]	LOD–1000	LOD–1000	LOD–1000
Accuracy (as RSD at 100 µg L^{-1}) [%]	2.7	5.7	4.8

LOD– limit of detection; LOQ– limit of quantification; RSD – relative standard deviation.

solution. On the other hand, the similar signal disproportion of these arsenic species was observed in literature [26]. Furthermore, in a view of asymmetry and peaks shape variability (dispersion) only calculations of peak areas were used in samples determination. Single–element chromatograms gave an information about significant peak resolution between As(V) and DMA due to the analytical signal response came back to the background level. The critical problem of efficiently separation could be the overlay of peak areas of As(III) and DMA until applied mobile phase concentration minimalized this effect. Due to small possibilities of separation conditions changes e.g. mobile phase concentration, retention times of investigated species can be reduced by the modification of unit construction e.g. shortening the tubing. Typical chromatograms obtained with described method were shown in Fig. 6.

What is more, validation parameters describing the analytical method, were determined (Table 2). The obtained detection limits as well as the precision (measured as RSD) are comparable with the results in literature, also with the usage of different separation systems

[27,28]. Importantly, obtain LODs are much better in comparison with different in-chamber hydride generation systems, FBMN [20,21], dual nebulizer system [29,30] and MSIS [31]. Matusiewicz & Ślachciński 2010 obtained better LODs using integrated continuous–microflow ultrasonic nebulizer–hydride generator sample introduction system with microwave inducted plasma optical emission spectrometer as a detector (μ-USN–DCS-HG-MIP-OES) [9]. On the other hand, their technique contained self-made devices instead of the described system where each part of the hyphenated technique is commercially available. In addition, all of mentioned authors determined the sum of As species only. The higher LOD values obtained for As(V) and DMA come from both: the chromatographic system (dispersion effect) and signal ratio disproportion between each arsenic form (analytical signal response of As (III) was approx. three time higher). The signal disproportion could be connected with the influence of DMA on analytical signal response of inorganic As species which was reported before [32]. On the other hand, the usage of anion-exchange column before HG process minimalizes this effect what was reported before [14].

There is a certified reference material, ERM®–BC211, which allows to determine these arsenic species, although there is a lack of reference materials for arsenic species in samples extracted by phosphoric acid [33]. Therefore, the standard addition method was used to traceability measurements and arsenic standard solutions were added to the final extracts volume of three different real samples. Final concentrations of standards in samples solution were 100 μg As L^{-1} and 500 μg As L^{-1}. Recovery from each of investigated forms (n = 3) of three samples (P1, P2, P3) was determined (Table 3). Recovery was high and acceptable and ranged: 95–106% for the lower concentration of 100 μg As L^{-1} and 98–104% for the higher concentration of 500 μg As L^{-1} (Table 3). According to results of the method validation, the hyphenated technique was applied to determine of As(III), As(V) and DMA in food and environmental samples.

3.5. Application

The developed method of simultaneous determination of three arsenic species within a single analysis was used in environmental and food samples analyses. There were three groups of samples: soil samples located in the proximity of industry wastes disposal site, 2 years old common oaks (Quercus robur) growing in hydroponic experiments with Knop solution enriched with arsenic forms and yerba mate (Ilex paraguariensis) available on the Polish market.

The first group of environmental samples appeared soil samples (n = 3) located in the proximity of industry wastes disposal site were investigated. Assuming a very high contamination level of inorganic arsenic forms, samples were diluted respectively. Results, shown in Table 4, confirmed the thesis about high level of arsenic contamination and contents of inorganic arsenic forms was presented as mg As kg^{-1} instead of other samples in this paper. The high content of As(V) was detected in each soil sample and a substantial domination of this form was observed (4960–5,920 mg kg^{-1}). Obtained results are similar to [34] (above 4,000 mg kg^{-1}) and [35] (4,530 mg kg^{-1}) or significant higher in comparison with [36] (1,725 mg kg^{-1}) and [37] (2,500 mg kg^{-1}), although some author presented substantial higher total arsenic contents [39,40]. The ratio between contents of As(V) and As(III) is in the range from 450 (sample II) to 713 (sample I). What is more, the slight content of As(III) was found (8–13 mg kg^{-1}) instead of DMA which was not detected. Results suggest that As(V) is more preferred in soil samples located in the proximity of industry wastes disposal site what was confirmed in literature [34,36].

Table 4
The content of As(III), DMA and As(V) with the ratio of As(V) and As(III) in soil samples located in the proximity of industry wastes disposal site (peak area), [mg kg^{-1}].

Sample	As(III)	DMA	As(V)	As(V)/As(III)
I	8.0	< LOD	5700	713
II	11	< LOD	4960	450
III	13	< LOD	5920	455

< LOD– below limit of detection.

The second group of environmental samples were parts of 2 years old common oaks (Quercus robur) (n = 6), which were grown in hydroponic experiments with Knop solution enriched with one of determined As forms (As enriched). Results were shown in Table 5. As (III), DMA and As(V) were not detected in leaves (sample B) or sprouts growing on solution enriched with As(V) and DMA (sample D and E respectively). Moreover, arsenic species were not detected together. On the other hand, a dominant content of organic arsenic species was detected in Quercus robur by Budzyńska et al., 2019. Due to this, undetectable arsenic species such as As(III), DMA and As(V) do not equal its absence in these trees [40]. In the case of sprout growing on solution enriched with As(V) (sample D), arsenic species were not detected what confirmed the accumulation and translocation of As(V) [41]. As(V) was only found in root growing on solution enriched with DMA (sample F). The highest content of As(III) was detected in sprout growing in Knop solution enriched with As(III) (sample C) and this species was the only detected. Furthermore, DMA and As(III) were found in leaves growing in Knop solution enriched with DMA (sample A). The dominance of DMA may suggest a direction of probable arsenic metabolism path of 2 years old common oak (Quercus robur) growing in hydroponic experiments with Knop solution enriched with arsenic forms. Results confirmed mechanism to cope inorganic arsenic excess in plants [42] (see Table 6).

The last group appeared food samples representing by yerba mate (Ilex paraguariensis) samples (n = 6), available on the Polish market. The content of investigated arsenic species was identical for each sample, As(III) < DMA ≤ As(V). Additionally, the sum of separated species were counted (As total) due to a detection of these species in all of six samples. The sum of arsenic content (As total) was in the range

Table 3
Recovery of arsenic species at the addition of standard solution (n = 3, peak area).

Sample	As(III)			DMA			As(V)		
	Added [μg L^{-1}]	Found [μg L^{-1}]	Recovery [%]	Added [μg L^{-1}]	Found [μg L^{-1}]	Recovery [%]	Added [μg L^{-1}]	Found [μg L^{-1}]	Recovery [%]
P1	0	< LOQ	–	0	< LOD	–	0	< LOQ	–
	100	105 ± 3	105 ± 3	100	95 ± 11	95 ± 11	100	101 ± 8	101 ± 8
	500	509 ± 3	102 ± 1	500	514 ± 11	103 ± 2	500	500 ± 8	100 ± 2
P2	0	< LOQ	–	0	< LOD	–	0	< LOD	–
	100	104 ± 3	104 ± 3	100	101 ± 11	101 ± 11	100	95 ± 8	95 ± 8
	500	515 ± 3	103 ± 1	500	490 ± 11	98 ± 2	500	491 ± 8	98 ± 2
P3	0	< LOQ	–	0	< LOD	–	0	< LOQ	–
	100	106 ± 3	106 ± 3	100	97 ± 11	97 ± 11	100	99 ± 8	99 ± 8
	500	519 ± 3	104 ± 1	500	499 ± 11	100 ± 2	500	491 ± 8	98 ± 2

LOD– limit of detection, LOQ– limit of quantification.

Table 5
The content of As(III), DMA and As(V) in part of 2 years old common oaks (*Quercus robur*) (peak area), [μg kg^{-1}].

Sample	Part	As enriched	As(III)	DMA	As(V)
A	Leaf	DMA	27	266	< LOD
B	Leaf	DMA	< LOD	< LOD	< LOD
C	Sprout	As(III)	44	< LOD	< LOD
D	Sprout	As(V)	< LOD	< LOD	< LOD
E	Sprout	DMA	< LOD	< LOD	< LOD
F	Root	DMA	< LOD	750	197

< LOD– below limit of detection.

Table 6
The content of As(III), DMA and As(V) and As total in yerba mate (*Ilex paraguariensis*) (peak area), [μg kg^{-1}].

Sample	As(III)	DMA	As(V)	As total
1	26	61	94	181
2	12	51	51	114
3	17	34	46	97
4	31	93	103	227
5	32	97	108	237
6	20	44	66	130

As total – the sum of As(III), DMA and As(V).

from 97 (sample 2) to 237 μg kg^{-1} (sample 5). Moreover, sample 5 contained the maximum values of As total and arsenic species. A domination of As(V) was observed in samples and the content was not higher than 108 μg kg^{-1} (sample 5). On the other hand, the content of As(III) was found as the lowest in all samples (12–32 μg kg^{-1}). Moreover, the DMA content was in the range from 34 (sample 3) to 97 μg kg^{-1} (sample 5). It is worth noting that results are interesting in comparison with literature. Presented results are 4 times [43] or 3 times higher [44], according to mean concentration. On the other hand, sample preparation procedure influences significantly on arsenic content in sample extracts what was confirmed experimentally by Wełna et al. 2015 during investigation of coffee products [45]. Significant contents of each arsenic species suggest that bushes of Ilex paraguariensis grew on soil contaminated with arsenic [43]. What is more, the higher content of arsenic species can occur if fertilizer, herbicide, pesticide and fungicide are used in yerba mate plantation [44]. It is surprising that LOD, obtained with ICP-MS by Marcelo et al., 2014, is higher (21 μg kg^{-1}) [44] than LODs of arsenic species in this work. It is worth mentioning that the determination of arsenic species in yerba mate (Ilex paraguariensis) is a novel and no authors did it before.

4. Conclusions

The usage of MSIS, as a hydride generator and a connecter between high performance liquid chromatography and inductively coupled plasma optical emission spectrometry, allows to perform simultaneous determinations of three speciation forms of arsenic: As(III), As(V) and DMA. The proposed function of MSIS was confirmed during the work. The presented results shown that MSIS can be applied between chromatography and spectrometry techniques and the unit is able to be applied as a connecter in different hyphenated systems in further perspective. The presented work confirmed suppositions that optimization of separation and hydride generation parameters have to be extensive and every single parameter e.g. reagents and mobile phase concentration affects significantly on obtained results.

Considerably low LODs, especially As(III), make the described method a useful analytical tool in simultaneous determination of three arsenic species within a single analysis. Moreover, low RSD values and acceptable recovery confirm its propriety. The system is more suitable and flexible for an expansion and an improvement than a commercial available hyphenated systems. What is more, this system is less expensive in purchase and maintain when it is compared with commercial available device, HPLC/ICP–MS. Obtained LODs and LOQ of these arsenic species are better in comparison with different systems based on the MSIS unit and different in-chamber hydride generation systems i.e. FBMN, dual nebulizer system. It allows to compare results from HPLC/HG–ICP–OES with different hyphenated techniques in optical emission systems. In the case of yerba mate (Ilex paraguariensis) samples, LODs were slight better in comparison with ICP–MS. What is more, the content of arsenic species in these samples was presented the first time and further studies seem to be interesting in this field.

The described application allows to conduct the direct investigation of environmental and food samples, which could be exposed on arsenic contamination. Results are good perspective for further studies including a separation of different volatile hydride forming elements e.g. selenium, antimony and the dual–mode application for a separation and a determination of non–hydride forming elements.

Acknowledgments

The work was supported by grant no. POWR.03.02.00–00–I026/16 co–financed by the European Union through the European Social Fund under the Operational Program Knowledge Education Development.

References

[1] W. Holak, Gas-sampling technique for arsenic determination by atomic absorption spectrophotometry, Anal. Chem. 41 (12) (1969) 1712–1713, https://doi.org/10.1021/ac60281a025.
[2] H. Brandenberger, H. Bader, Determination of nanograms levels of mercury in solution by a flameless atomic absorption technique, At. Absorpt. Newsl. 6 (5) (1967) 101.
[3] Z. Long, C. Chen, X. Hou, C. Zheng, Recent advance of hydride generation–analytical atomic spectrometry: Part II—analysis of real samples, Appl. Spectrosc. Rev. 47 (7) (2012) 495–517, https://doi.org/10.1080/05704928.2012.666776.
[4] C. Ericzon, J. Pettersson, M. Andersson, A. Olin, Determination and speciation of selenium in end products from a garbage incinerator, Environ. Sci. Technol. 23 (12) (1989) 1524–1528, https://doi.org/10.1021/es00070a012.
[5] A. Asfaw, G. Wibetoe, Dual mode sample introduction for multi-element determination by ICP-MS: the optimization and use of a method based on simultaneous introduction of vapor formed by NaBH4 reaction and aerosol from the nebulizer, J Anal At Spectrom 21 (10) (2006) 1027, https://doi.org/10.1039/b604116g.
[6] I. Rojas, M. Murillo, N. Carrión, J. Chirinos, Investigation of the direct hydride generation nebulizer for the determination of arsenic, antimony and selenium in inductively coupled plasma optical emission spectrometry, Anal. Bioanal. Chem. 376 (1) (2003) 110–117, https://doi.org/10.1007/s00216-003-1856-7.
[7] A. Asfaw, D. Beauchemin, Combination of a multimode sample introduction system with a pre-evaporation tube to improve multi-element analysis by ICP-OES, J Anal At Spectrom 27 (1) (2012) 80–91, https://doi.org/10.1039/c1ja10224a.
[8] H. Matusiewicz, M. Ślachciński, Simultaneous determination of hydride forming elements (As, Sb, Se, Sn) and Hg in sonicate slurries of biological and environmental reference materials by hydride generation microwave induced plasma optical emission spectrometry (SS-HG-MIP-OES), Microchem. J. 82 (1) (2006) 78–85, https://doi.org/10.1016/j.microc.2005.08.001.
[9] H. Matusiewicz, M. Ślachciński, Method development for simultaneous multi-element determination of hydride forming elements (As, Bi, Ge, Sb, Se, Sn) and Hg by microwave induced plasma-optical emission spectrometry using integrated continuous-microflow ultrasonic nebulizer-hydride generator sample introduction system, Microchem. J. 95 (2) (2010) 213–221, https://doi.org/10.1016/j.microc.2009.12.004.
[10] C. Tanabe, H. Hopfer, G. Gilleland, A. Liba, S. Ebeler, J. Nelson, Total arsenic analysis in Californian wines with hydride generation – microwave plasma – atomic emission spectroscopy (HG-MP-AES), J Anal At Spectrom 31 (6) (2016) 1223–1227, https://doi.org/10.1039/c6ja00051g.
[11] I. Mikheev, E. Karpukhina, L. Usol'tseva, T. Samarina, D. Volkov, M. Proskurnin, Application of microwave plasma atomic emission spectrometry and hydride generation for determination of arsenic and selenium in mineral water, Inorg. Mater. 53 (14) (2017) 1422–1426, https://doi.org/10.1134/s0020168517140126.
[12] R. Machado, C. Amaral, J. Nóbrega, A. Araujo Nogueira, Multielemental determination of as, Bi, Ge, Sb, and Sn in agricultural samples using hydride generation coupled to microwave-induced plasma optical emission spectrometry, J. Agric. Food Chem. 65 (23) (2017) 4839–4842, https://doi.org/10.1021/acs.jafc.7b01448.
[13] M. Welna, A. Szymczycha-Madeja, P. Pohl, Critical evaluation of strategies for single and simultaneous determinations of As, Bi, Sb and Se by hydride generation inductively coupled plasma optical emission spectrometry, Talanta 167 (2017) 217–226, https://doi.org/10.1016/j.talanta.2017.01.029.
[14] M. Welna, P. Pohl, Potential of the hydride generation technique coupled to

inductively coupled plasma optical emission spectrometry for non-chromatographic as speciation, J Anal At Spectrom 32 (9) (2017) 1766–1779, https://doi.org/10.1039/c7ja00107j.
[15] P. Cava-Montesinos, K. Nilles, M. Cervera, M. Guardia, Non-chromatographic speciation of toxic arsenic in fish, Talanta 66 (4) (2005) 895–901, https://doi.org/10.1016/j.talanta.2004.12.042.
[16] P. Niedzielski, The new concept of hyphenated analytical system: simultaneous determination of inorganic arsenic(III), arsenic(V), selenium(IV) and selenium(VI) by high performance liquid chromatography–hydride generation–(fast sequential) atomic absorption spectrometry during single analysis, Anal. Chim. Acta 551 (1–2) (2005) 199–206, https://doi.org/10.1016/j.aca.2005.06.073.
[17] P. Niedzielski, M. Rudnicka, M. Wachelka, et al., Selenium species in selenium fortified dietary supplements, Food Chem. 190 (2016) 454–459, https://doi.org/10.1016/j.foodchem.2015.05.125.
[18] B. Deng, X. Xu, Y. Xiao, P. Zhu, Y. Wang, Response to “Comment on understanding the effects of potassium ferricyanide on lead hydride formation in tetrahydroborate system and its application of lead in milk using hydride generation inductively coupled plasma optical emission spectrometry” by Alessandro D'Ulivo, Anal. Chim. Acta 884 (2015) 28, https://doi.org/10.1016/j.aca.2015.04.004.
[19] V. dos Santos, M. Grassi, G. Abate, Speciation of antimony(III) and antimony(V) in bottled water by hydride generation-inductively coupled plasma optical emission spectrometry, Anal. Lett. 48 (18) (2015) 2921–2935, https://doi.org/10.1080/00032719.2015.1052971.
[20] M. García, M. Aguirre, A. Canals, Determination of As, Se, and Hg in fuel samples by in-chamber chemical vapor generation ICP OES using a Flow Blurring® multinebulizer, Anal. Bioanal. Chem. 409 (23) (2017) 5481–5490, https://doi.org/10.1007/s00216-017-0484-6.
[21] C. Pereira, M. Aguirre, J. Nóbrega, M. Hidalgo, A. Canals, Aerosol generation of as and Se hydrides using a new Flow Blurring® multiple nebulizer for sample introduction in inductively coupled plasma optical emission spectrometry, Microchem. J. 112 (2014) 82–86, https://doi.org/10.1016/j.microc.2013.09.006.
[22] E. Barrientos, K. Wrobel, J. Torres Guzman, A. Corrales Escobosa, K. Wrobel, Determination of SeMet and Se(iv) in biofortified yeast by ion-pair reversed phase liquid chromatography-hydride generation-microwave induced nitrogen plasma atomic emission spectrometry (HPLC-HG-MP-AES), J Anal At Spectrom 31 (1) (2016) 203–211, https://doi.org/10.1039/c5ja00276a.
[23] P. Niedzielski, M. Mleczek, Z. Magdziak, M. Siwulski, L. Kozak, Selected arsenic species: as(III), As(V) and dimethylarsenic acid (DMAA) in Xerocomus badius fruiting bodies, Food Chem. 141 (4) (2013) 3571–3577, https://doi.org/10.1016/j.foodchem.2013.06.103.
[24] J. Stummeyer, B. Harazim, T. Wippermann, Speciation of arsenic in water samples by high-performance liquid chromatography-hydride generation-atomic absorption spectrometry at trace levels using a post-column reaction system, Anal. Bioanal. Chem. 354 (3) (1996) 344–351, https://doi.org/10.1007/s0021663540344.
[25] M. Villa-Lojo, Coupled high performance liquid chromatography–microwave digestion–hydride generation–atomic absorption spectrometry for inorganic and organic arsenic speciation in fish tissue, Talanta 57 (4) (2002) 741–750, https://doi.org/10.1016/s0039-9140(02)00094-2.
[26] D. Zhang, S. Yang, H. Cheng, Y. Wang, J. Liu, Speciation of inorganic and organic species of mercury and arsenic in lotus root using high performance liquid chromatography with inductively coupled plasma mass spectrometric detection in one run, Talanta 199 (2019) 620–627, https://doi.org/10.1016/j.talanta.2019.03.023.
[27] M. Amran, F. Lagarde, M. Leroy, Determination of arsenic species in marine organisms by HPLC-ICP-OES and HPLC-HG-QFAAS, Mikrochim. Acta 127 (3–4) (1997) 195–202, https://doi.org/10.1007/bf01242722.
[28] J. Gómez-Ariza, F. Lorenzo, T. García-Barrera, D. Sánchez-Rodas, Analytical approach for routine methylmercury determination in seafood using gas chromatography-atomic fluorescence spectrometry, Anal. Chim. Acta 511 (1) (2004) 165–173, https://doi.org/10.1016/j.aca.2004.01.051.
[29] L. Gómez, G. Márquez, J. Chirinos, Dual nebulizer sample introduction system for simultaneous determination of volatile elemental hydrides and other elements, Anal. Bioanal. Chem. 386 (1) (2006) 188–195, https://doi.org/10.1007/s00216-006-0578-z.
[30] D. Maldonado, J. Chirinos, Z. Benzo, C. Gómez, E. Marcano, Analytical evaluation of a dual micronebulizer sample introduction system for inductively coupled plasma spectrometry, J Anal At Spectrom 21 (8) (2006) 743–749, https://doi.org/10.1039/b604044f.
[31] H. Wiltsche, I. Brenner, K. Prattes, G. Knapp, Characterization of a multimode sample introduction system (MSIS) for multielement analysis of trace elements in high alloy steels and nickel alloys using axially viewed hydride generation ICP-AES, J Anal At Spectrom 23 (9) (2008) 1253, https://doi.org/10.1039/b803943g.
[32] S. Musil, Á. Pétursdóttir, A. Raab, H. Gunnlaugsdóttir, E. Krupp, J. Feldmann, Speciation without chromatography using selective hydride generation: inorganic arsenic in rice and samples of marine origin, Anal. Chem. 86 (2) (2014) 993–999, https://doi.org/10.1021/ac403438c.
[33] S. Budzyńska, Z. Magdziak, P. Goliński, P. Niedzielski, M. Mleczek, Arsenic forms in phytoextraction of this metalloid in organs of 2-year-old Acer platanoides seedlings, Environ. Sci. Pollut. Control Ser. 25 (27) (2018) 27260–27273, https://doi.org/10.1007/s11356-018-2739-y.
[34] G. Camm, H. Glass, D. Bryce, A. Butcher, Characterisation of a mining-related arsenic-contaminated site, Cornwall, UK, J. Geochem. Explor. 82 (1–3) (2004) 1–15, https://doi.org/10.1016/j.gexplo.2004.01.004.
[35] M. Casado, H. Anawar, A. Garcia-Sanchez, I. Regina, Arsenic bioavailability in polluted mining soils and uptake by tolerant plants (El Cabaco mine, Spain), Bull. Environ. Contam. Toxicol. 79 (1) (2007) 29–35, https://doi.org/10.1007/s00128-007-9214-7.
[36] T. Frentiu, M. Ponta, E. Levei, E. Cordos, Study of partitioning and dynamics of metals in contaminated soil using modified four-step BCR sequential extraction procedure, Chem. Pap. 63 (2) (2009), https://doi.org/10.2478/s11696-008-0102-3.
[37] M. Jung, I. Thornton, H. Chon, Arsenic, Sb and Bi contamination of soils, plants, waters and sediments in the vicinity of the Dalsung Cu–W mine in Korea, Sci. Total Environ. 295 (1–3) (2002) 81–89, https://doi.org/10.1016/s0048-9697(02)00042-6.
[39] P. Visoottiviseth, K. Francesconi, W. Sridokchan, The potential of Thai indigenous plant species for the phytoremediation of arsenic contaminated land, Environ. Pollut. 118 (3) (2002) 453–461, https://doi.org/10.1016/s0269-7491(01)00293-7.
[40] S. Budzyńska, P. Mleczek, M. Szostek, et al., Phytoextraction of arsenic forms in selected tree species growing in As-polluted mining sludge, J. Environ. Sci. Health, Part A. (2019) 1–10, https://doi.org/10.1080/10934529.2019.1609322.
[41] S. Budzyńska, M. Krzesłowska, P. Niedzielski, P. Goliński, M. Mleczek, Arsenate phytoextraction abilities of one-year-old tree species and its effects on the nutritional element content in plant organs, Int. J. Phytoremediation (2019) 1–13, https://doi.org/10.1080/15226514.2019.1594684.
[42] N. Verbruggen, C. Hermans, H. Schat, Mechanisms to cope with arsenic or cadmium excess in plants, Curr. Opin. Plant Biol. 12 (3) (2009) 364–372, https://doi.org/10.1016/j.pbi.2009.05.001.
[43] R. Pardinho, P. Dalla Vecchia, A. Mendes, C. Bizzi, P. Mello, F. Duarte, E. Flores, Determination of toxic elements in yerba mate by ICP-MS after diluted acid digestion under O2 pressure, Food Chem. 263 (2018) 37–41, https://doi.org/10.1016/j.foodchem.2018.04.112.
[44] M. Marcelo, C. Martins, D. Pozebon, V. Dressler, M. Ferrão, Classification of yerba mate (Ilex paraguariensis) according to the country of origin based on element concentrations, Microchem. J. 117 (2014) 164–171, https://doi.org/10.1016/j.microc.2014.06.027.
[45] M. Welna, A. Szymczycha-Madeja, P. Pohl, Improvement of determination of trace amounts of arsenic and selenium in slim coffee products by HG-ICP-OES, Food Anal Methods 7 (5) (2013) 1016–1023, https://doi.org/10.1007/s12161-013-9707-4.

Talanta 231 (2021) 122403

Contents lists available at ScienceDirect

Talanta

journal homepage: www.elsevier.com/locate/talanta

Iron species determination by high performance liquid chromatography with plasma based optical emission detectors: HPLC–MIP OES and HPLC–ICP OES

Jędrzej Proch, Przemysław Niedzielski *

Adam Mickiewicz University, Faculty of Chemistry, Department of Analytical Chemistry, Uniwersytetu Poznańskiego 8, 61–614, Poznań, Poland

ARTICLE INFO

Keywords:
Hyphenated techniques
HPLC–MIP OES
HPLC–ICP OES
Iron speciation
Method evaluation

ABSTRACT

The paper presents an independent application of two hyphenated techniques, wherein an identical chromatographic system i.e. high performance liquid chromatography (HPLC) was coupled to microwave induced plasma optical emission spectrometry (MIP OES) or inductively coupled plasma optical emission spectrometry (ICP OES). A cation–exchange column and a mobile phase based on pyridine–2,6–dicarboxylic acid (PDCA) were employed to separate Fe(II) and Fe(III) within 300 s. Additionally, two methods of sample preparation were employed. Optimization and validation of both methods were conducted parallel. The applicability was presented with different sample matrix types: post–glacial sediments, archaeological pottery, soils located in the proximity of industry wastes disposal site, river sediments and yerba mate *(Ilex paraguariensis)*. Obtained results were compared in terms of the excitation source (microwave induced or inductively coupled) and supplied gas (nitrogen or argon). The research introduces HPLC–MIP OES for iron speciation analysis and its applicability were critically evaluated with HPLC–ICP OES.

1. Introduction

Iron is the fourth most abundant element in the Earth's crust and two main species, Fe(II) and Fe(III), are thermodynamically stable and kinetically reactive. Living organisms continuously require interconversion of molecules at specific moments in reactions where neither inert nor very unstable metallic species would be adequate substitutes [1]. Moreover, iron cycling was observed in the environment e.g. salt–marsh sediments [2] or dam water [3]. On one hand, iron speciation analysis should be one of the major challenges in environmental analytical chemistry. On the other hand, in comparison to metalloids (e.g. As, Sb, Se) and other metals (e.g. Al, Cr, Hg), a lack of new methods for fast simultaneous determination of Fe species is surprising, especially in the area of commercialized hyphenated techniques as HPLC–ICP MS [4–6].

Simultaneous separation and determination of element species plays an important role in modern analytical chemistry. In the case of iron species separation, the composition of mobile phase (eluent) seems to be crucial. Pyridine–2,6–dicarboxylic acid (PDCA), as a mobile phase component for a separation of transition metals, was described in 1995 with the comparison of two mixed–bed resin columns [7]. Possibility of Fe(II) and Fe(III) separation, with the mixture of PDCA and acetic acid, using mixed–bed resin column, Dionex IonPac CS5A (Thermo Fisher Scientific, USA) was presented later [8]. In turn, Cardellicchio et al. firstly applied the eluent, containing PDCA, formic acid, potassium hydroxide and potassium sulfate, which was able to separate eight metals, including Fe(II) and Fe(III) within 20 min in industrial waste water [9]. In the following years, related systems were developed for iron species separation [10–14]. Moreover, other components were investigated with PDCA as a mobile phase, usually with the introduction of new detectors for HPLC or IC [15–17]. Unfortunately, all above methods with dedicated detectors for HPLC or IC systems e.g. require a usage of additional post–column reagents such as 4–(2–pyridylazo)resorcinol (PAR) [7–15] and luminol [16,17] to obtain or to increase the analytical signal. The most desirable way is to introduce the post–column solution directly to the detector.

The development and higher accessibility of inductively coupled plasma optical emission spectrometry (ICP OES) or microwave induced plasma optical emission spectrometry (MIP OES) gave new possibilities of analyses. Greenfield et al. [18] reported independently with Wendt and Fassel [19], the first applications of ICPs. Since then, ICP OES was being developed as a method for multielement analysis of liquids and

* Corresponding author.
E-mail address: pnied@amu.edu.pl (P. Niedzielski).

https://doi.org/10.1016/j.talanta.2021.122403
Received 16 February 2021; Received in revised form 30 March 2021; Accepted 3 April 2021
Available online 9 April 2021

commercial devices appeared on the market in early 1970s [20]. Nowadays (2020), despite worse limits of detection (LODs) and quantification (LOQs), in comparison with inductively coupled plasma mass spectrometry (ICP MS), ICP OES could be its profitable alternative (less apparatus costs, lower reagents consumption, less interferences etc.) [21]. MIPs have evolved as atomization and excitation sources that could potentially be used as alternatives to ICPs in OES [22]. It was described in 1951 by Cobine and Wilbur [23]. In turn, the first use of MIP as excitation source for OES was reported in 1965 [24]. Despite ICP, MIPs can be operated with different working gases (helium, argon, nitrogen) and its consumption can be lower [25]. The first commercially available MIP OES, which uses nitrogen as the working gas, was released in serial production in 2012 and its analytical capabilities have being evaluated in the following years [26]. Nevertheless, neither ICP OES nor MIP OES are able to directly determine of any element species.

This problem can be solved by coupling and application of two (and more) techniques e.g. chromatography (HPLC or IC) and spectrometry (MS or OES) as the hyphenated system. In the case of HPLC or IC coupled to MIP OES, no hyphenated technique has been developed for iron speciation analysis yet. However, there are significant application of MIP OES to determine Fe total content in slurry samples [27], geological samples [28], fishes [29] and beer [30]. In the case of ICP OES, there are few systems to simultaneously determine Fe(II) and Fe(III) in rat brain extracts by IC–ICP OES [31]. However, the method was applied for specific material only (rat brain extracts). Therefore quantification range of this system was slightly narrow. It is worth mentioning that Solovyev et al. was presented an interesting method for Fe, Cu and Mn species determination in cerebrospinal fluid [32]. Moreover, Wolle et al. developed the method for redox speciation analysis of iron [33]. However, there were examples of HPLC–ICP MS and applications were narrowed down to biological samples [32] or aqueous standard solutions [33]. Summarizing the above, there is a gap in Fe species determination which can be filled by HPLC coupled to OES detectors (both MIP and ICP).

On one hand, the iron speciation in biological and clinical samples attracts much attention, where mainly iron contained biomolecules are target (transferrin, myoglobin etc.) [34]. On the other hand, mass spectrometry (MS) is preferred as a chromatographic detector considering the low concentrations of iron species. Assuming high Fe concentrations in samples (soils, sediments, pottery etc.), MS becomes an overly demanding chromatographic detector (requiring hundred– or thousand–fold dilution) [35]. Moreover, over–dilution adversely affects the limits of quantification, repeatability and precision of the results. MIP OES and ICP OES are more resistant to low pH and high concentrations of elements in comparison to ICP–MS. Summarizing all above, with all due respect to MS advantages, determination of iron species in environmental samples is more appropriate by coupling HPLC and OES.

In this study, the optimization of two hyphenated techniques, HPLC coupled with nitrogen plasma MIP OES and ICP OES, were conducted parallel. A cation–exchange column and PCDA eluent were employed to separate and determine Fe(II) and Fe(III) simultaneously with the additional post–column agents avoiding. Wide method applicability was performed with real samples of post–glacial sediments (Spitsbergen, Svalbard), archaeological pottery, soil samples located in the proximity of industry wastes disposal site, river sediments (Mekong, Vietnam) and yerba mate *(Ilex paraguariensis)*. Obtained parameters by HPLC–MIP OES and HPLC–ICP OES, i.e. analytical figures of merit (e.g. LODs, accuracy), standard addition recovery and contents of iron species were compared and critically evaluated. The novel is the introduction of HPLC–MIP OES as a complementary analytical tool for HPLC–ICP OES in iron speciation analyses.

2. Materials and methods

2.1. Gases and reagents

Pure nitrogen (purity >99.5%), produced using pressure swing absorption technology by on–line nitrogen generator ZEFIRO MP (CINEL S. r.l. Gas Generators Technology), was employed as a working gas for HPLC–MIP OES. High–pure argon (N–5.0, purity 99.999%), obtained from Linde (Poland), was employed as a working gas for HPLC–ICP OES. All reagents were diluted by high–pure deionized water (≥18 MΩ cm resistivity) obtained from a Milli–Q water purification system (Millipore, USA). Ferrous ammonium sulfate hexahydrate and ferric ammonium sulfate dodecahydrate were obtained from Acros Organics (USA). Stock standard solutions (1000 mg L^{-1} in a single solution) were prepared by dissolving appropriate amounts powder in water. Less concentrated standard solutions obtained by a dilution of the stock solutions were prepared daily. Stock standard solutions were stored in glass bottles at 4 °C in darkness.

A PDCA eluent was prepared by mixing appropriate volumes of pyridine–2,6–dicarboxylic acid (PDCA) and formic acid (HCOOH) (Sigma–Aldrich, USA), then appropriate amounts of potassium hydroxide (KOH) and potassium sulfate (K_2SO_4) (Merck, Germany) were dissolved and the solution was filled up with deionized water to the final volume. Final molar concentrations of PDCA, KOH, K_2SO_4 and HCOOH were 7.0, 66, 5.6 and 74 mmol L^{-1} respectively and the pH of the eluent was 4.2 ± 0.2. 100 mmol L^{-1} sodium sulfite (Merck) was obtained by dissolving appropriate amounts of powder (Na_2SO_3) in water and the solution was used to the periodic column condition. 2 mol L^{-1} HCl solution was prepared from 30% HCl (Suprapur®, Merck). A phosphate buffer was prepared by mixing disodium hydrophosphate (Na_2HPO_4) and potassium dihydrophosphate ($KH_2PO_4{\cdot}2H_2O$) obtained from Merck. Appropriate amounts of powder reagents were dissolved and mixed to obtain the solution, 25 mmol L^{-1} KH_2PO_4 and 2.5 mmol L^{-1} Na_2HPO_4, pH adjusted 6.0 ± 0.2.

2.2. Instrumentation

2.2.1. High performance liquid chromatography

The HPLC system was constructed from a HPLC pump, Shimadzu LC–10AT (Shimadzu, Japan) and a cation–exchange HPLC column, Dionex IonPac CS5A, 250 mm × 4.0 mm i.d., resin particle size 5 μm (Thermo Fisher Scientific, USA). Mobile phase flow rate was isocratic at 2 mL min^{-1} and an injection volume (sample loop volume) was 200 μL. PEEK tubing, which was used to transfer the eluent from LC column, was inserted into a Tygon sleeve. The outlet of the cation–exchange HPLC column was connected with the nebulizer sample channel. Due to cohesion of mobile phase from the column, the eluent was introduced directly to nebulizer (peristaltic pump avoiding). Tubing length (including the column outlet) was identical independently of the applied detector.

2.2.2. Microwave induced plasma optical emission spectrometry

The MIP OES, MP–AES 4200 (Agilent Technologies, USA), was used as a detector of the novel hyphenated system. The spectrometer was equipped with Czerny–Turner monochromator with 600 mm focal length with fixed entrance slit, holographic diffraction grating with 2400 lines mm^{-1} (wavelength range 178–780 nm) and charge coupled device (CCD) detector (532 × 128 pixel) directly cooled to 0 °C using a thermoelectric Peltier device. The microwave excitation assembly was an air cooled magnetron operating at 2450 MHz (fixed plasma power of 1000 W, vertically–oriented plasma with axial viewing). Cyclonic spray chamber and OneNeb nebulizer (Agilent Technologies, USA) were used. Nitrogen (N_2) was employed as a working gas. Nebulizer gas flow rate was 0.70 L min^{-1}. Plasma and auxiliary gas flow rates were fixed at 20 and 1.5 L min^{-1} respectively. Peristaltic pump was only used to drain the waste. Analytical wavelengths (emission lines) of element were chosen

according to available data, both literature and instrument software.

2.2.3. The inductively coupled plasma optical emission spectrometry

The ICP OES, Agilent 5110 ICP–OES (Agilent Technologies, USA), was used as a detector of the reference hyphenated system. The synchronous vertical dual view (SVDV) of the plasma allowed the axial and radial view analyses simultaneously and it was used in this study. Echelle grading fixed optics was thermostated at 35 °C and a detector, VistaChip II with CCD detector was cooled to −40 °C using triple Peltier system. Radio frequency (RF) power was set up at 1200 W. Multi–mode Sample Introduction System (MSIS) and OneNeb nebulizer (both Agilent Technologies, USA) were used. The MSIS unit is a modified cyclonic spray chamber which is able to work as a conventional spray chamber (PN mode), a hydride generation system (HG mode) or combining both functions (dual mode). HG mode was not used in the research. Therefore, MSIS is described as 'cyclonic spray chamber' (Table 1) in the further part of the text. Argon (Ar) was employed as a working gas. Nebulizer, plasma and auxiliary argon flow rates were 0.70, 12 and 1.0 L min^{-1} respectively. Peristaltic pump was only used to drain the waste. Analytical wavelengths (emission lines) of element were chosen according to available data, both literature and instrument software. Full experimental conditions were shown in Table 1.

2.3. Sample collection and preparation

2.3.1. Sample collection

All samples were collected in the past by authors. Post-glacial sediments (Spitsbergen, Svalbard), archaeological pottery (Wielkopolskie, Poland), soils located in the proximity of industry wastes disposal site (Dolnośląskie, Poland) and river sediments (Mekong, Vietnam) were collected by Przemysław Niedzielski. Yerba mate *(Ilex paraguariensis)*, distributed on the Polish market, was obtained online by Jędrzej Proch. Additional and detailed rationale for selecting the following sample matrix types in the Application section.

2.3.2. Sample hydrochloric acid leaching

The procedure of hydrochloric acid extraction (acid leaching) was repeated after Niedzielski et al. [28]. Accurately weighted 1.00 ± 0.01 g of a dry sample was placed in a conical flask and 2 mol L^{-1} hydrochloric acid solution (HCl) was added carefully in small portions (20 mL). After the reflux condenser was connected, the flask was heated up to approx. 80 °C. Then this temperature was held for 30 min. After extraction, sample was drained quantitatively through a paper filter (previously rinsed with 200 mL of high–pure deionized water) using polyethylene funnel into a plastic test tube. Finally, water was added up to a volume of 50.0 mL.

Table 1
Experimental conditions for HPLC–MIP OES and HPLC–ICP OES.

HPLC conditions		
Pump	Shimadzu LC–10AT	
Column	Dionex IonPac CS5A (250 mm × 4.0 mm i.d., 5 μm)	
Mobile phase	7.0 mmol L^{-1} pyridine–2,6–dicarboxylic acid (PDCA), 66 mmol L^{-1} potassium hydroxide (KOH), 5.6 mmol L^{-1} potassium sulfate (K_2SO_4), 74 mmol L^{-1} formic acid (HCOOH)	
Mobile phase flow rate [mL min^{-1}]	2.0[a]	
Injection volume [mL]	0.2	
	MIP OES conditions	ICP OES conditions
Spectrometer	Agilent Technologies MP–AES 4200	Agilent Technologies ICP 5110 Dual–View
RF power [W]	1000	1200
Working gas	Nitrogen (N_2)	Argon (Ar)
Nebulizer gas flow rate [L min^{-1}]	0.7	0.7
Plasma gas flow rate [L min^{-1}]	20	12
Auxiliary gas flow rate [L min^{-1}]	1.5	1.0
Nebulizer/spray chamber type	pneumatic (OneNeb)/ cyclonic	pneumatic (OneNeb)/MSIS (as cyclonic)
Viewing Position	0	N/A
Torch view	axial	synchronous vertical dual view (SVDV)
Analytical wavelengths [nm]	Fe 259.940, Fe 371.993[a]	Fe 234.350, Fe 238.204[a], Fe 259.940, Fe 261.382

[a] optimized parameter, N/A – not applicable.

2.3.3. Ultrasound assisted extraction

The procedure was similar to Proch and Niedzielski [36,37]. Accurately weighted 0.50 ± 0.01 g of a dry sample was placed in polyethylene test tube. 8.0 mL of 1 mol L^{-1} orthophosphoric acid (H_3PO_4) was added to each sample and the ultrasound assisted extraction was conducted by 30 min at ambient temperature. In the next step, sample was drained quantitatively through a paper filter (previously rinsed with 200 mL of high–pure deionized water and 20 mL of phosphate buffer). Sample solutions were neutralized (up to pH 6.0–6.5) with a few drops of 15 mol L^{-1} NaOH and filled up to 10 mL with phosphate buffer (25 mmol L^{-1} KH_2PO_4 and 2.5 mmol L^{-1} Na_2HPO_4, pH adjusted 6.0 ± 0.2). Samples were determined rapidly after preparation.

3. Results and discussion

3.1. Optimization

3.1.1. Plasma ignition and nebulization parameters

The hyphenated techniques presented in this work, HPLC–MIP OES and HPLC–ICP OES were simple modifications of HPLC–HG–ICP OES [36,37] In contrast to the mentioned studies, Multi–mode Sample Introduction System (MSIS, Agilent Technologies, USA), was used as a conventional cyclonic spray chamber (Table 1). Elaborate optimization was conducted previously for MIP OES [28] and ICP OES [36,37]. It is worth mentioning that nebulizer gas flow rate was similar to IC–ICP OES, however the described system consumed less argon keeping up the plasma (12 L min^{-1}) and lower RF power (1200 W) in comparison to Fernsebner et al. (15 L min^{-1} and 1350 W) [31]. Full parameters of both hyphenated systems were placed in Table 1.

3.1.2. Eluent composition

The PDCA eluent, 7.0 mmol L^{-1} PDCA, 66 mmol L^{-1} KOH, 5.6 mmol L^{-1} K_2SO_4 and 74 mmol L^{-1} HCOOH adjusted to pH 4.2 ± 0.2, was repeated after various authors [9–12]. Chen et al. observed that higher concertation of neutral salt shortened retention time (RT) and decreased mutual RT ratio of Fe(II) and Fe(III). Due to this, 80 mmol L^{-1} KCl was used instead of 5.6 mmol L^{-1} K_2SO_4 and 10 mmol L^{-1} PDCA, 33 mmol L^{-1} KOH and 37 mmol L^{-1} HCOOH (pH 4.0) were other components of the mobile phase [16]. However, the increase of salt load on ICP (such as chlorides or sulfates) may cause several problems, including nebulizer clogging, ionization interferences, plasma instability and extinction, even torch damage [32]. To determine Fe(II) and Fe(III) in biological sample, the following mobile phase were applied in the literature: PDCA + acetate buffer [15], PDCA + Tris–HAc + NH_4Ac [31] and PDCA + ammonium citrate [32]. However, the column overload was dangerously possible by most abundant elements (occurring as trace elements in biological samples). Summarizing all the above, the chosen eluent composition was suitable well for environmental samples to separate efficiently Fe(II) and Fe(III) on Dionex IonPac CS5A with significantly short RTs and acceptable signal–to–noise ratio.

3.1.3. Chromatographic run

In the HPLC optimization, both spectrometers were used independently. Mobile phase flow rate was investigated in the range from 0.5 to 2.0 mL min^{-1} and the influence of mobile phase flow rate [mL min^{-1}] on the retention time [s] was shown (Fig. 1). Single–element

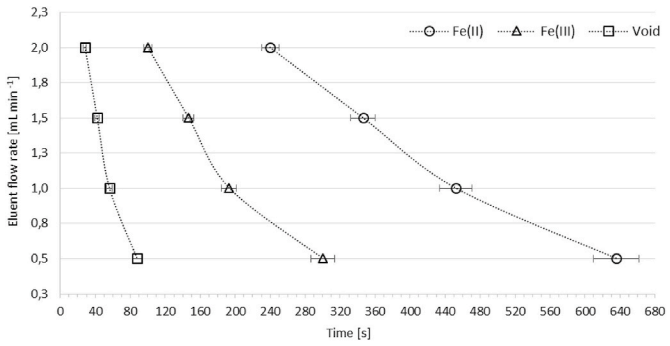

Fig. 1. The influence of mobile phase flow rate [mL min^{-1}] on the retention time [s] performed with Fe(II)+Fe(III) standard solution, 1.00 + 1.00 [mg L^{-1}].

chromatograms gave an information about significant peak resolution. Peaks areas were proportional to the height in the investigated range. Peak areas of Fe(II) and Fe(III) did not overlay and significant good resolution was obtained in whole investigated range (0.5–2.0 mL min^{-1}). The optimal eluent flow rate was established at 2.0 mL min^{-1}. Under optimal conditions, retention times (mean ± SD) were calculated, i.e. 103 ± 3 s and 242 ± 13 s for Fe(III) and Fe(II) respectively. Void time was 28 ± 2 s.

Moreover, the influence of iron standard concentration [mg L^{-1}] on the retention times [s] was investigated under optimal conditions in the range from 0.10 to 20.0 mg L^{-1}. Results were shown in Fig. 2. The RT ratio of Fe(II) and Fe(III) was calculated and equal to 2.36 ± 0.09 (mean ± SD). According to obtained data, retention time of Fe(II) could be established theoretically, however the RT ratio might be fixed only within the same chromatographic conditions (the column, the eluent, mobile phase flow rates etc.). In the literature, authors who used the same components, obtained similar values of the RT ratio: 2.34 [10], 2.45 [11], 2.46 [14], 2.54 [9], 2.72 [12].Moreover, no significant changes were observed in peak shapes and heights for mentioned species. In a view of asymmetry and peaks shape variability (dispersion) only calculations of peak areas were used in iron species determination. Obtained results proved that RTs are consistent and independent of Fe concentration in the whole investigated range.

It is worth mentioning that both hyphenated techniques allowed to determine Fe(II) and Fe(III) within 300 s. Obtained retention times were significantly better in comparison to reported systems, i.e. IC–Vis [9–14], IC–CLD [16,17], HPLC–ICP MS [32]. Only RT of Fe(III) obtained by Fernsebner et al. was slightly better, 0.8 min, and RT of Fe(II) were similar, 4.1 min. Instead of Dionex IonPac CS5A, only the guard column, CG5A (Thermo Fisher Scientific both) was used as analytical column which shortened the separation [31]. Nevertheless, it significantly deteriorated the quality of IC–ICP OES and its applicability. To keep up correct results of Fe(II) and Fe(III), cation–exchange column was

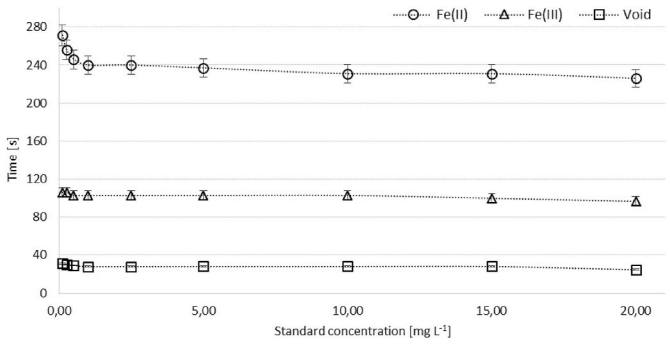

Fig. 2. The influence of Fe(II)+Fe(III) standard concentration [mg L^{-1}] on the retention time [s] performed with the optimal mobile phase flow rate, 2.0 mL min^{-1}.

periodically conditioned with 100 mmol L^{-1} sodium sulfite to eliminate any oxygen build–up on the column (60 min purging). The changes of retention time within longer time intervals (longer than a month) were observed during an analytical work. According to this, periodic controls were conducted with a single element form standard solutions to confirm respective retention times.

3.2. Analytical figures of merit

3.2.1. Linear calibration range and analytical wavelengths

Two most recommended analytical wavelengths (emission lines) were investigated in the MIP OES optimization, Fe 371.993 nm (atomic) and Fe 259.940 nm (ionic). Results obtained with Fe 259.940 nm were rejected due to significant high limit of detections (LODs), 7.4 mg L^{-1} and 6.0 mg L^{-1} of Fe(II) and Fe(III) respectively. However, the linear range of calibration curve was observed from 20 to 50 mg L^{-1} (the last investigated standard solution). For Fe 371.993 nm, the calibration curve, was linear from the limit of quantification (LOQ) to 20.0 mg L^{-1} with acceptable coefficient of correlation (R^2 > 0.9900). Worth mentioning that signals of both Fe species increased much disproportionately above 20.0 mg L^{-1} and 'a tail' of Fe(III) peak was observed. Summarizing the above observations, Fe 259.940 nm could be supply for geological samples (high concentration of Fe species) to avoid over–diluting of samples. However, the optics (Czerny–Turner monochromator) allows to employ one analytical wavelength in the chromatographic run and Fe 371.993 nm was used in the application (Table 2). Moreover, a higher concentration of standards and samples might require to clean the system more frequently, especially a plasma torch (both ICP and MIP) which can be damaged by salting out.

In the case of ICP OES, echelle fixed–grating optics allows to simultaneously employ more than one analytical wavelength in one run. Due to this, four Fe analytical wavelengths were chosen to optimize HPLC–ICP OES i.e. Fe 234.350 nm (ionic), Fe 238.204 nm (ionic), Fe 259.940 nm (ionic), Fe 261.382 nm (ionic). Results were presented in Table 2. Significant better LOD and LOQ were obtained with Fe 238.204 nm, however better precision (as relative standard deviation, RSD) was obtained with Fe 259.940 nm than Fe 238.204 nm. Worth noting, precision was significantly low irrespective of applied analytical wavelength, 1.7–4.1% [Fe(II)] and 2.0–4.2% [Fe(III)]. Acceptable coefficient of correlation (R2>0.9900) were obtained for each emission line with the highest values for Fe 234.350 nm. Summarizing the collected data, Fe 238.204 nm was applied in ICP OES for the further studies, in opposite to 237.532 nm, employed in IC–ICP OES by Fernsebner et al. [31]. Therefore the difference in background level was significant and it was equal to 1379 ± 59 [cps] (mean ± SD) for blank measurements (n = 6). Moreover, this difference was increasing for standard measurements in the range from 0.1 to 5.0 mg L^{-1} and it was ranging from 1658 ± 64 to 2260 ± 94 [cps] respectively. The background correction was required to compare a relative signal (intensity) of Fe species obtained by both techniques. After this, typical chromatograms were imposed on each other and shown in Fig. 3.

3.2.2. Limits of detection/quantification and precision

Instrumental LODs (as 3–sigma) and LOQs (as 3 LOD) obtained by HPLC–ICP OES were 10–20 times lower than HPLC–MIP OES. In the case of HPLC–MIP OES, no similar system for iron speciation analysis was described in the literature. However, obtained LODs for Fe(II) and Fe(III) were comparable [27] or slightly worse [29,30] with LODs obtained by MIP OES in determination of total iron content. In turn, LODs measured with HPLC–ICP OES, 6.31 and 5.41 μg L^{-1}, were slightly better than IC–ICP OES, 9.11 and 6.33 μg L^{-1}, for Fe(II) and Fe(III) respectively [31]. Moreover, this system was less economic (higher RF power and argon consumption) and more specific (only applied for rat brain extracts). Unreachable low LODs were obtained with HPLC–ICP–MS (0.6 μg L^{-1}) however with significantly worse RTs i.e. 370 and 120 s for Fe (II) and Fe(III) respectively [32]. Comparing to the reported IC systems,

Table 2
Analytical figures of merit (n = 3, peak area).

Species	RT [s]	Plasma	Analytical wavelength [nm]	Linear calibration range [mg L^{-1}]	R^2	LOD [μg L^{-1}]	LOQ [μg L^{-1}]	Precision (as RSD) [%]
Fe(II)	242 ± 13	MIP (N_2)	371.993	LOQ–20.0	0.9941	108	324	2.8 (at 1000 μg L^{-1})
		ICP (Ar)	234.350	LOQ–5.00	0.9966	11.4	34.2	1.8 (at 100 μg L^{-1})
			238.204	LOQ–5.00	0.9933	6.31	18.9	4.1 (at 100 μg L^{-1})
			259.940	LOQ–5.00	0.9924	9.90	29.7	1.7 (at 100 μg L^{-1})
			261.382	LOQ–5.00	0.9905	16.6	49.8	3.9 (at 100 μg L^{-1})
Fe(III)	103 ± 3	MIP (N_2)	371.993	LOQ–20.0	0.9901	93.6	281	2.1 (at 1000 μg L^{-1})
		ICP (Ar)	234.350	LOQ–5.00	0.9972	9.49	28.5	4.2 (at 100 μg L^{-1})
			238.204	LOQ–5.00	0.9942	5.41	16.2	3.6 (at 100 μg L^{-1})
			259.940	LOQ–5.00	0.9927	6.80	20.4	2.7 (at 100 μg L^{-1})
			261.382	LOQ–5.00	0.9907	10.9	32.8	2.0 (at 100 μg L^{-1})

RT – retention time (mean ± SD); LOD– limit of detection (as 3σ); LOQ– limit of quantification (as 3 LOD); RSD – relative standard deviation.

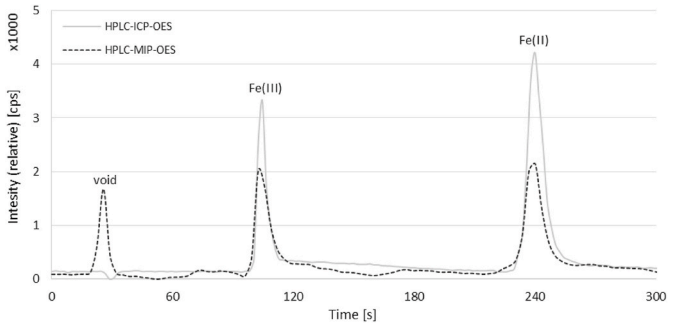

Fig. 3. Typical chromatograms (after the background correction) presenting separation of Fe(II)+Fe(III) standard solution (1.00 + 1.00 mg L^{-1}), obtained in optimal conditions by HPLC–MIP OES (Fe I 371.993 nm) and HPLC–ICP OES (Fe II 238.204 nm).

both of hyphenated techniques obtained better LODs [12,38]. In turn, obtained LODs were similar [13,15] or slightly better [9,10] in comparison to HPLC–ICP OES. Precision was measured at the concentration which was approx. 3–5 times higher than LOQs. According to this, different concentrations of standard solution were used for each detector, 100 and 1000 μg L^{-1}, for ICP OES and MIP OES respectively. For chosen analytical wavelengths, slightly better precision was obtained by MIP OES (2.1–2.8%) than ICP OES (3.6–4.1%). Irrespective of the applied method, lower RSD was for Fe(III), 2.1–3.6%, than Fe(II), 2.8–4.1%.

3.2.3. Standard addition method

There is a lack of Certified Reference Materials (CRMs) which is able to simultaneously determine Fe(II) and Fe(III), and there is an example of the material developing in the literature, however it is not commercially available [39]. Determination of CRMs for total content of elements is not inappropriate using chromatographic methods. Therefore, the standard addition method was chosen for recovery measurements. Standard solutions of each element species were added in two concentrations (low and high) to the final extracts volume of three different real samples. Final concentrations of standards in sample solutions were established individually due to a spectrometry type. The concentration of the first standard addition was approx. 3–5 times higher than LOQs, i.e. 100 (ICP OES) and 1000 μg L^{-1} (MIP OES). High concentration was respectively 10 times higher than the first standard addition, i.e. 1.00 mg L^{-1} (ICP OES) and 10.0 mg L^{-1} (MIP OES). Sample matrix types were inorganic (P1, P2) and organic (P3). Moreover, two sample preparation procedure were applied i.e. acid leaching (P1) and ultrasound assisted extraction (P2, P3). Acceptable recoveries, 94–109% for Fe(II) and 99–115% for Fe(III), were presented for each sample matrix type. More consistent recoveries were obtained with HPLC–ICP OES (97–113%) than HPLC–MIP OES (94–115%). In the comparison with IC–ICP OES, recoveries were significantly higher, 86–105% for Fe(II) and 43–66% for Fe(III) [31]. Full results of the standard addition method were showed in Table 3.

3.3. Application

The applicability of the methods, HPLC–MIP OES and HPLC–ICP OES, was performed parallel with fifteen samples (three samples of five sample matrix types): post–glacial sediments (Spitsbergen, Svalbard) (A1–A3), archaeological pottery (B1–B3), soils located in the proximity of industry wastes disposal site (C1–C3), river sediments (Mekong, Vietnam) (D1–D3), yerba mate *(Ilex paraguariensis)* (E1–E3). The following selection of samples was performed to prove the wide applicability of both methods. Samples of soils located in the proximity of industry wastes disposal site represented high anthropogenic impact on the environment. In turn, post-glacial and river sediments represented samples with none or low anthropogenic impact on the environment. Samples of archaeological pottery were selected to demonstrate the applicability in archaeometry. As both the infusion type and the cultivated plant, yerba mate samples represented examples of food or plant analysis.

Post–glacial sediments and archaeological pottery were prepared with the procedure of hydrochloric acid leaching [28] in contrast to soils located in the proximity of industry wastes disposal site, river sediments and yerba mate which were extracted with ultrasound assistance by phosphoric acid [36,37]. Worth noticing that Fe(II) and Fe(III) are not totally extracted from soils and sediments by extractants as hydrochloric and orthophosphoric acids. Proposed extraction procedures are more effective for biological samples and less effective for geological samples due to some iron species are built in silicates. However, from the point of view of speciation research, the proposed extraction procedures allow for the determination of Fe (III) and Fe (II), while Fe (II) is oxidized by the decomposition of the sample, e.g. with aqua regia. Assuming high concentration of Fe(II) and Fe(III) in inorganic samples, extracts were respectively diluted (Table 4) before an analysis. Method LOQs for complete analytical process (including sample preparation and dilution), were calculated and presented (Table 4). The uncertainty for complete analytical process was at the level of 20%.

Results obtained in the two methods have been compared using statistical tools. Because of the dual nature of data distribution detected by the Lilliefors and Shapiro-Wilk normality tests (non-normal distribution of Fe(III) and normal distribution of Fe(II)) the nonparametric tests (sign test and Wilcoxon signed-rank test) have been used. Statistical analysis showed that the results obtained with the use of two analytical methods did not show statistically significant differences ($p > 0.05$).

In comparison to the literature, obtained results by both methods were generally lower for post–glacial sediments and archaeological pottery [40–42]. It was related to the use of other extractants. Cloudhary et al. determined 3.89–5.84% of total Fe in post–glacial sediments (Svalbard), however samples were digested in the mixture of HF, HNO_3 and $HClO_4$ acid with the ratio of 7:3:1 [40]. Also Krajcarova et al. found total Fe in the range from 15.8 to 46.2 g kg^{-1} in arctic soils

Table 3
Recovery at the addition of standard solution (n = 3, peak area).

MIP OES	Fe I 371.993 nm				ICP OES	Fe II 238.204 nm			
	Sample solution	Added	Found	Recovery		Sample solution	Added	Found	Recovery
P1	[mg L^{-1}]	[mg L^{-1}]	[mg L^{-1}]	[%]	P1	[μg L^{-1}]	[μg L^{-1}]	[μg L^{-1}]	[%]
Fe(II)	<0.32	1.00	0.97 ± 0.06	97 ± 6	Fe(II)	74 ± 5	100	172 ± 12	98 ± 7
	<0.32	10.0	10.9 ± 0.7	109 ± 7		74 ± 5	1000	1042 ± 73	97 ± 7
Fe(III)	0.66 ± 0.04	1.00	1.76 ± 0.12	109 ± 7	Fe(III)	641 ± 32	100	742 ± 37	113 ± 6
	0.66 ± 0.04	10.0	12.2 ± 0.8	115 ± 8		641 ± 32	1000	1699 ± 85	108 ± 5
P2	[mg L^{-1}]	[mg L^{-1}]	[mg L^{-1}]	[%]	P2	[μg L^{-1}]	[μg L^{-1}]	[μg L^{-1}]	[%]
Fe(II)	<0.32	1.00	0.94 ± 0.06	94 ± 6	Fe(II)	55 ± 4	100	163 ± 11	107 ± 8
	<0.32	10.0	10.4 ± 0.6	104 ± 6		55 ± 4	1000	1098 ± 77	104 ± 7
Fe(III)	<0.28	1.00	1.36 ± 0.09	113 ± 7	Fe(III)	222 ± 11	100	326 ± 16	107 ± 5
	<0.28	10.0	11.7 ± 0.8	115 ± 8		222 ± 11	1000	1120 ± 56	100 ± 5
P3	[mg L^{-1}]	[mg L^{-1}]	[mg L^{-1}]	[%]	P3	[μg L^{-1}]	[μg L^{-1}]	[μg L^{-1}]	[%]
Fe(II)	<0.32	1.00	1.06 ± 0.06	106 ± 6	Fe(II)	<18.9	100	99 ± 7	99 ± 7
	<0.32	10.0	9.51 ± 0.57	95 ± 6		<18.9	1000	1031 ± 7	103 ± 7
Fe(III)	<0.28	1.00	1.15 ± 0.08	115 ± 8	Fe(III)	183 ± 9	100	282 ± 14	99 ± 5
	<0.28	10.0	10.9 ± 0.7	109 ± 7		183 ± 9	1000	1315 ± 66	113 ± 6

<x.xx – below limit of quantification.

Table 4
Applicability of hyphenated techniques: HPLC–MIP OES (Fe I 371.993 nm) and HPLC–ICP OES (Fe II 238.204 nm) performed on five groups of real samples (n = 3) (peak area) [mg kg^{-1}].

Methods				HPLC–MIP OES		HPLC–ICP OES		Accuracy [%]	
Sample matrix	Preparation	DF	No.	Fe(II)	Fe(III)	Fe(II)	Fe(III)	Fe(II)	Fe(III)
post–glacial sediments	Acid leaching	20 (1)	A1	547 ± 91	10019 ± 1670	565 ± 94	10621 ± 1770	97 ± 8	94 ± 5
		50 (2)	A2	<324	17206 ± 2868	146 ± 24	17655 ± 2943	–	97 ± 5
			A3	1209 ± 201	16592 ± 2765	1573 ± 262	15542 ± 2590	77 ± 7	107 ± 6
archaeological potshards	Acid leaching	20 (1)	B1	<324	9825 ± 1638	311 ± 52	9874 ± 1646	–	100 ± 7
		50 (2)	B2	413 ± 69	10204 ± 1701	432 ± 72	9751 ± 1625	96 ± 5	105 ± 5
			B3	648 ± 108	12560 ± 2093	754 ± 126	12975 ± 2162	86 ± 4	97 ± 4
soils located in the proximity of industry wastes disposal site	Ultrasound assisted extraction	20 (1)	C1	516 ± 86	3270 ± 545	503 ± 84	3252 ± 542	103 ± 7	101 ± 5
		50 (2)	C2	<130	3698 ± 616	61 ± 10	3638 ± 606	–	102 ± 6
			C3	<130	4297 ± 716	<18.9	4234 ± 706	–	101 ± 6
river sediments	Ultrasound assisted extraction	20 (1)	D1	<130	858 ± 143	<18.9	877 ± 146	–	98 ± 7
		50 (2)	D2	<130	3959 ± 660	<18.9	3588 ± 598	–	110 ± 8
			D3	440 ± 73	4172 ± 695	449 ± 75	4310 ± 718	98 ± 9	97 ± 8
yerba mate	Ultrasound assisted extraction	–	E1	16 ± 3	15 ± 3	15 ± 3	16 ± 3	105 ± 3	97 ± 2
			E2	32 ± 5	41 ± 7	31 ± 5	38 ± 6	102 ± 3	107 ± 3
			E3	<6.48	45 ± 7	<0.38	43 ± 7	–	103 ± 5

<xx.x – below method LOQ (including sample preparation and dilution); DF – dilution factor (before an analysis, excluding sample preparation).
Accuracy as the ratio HPLC–MIP OES to HPLC–ICP OES results in %.

(Spitsbergen), however samples were extracted by aqua regia [41]. Hatcher et al. used ICP OES and the mixture of HF and $HClO_4$ (2:1) to find iron in ceramics and results were in the range from 0.05 to 13.64% (presented as Fe_2O_3) [42]. Worth noticing that above extractants prevent iron speciation analysis. In the case of river sediments, the iron content varied considerably and resulted mainly from the tested fraction [43,44]. Howari & Banat, using sequential extraction procedure, found total Fe in mud and clay fraction in the range, 1508–1613 mg kg^{-1} and 1265.6–1370.5 mg kg^{-1} respectively [43]. In turn, Postma et al. reported that 1,1–5,6 g kg^{-1} of Fe was extracted with HCl and ascorbic acid from Red River mud (Vietnam) [44]. In the case of yerba mate (Ilex paraguariensis), total Fe was only determined after wet digestion in concentrated HNO_3 or the HNO_3/H_2O_2 mixture [45,46]. Nevertheless, results obtained by both methods were comparable to Olivari et al. Author used 65% HNO_3 digestion and ICP OES to determine total Fe in the range 9.11–54.7 mg kg^{-1} [45]. In turn, Pozebon et al. used the mixture of HNO_3 and H_2O_2 (2:1) mixture and ICP OES. Total Fe was found in the range, 154–318 mg kg^{-1} [46].

Comparing both of analytical methods, a high compatibility of the results was observed (Table 4). Accuracy [%], as the ratio HPLC–MIP OES to HPLC–ICP OES results, was in the acceptable range (80–120%) with an exception, 77% for Fe(II) in A3 (post–glacial sediment). This

difference could be related to the high dilution factor. RSD of results accuracy was below 10%. Typically, results obtained with HPLC–MIP OES were slightly higher in comparison to HPLC–ICP OES. According to sample preparation, accuracy was in the ranges, 77–107% (acid leaching) and 97–110% (ultrasound assisted extraction). Fe(III) was detected parallel by both methods in the whole population of investigated samples (n = 15) with the accuracy from 94 to 110%. In turn, Fe(II) was found in 8 (53%) and 11 (73%) of 15 investigated samples by HPLC–MIP OES and HPLC–ICP OES respectively. On one hand, the applicability of HPLC–MIP OES was a limiting factor as Fe(II) was detected parallel in 8 samples (the accuracy from 77 to 105%). On the other hand, the main advantage of HPLC–MIP OES was the usage of nitrogen generator which made a single analysis much cheaper than argon consuming HPLC–ICP OES.

In comparison of HPLC detectors, the following observations was noted. If the ratio of Fe(III) and Fe(II) was 25 (B3) or lower, the applicability of both methods could be similar. Therefore, if very high concentration (>10 g kg^{-1}) of total Fe or Fe(III) was expected (especially soils or sediments), MIP OES would be more appropriate as a detector to avoid the sample over–dilution. In turn, high dilution factor (DF > 20) led to higher method LOQs, which significantly adversely affected low concentrations, especially Fe(II). However, even 50–fold dilution gave significantly better response of Fe(II) using ICP OES as a detector. Therefore, ICP OES should be applied if the ratio of Fe(III) and Fe(II) was 32 (B1) or higher. According to this, expected iron concentration as well as the mutual ratio of Fe(III) and Fe(II) were crucial parameters to evaluate the choice of the appropriate detector for specific sample types. Worth noting that the linear calibration range of HPLC–MIP OES could be significantly extended using Fe 259.940 nm instead of Fe 371.993 nm. Summarizing all collected data, HPLC–MIP OES could be a complementary analytical tool in determination of Fe species for HPLC–ICP OES.

4. Conclusions

The parallel usage of high performance liquid chromatography coupled with two different types of optical emission spectrometers, such as microwave induced and inductively coupled plasma, was presented. Both of spectrometers, i.e. MIP OES and ICP OES, are able be applied as a specific detectors in hyphenated techniques. Described methods allows to simultaneously determine of two iron species: Fe(II) and Fe(III) within 300 s of single analysis. In comparison to related systems, both presented methods obtained significantly shorter retention times. In addition, the post–column solution was directly introduced to the detector (avoiding a usage of additional post–column reagents).

Considerably low LOQs, low RSD values and acceptable recoveries was comparable with the literature. The application, performed with different sample matrix types, confirmed that described methods are complementary analytical tools in simultaneous determination of iron species. Moreover, the high compatibility of the results was proved despite the high dilution factor. An indisputable advantage of HPLC–MIP OES is the usage of a nitrogen generator to supply working gas. Comparing with HPLC–ICP OES, a single analysis is much cheaper while LOQs are respectively higher. Probably some limitations could be equated, however it would require more extensive optimization (including the sample preparation), which was not crucial in this study. Choosing the appropriate detector for specified sample types, two parameters could be crucial: the expected level of iron concentration as well as the mutual ratio of Fe species in the investigated material. For example, expecting high Fe concentration in the sample, the usage of HPLC–MIP OES is more recommended than HPLC–ICP OES to avoid over–diluting. However, HPLC–ICP OES is more appropriate if the ratio of Fe(III) and Fe(II) is higher than 25. Summarizing all observations, HPLC–MIP OES is rather complementary of HPLC–ICP OES than is an alternative. Described systems are more suitable and flexible for an expansion and an improvement than a commercial available hyphenated systems e.g. HPLC–ICP MS. It shows a good perspective for further study with hyphenated techniques, using other types of chromatography or spectrometry.

Credit author statement

Jędrzej Proch: Conceptualization; Investigation; Methodology; Data curation; Funding acquisition; Validation; Writing - original draft; Writing - Review & Editing. Przemysław Niedzielski: Conceptualization; Investigation; Methodology; Formal analysis; Writing - original draft; Writing - Review & Editing

Declaration of competing interest

The authors declare that they have no known competing financial interests or personal relationships that could have appeared to influence the work reported in this paper.

Acknowledgments

The work was supported by grant no. POWR.03.02.00–00–I026/16 co–financed by the European Union through the European Social Fund under the Operational Program Knowledge Education Development.

References

[1] M. Sánchez, L. Sabio, N. Gálvez, M. Capdevila, J. Dominguez-Vera, Iron chemistry at the service of life, IUBMB Life 69 (6) (2017) 382–388, https://doi.org/10.1002/iub.1602.
[2] G. Luther III, J. Kostka, T. Church, B. Sulzberger, W. Stumm, Seasonal iron cycling in the salt–marsh sedimentary environment: the importance of ligand complexes with Fe(II) and Fe(III) in the dissolution of Fe(III) minerals and pyrite, respectively, Mar. Chem. 40 (1–2) (1992) 81–103, https://doi.org/10.1016/0304–4203(92)90049–g.
[3] M. Zaw, B. Chiswel, Speciation of iron and manganese in dam water particles using electron spectroscopy for chemical analysis (ESCA), Talanta 42 (1) (1995) 27–40, https://doi.org/10.1016/0039–9140(94)00211–a.
[4] R. Michalski, Applications of ion chromatography for the determination of inorganic cations, Crit. Rev. Anal. Chem. 39 (4) (2009) 230–250, https://doi.org/10.1080/10408340903032453.
[5] R. Michalski, M. Jabłonska, S. Szopa, A. Łyko, Application of ion chromatography with ICP–MS or MS detection to the determination of selected halides and metal/metalloids species, Crit. Rev. Anal. Chem. 41 (2) (2011) 133–150, https://doi.org/10.1080/10408347.2011.559438.
[6] M. Grotti, A. Terol, J. Todolí, Speciation analysis by small–bore HPLC coupled to ICP–MS, Trac. Trends Anal. Chem. 61 (2014) 92–106, https://doi.org/10.1016/j.trac.2014.06.009.
[7] P. Janvion, S. Motellier, H. Pitsch, Ion–exchange mechanisms of some transition metals on a mixed–bed resin with a complexing eluent, J. Chromatogr. A 715 (1) (1995) 105–115, https://doi.org/10.1016/0021–9673(95)00576–9.
[8] M. Šikovec, M. Novič, M. Franko, Application of thermal lens spectrometric detection to the determination of heavy metals by ion chromatography, J. Chromatogr. A 739 (1–2) (1996) 111–117, https://doi.org/10.1016/0021–9673(96)00054–4.
[9] N. Cardellicchio, P. Ragone, S. Cavalli, J. Riviello, Use of ion chromatography for the determination of transition metals in the control of sewage–treatment–plant and related waters, J. Chromatogr. A 770 (1–2) (1997) 185–193, https://doi.org/10.1016/s0021–9673(97)00086–1.
[10] B. Divjak, M. Franko, M. Novič, Determination of iron in complex matrices by ion chromatography with UV–Vis, thermal lens and amperometric detection using post–column reagents, J. Chromatogr. A 829 (1–2) (1998) 167–174, https://doi.org/10.1016/s0021–9673(98)00837–1.
[11] N. Cardellicchio, S. Cavalli, P. Ragone, J. Riviello, New strategies for determination of transition metals by complexation ion–exchange chromatography and post column reaction, J. Chromatogr. A 847 (1–2) (1999) 251–259, https://doi.org/10.1016/s0021–9673(99)00426–4.
[12] A. Atanassova, R. Lam, D. Zamble, A high–performance liquid chromatography method for determining transition metal content in proteins, Anal. Biochem. 335 (1) (2004) 103–111, https://doi.org/10.1016/j.ab.2004.08.013.
[13] H. Kaasalainen, A. Stefánsson, G. Druschel, Determination of Fe(II), Fe(III) and Fe total in thermal water by ion chromatography spectrophotometry (IC–Vis), Int. J. Environ. Anal. Chem. 96 (11) (2016) 1074–1090, https://doi.org/10.1080/03067319.2016.1232717.
[14] C. Ashworth, C. Weller, G. Frisch, Quantifying indium with ion chromatography in hydro- and biohydrometallurgical leaching solutions, J. Separ. Sci. 42 (15) (2019) 2517–2522, https://doi.org/10.1002/jssc.201900295.
[15] Y. Kim, H. Chung, H. Kong, D. Choi, D. Cho, The application of Ion chromatographic method for bioavailability and stability test of iron preparations,

Arch Pharm. Res. (Seoul) 22 (3) (1999) 288–293, https://doi.org/10.1007/bf02976364.
[16] Y. Chen, Y. Jian, K. Chiu, H. Yak, Simultaneous speciation of iron(II) and iron(III) by ion chromatography with chemiluminescence detection, Anal. Sci. 28 (8) (2012) 795–799, https://doi.org/10.2116/analsci.28.795.
[17] S. Scott, A. Housh, G. Powell, A. Anstaett, A. Gerheart, M. Benoit, S. Wilder, M. Schueller, R. Ferrieri, Crop yield, ferritin and Fe(II) boosted by azospirillum brasilense (HM053) in corn, Agronomy 10 (3) (2020) 394, https://doi.org/10.3390/agronomy10030394.
[18] S. Greenfield, I. Jones, C. Berry, High–pressure plasmas as spectroscopic emission sources, Analyst 89 (1064) (1964) 713, https://doi.org/10.1039/an9648900713.
[19] R. Wendt, V. Fassel, Induction–coupled plasma spectrometric excitation source, Anal. Chem. 37 (7) (1965) 920–922, https://doi.org/10.1021/ac60226a003.
[20] P. Boumans, Inductively coupled plasma–atomic emission spectroscopy: its present and future position in analytical chemistry, Fresenius' Z. für Anal. Chem. 299 (5) (1979) 337–361, https://doi.org/10.1007/bf00704968.
[21] M. Ślachciński, Recent achievements in sample introduction systems for use in chemical vapor generation plasma optical emission and mass spectrometry: from macro– to microanalytics, Appl. Spectrosc. Rev. 49 (4) (2014) 271–321, https://doi.org/10.1080/05704928.2013.823547.
[22] C. Williams, R. Amais, B. Fontoura, B. Jones, J. Nóbrega, G. Donati, Recent developments in microwave–induced plasma optical emission spectrometry and applications of a commercial Hammer–cavity instrument, Trac. Trends Anal. Chem. 116 (2019) 151–157, https://doi.org/10.1016/j.trac.2019.05.007.
[23] J. Cobine, D. Wilbur, The electronic torch and related high frequency phenomena, J. Appl. Phys. 22 (6) (1951) 835–841, https://doi.org/10.1063/1.1700055.
[24] A. McCormack, S. Tong, W. Cooke, Sensitive selective gas chromatography detector based on emission spectrometry of organic compounds, Anal. Chem. 37 (12) (1965) 1470–1476, https://doi.org/10.1021/ac60231a007.
[25] A. Tyburska, K. Jankowski, Determination of selenium in dietary supplements by optical emission spectrometry after alkaline dissolution and subsequent headspace solid phase microextraction, J. Pharmaceut. Biomed. Anal. 74 (2013) 268–272, https://doi.org/10.1016/j.jpba.2012.11.011.
[26] I. Mikheev, E. Karpukhina, L. Usol'tseva, T. Samarina, D. Volkov, M. Proskurnin, Application of microwave plasma atomic emission spectrometry and hydride generation for determination of arsenic and selenium in mineral water, Inorg. Mater. 53 (14) (2017) 1422–1426, https://doi.org/10.1134/s0020168517140126.
[27] H. Matusiewicz, M. Ślachciński, Simultaneous determination of hydride forming (As, Bi, Ge, Sb, Se, Sn) and Hg and non–hydride forming (Ca, Fe, Mg, Mn, Zn) elements in sonicate slurries of analytical samples by microwave induced plasma optical emission spectrometry with dual–mode sample introduction system, Microchem. J. 86 (1) (2007) 102–111, https://doi.org/10.1016/j.microc.2006.12.002.
[28] P. Niedzielski, L. Kozak, M. Wachelka, K. Jakubowski, J. Wybieralska, The microwave induced plasma with optical emission spectrometry (MIP–OES) in 23 elements determination in geological samples, Talanta 132 (2015) 591–599, https://doi.org/10.1016/j.talanta.2014.10.009.
[29] S. Gallego Ríos, G. Peñuela, C. Ramírez Botero, Method validation for the determination of mercury, cadmium, lead, arsenic, copper, iron, and zinc in fish through microwave–induced plasma optical emission spectrometry (MIP OES), Food Analytical Methods 10 (10) (2017) 3407–3414, https://doi.org/10.1007/s12161–017–0908–0.
[30] L. Pires, F.de S. Dias, L. Teixeira, Assessing the internal standardization of the direct multi–element determination in beer samples through microwave–induced plasma optical emission spectrometry, Anal. Chim. Acta 1090 (2019) 31–38, https://doi.org/10.1016/j.aca.2019.09.033.
[31] K. Fernsebner, J. Zorn, B. Kanawati, A. Walker, B. Michalke, Manganese leads to an increase in markers of oxidative stress as well as to a shift in the ratio of Fe(II)/(III) in rat brain tissue, Metall 6 (4) (2014) 921, https://doi.org/10.1039/c4mt00022f.
[32] N. Solovyev, M. Vinceti, P. Grill, J. Mandrioli, B. Michalke, Redox speciation of iron, manganese, and copper in cerebrospinal fluid by strong cation exchange chromatography – sector field inductively coupled plasma mass spectrometry, Anal. Chim. Acta 973 (2017) 25–33, https://doi.org/10.1016/j.aca.2017.03.040.
[33] M. Wolle, T. Fahrenholz, G. Rahman, M. Pamuku, H. Kingston, D. Browne, Method development for the redox speciation analysis of iron by ion chromatography–inductively coupled plasma mass spectrometry and carryover assessment using isotopically labeled analyte analogues, J. Chromatogr. A 1347 (2014) 96–103, https://doi.org/10.1016/j.chroma.2014.04.066.
[34] V. Trinta, P. Padilha, S. Petronilho, R. Santelli, B. Braz, A. Freire, C. Saunders, H.F. D. Rocha, A. Sanz–Medel, M.L. Fernández–Sánchez, Total metal content and chemical speciation analysis of iron, copper, zinc and iodine in human breast milk using high–performance liquid chromatography separation and inductively coupled plasma mass spectrometry detection, Food Chem. 326 (2020) 126978, https://doi.org/10.1016/j.foodchem.2020.126978.
[35] L. Zheng, D. Watson, J. Tettey, C. Clements, The determination of iron as its EDTA complex in Helix aspera by hydrophilic interaction liquid chromatography coupled to Fourier transform electrospray ionisation mass spectrometry, Talanta 76 (5) (2008) 1165–1169, https://doi.org/10.1016/j.talanta.2008.05.018.
[36] J. Proch, P. Niedzielski, In–spray chamber hydride generation by multi–mode sample introduction system (MSIS) as an interface in the hyphenated system of high performance liquid chromatography and inductivity coupled plasma optical emission spectrometry (HPLC–HG–ICP–OES) in arsenic species determination, Talanta 208 (2020) 120395, https://doi.org/10.1016/j.talanta.2019.120395.
[37] J. Proch, P. Niedzielski, Multi–mode Sample Introduction System (MSIS) as an interface in the hyphenated system 2 HPLC–MSIS–ICP–OES in simultaneous determination of metals and metalloids species, Anal. Chim. Acta 1147 (2021) 1–14, https://doi.org/10.1016/j.aca.2020.12.047.
[38] J. Dias, L. Kubota, P. Nesterenko, P. Haddad, Chelidamic acid as a new eluent for the determination of Fe(II) and Fe(III) species and other metals by high performance chelation ion chromatography, Chromatographia 75 (15–16) (2012) 867–873, https://doi.org/10.1007/s10337–012–2265–x.
[39] L. Alcott, A. Krause, E. Hammarlund, C. Bjerrum, F. Scholz, Y. Xiong, A. Hobson, L. Neve, B. Mills, C. März, B. Schnetger, A. Bekker, S. Poulton, Development of iron speciation reference materials for palaeoredox analysis, Geostand. Geoanal. Res. 44 (3) (2020) 581–591, https://doi.org/10.1111/ggr.12342.
[40] S. Choudhary, G. Nayak, N. Khare, Source, mobility, and bioavailability of metals in fjord sediments of Krossfjord–Kongsfjord system, Arctic, Svalbard, Environ. Sci. Pollut. Control Ser. (2020), https://doi.org/10.1007/s11356–020–07879–1.
[41] L. Krajcarová, K. Novotný, B. Chattová, J. Elster, Elemental analysis of soils and Salix polaris in the town of Pyramiden and its surroundings (Svalbard), Environ. Sci. Pollut. Res. 23 (10) (2016) 10124–10137, https://doi.org/10.1007/s11356–016–6213–4.
[42] H. Hatcher, M. Tite, J. Walsh, A comparison of inductively–coupled plasma emission spectrometry and atomic absorption spectrometry analysis on standard reference silicate materials and ceramics, Archaeometry 37 (1) (1995) 83–94, https://doi.org/10.1111/j.1475–4754.1995.tb00728.x.
[43] F. Howari, K. Banat, Assessment of Fe, Zn, Cd, Hg, and Pb in the Jordan and yarmouk river sediments in relation to their physicochemical properties and sequential extraction characterization, Water, Air, Soil Pollut. 132 (1/2) (2001) 43–59, https://doi.org/10.1023/a:1012062814873.
[44] D. Postma, S. Jessen, N. Hue, M. Duc, C. Koch, P. Viet, et al., Mobilization of arsenic and iron from Red River floodplain sediments, Vietnam, Geochem. Cosmochim. Acta 74 (12) (2010) 3367–3381, https://doi.org/10.1016/j.gca.2010.03.024.
[45] I. Olivari, S. Paz, Á. Gutiérrez, D. González–Weller, A. Hardisson, G. Sagratini, C. Rubio, Macroelement, trace element, and toxic metal levels in leaves and infusions of yerba mate (Ilex paraguariensis), Environ. Sci. Pollut. Res. 27 (17) (2020) 21341–21352, https://doi.org/10.1007/s11356–020–08681–9.
[46] D. Pozebon, V. Dressler, M. Marcelo, T. de Oliveira, M. Ferrão, Toxic and nutrient elements in yerba mate (Ilex paraguariensis), Food Addit. Contam. B 8 (3) (2015) 215–220, https://doi.org/10.1080/19393210.2015.1053420.

Analytica Chimica Acta 1147 (2021) 1–14

Contents lists available at ScienceDirect

Analytica Chimica Acta

journal homepage: www.elsevier.com/locate/aca

Multi–mode Sample Introduction System (MSIS) as an interface in the hyphenated system 2 HPLC–MSIS–ICP–OES in simultaneous determination of metals and metalloids species

Jędrzej Proch , Przemysław Niedzielski *

Adam Mickiewicz University, Faculty of Chemistry, Department of Analytical Chemistry, Uniwersytetu Poznańskiego 8, 61–614, Poznań, Poland

HIGHLIGHTS

- The new interface in hyphenated technique has been applied for multielemental analysis.
- The hyphenated technique HPLC/HPLC-MSIS-ICP-OES had been optimised and validated.
- The application for routine speciation analysis has been elaborated for different matrixes.

ARTICLE INFO

Article history:
Received 5 September 2020
Received in revised form
10 November 2020
Accepted 23 December 2020
Available online 27 December 2020

Keywords:
Hyphenated systems
Liquid chromatography
Inductively coupled plasma optical emission spectrometry
Multi–mode sample introduction system
Speciation analysis

ABSTRACT

The paper presents a usage of a new hyphenated technique, wherein a Multi–mode Sample Introduction System (MSIS) was applied as an interface of two high pressure liquid chromatography units and inductively coupled plasma optical emission spectrometry (2 HPLC–MSIS–ICP–OES). Simultaneous separation and detection of non–hydride forming and hydride forming elements was possible due to the application of two different HPLC column, cation–exchange and anion–exchange respectively. The method was able to determine 15 elements quantitatively with a distinction of three arsenic and two iron species and it was validated obtaining acceptable LODs (2.67–28.7 μg L^{-1}) and recoveries (80–120%). The method applicability was presented and confirmed on 5 varied sample matrix types i.e. post–glacial sediments, yerba mate *(Ilex paraguariensis)*, soil samples located in the proximity of industry wastes disposal site, river sediments, and archaeological pottery. In addition to the above, unknown Cu, Fe, Mn and Zn species were detected in real samples (qualitative speciation analysis) and the identification was attempted according to the literature.

1. Introduction

A simultaneous determination with a separation of element species plays an important role in modern analytical chemistry. A separation of element species using reverse phase (RP) high performance liquid chromatography (HPLC) or ion–exchange chromatography (IC) is one of the most satisfying procedure in speciation studies [1]. The choice of a mobile phase seems to be crucial in chromatographic separation conditions and efficiency. The usage of pyridine–2,6–dicarboxylic acid (PDCA) as a mobile phase component was described by Janvion et al. [2]. Two mixed–bed resin columns were compared in the IC with a diode–array detector at 520 nm. What is crucial, authors used a mixture of PDCA and acetic acid as the mobile phase to separate Cu, Co, Fe(III), Ni, Zn. Another significant usage of IC for the simultaneous determination of transition metals was presented in 1997. The selective separation of eight metals, i.e. Cd, Co, Cu, Fe(II), Fe(III), Mn, Ni, Zn, was obtained in 20 min and a variable wavelength absorbance detector at 530 nm was used. The method was applied to the analysis of natural and waste waters related to the maintenance of a sewage treatment plant [3]. What is more, authors presented the eluent based on pyridine–2,6–dicarboxylic acid (PDCA) which is able to separate Fe(II) and Fe(III) using ion–exchange column, Dionex IonPac CS5A (Thermo Fisher Scientific, USA). The same method was presented by Atanassova et al. for determining the transition metals in protein [4]. Chen et al. presented the method to determine Fe species using IC with chemiluminescence detection (CLD) [5]. Unfortunately, all above

* Corresponding author.
E-mail address: pnied@amu.edu.pl (P. Niedzielski).

https://doi.org/10.1016/j.aca.2020.12.047
0003-2670/

methods with dedicated detectors for HPLC or IC systems e.g. require a usage of an additional post–column reagents such as 4–(2–pyridylazo) resorcinol (PAR) [2–4] and luminol [5] to obtain or to increase the analytical signal. The most desirable way is to introduce the post–column solution directly to the detector.

In 1999, Guerin et al. collected numerous speciation analysis of arsenic and selenium compounds by HPLC hyphenated to specific detectors [1]. Nonetheless, inconsiderable amount of methods allowed for simultaneous determination As and Se in the one run. The development and higher accessibility of spectrometry techniques, especially ICP–OES with echelle fixed–grating, gave new possibilities of multi-elemental determination and speciation analysis. Primarily, hyphenated systems based on ICP–OES could be complementation, not an alternative to the commercially available devices such as HPLC–ICP–MS [6]. Secondarily, these spectrometers allow to determine co–eluting elements in comparison with conventional liquid chromatography (LC) detectors. Therefore, hydride generation reaction (HG), coupled originally with atomic absorption spectrometry (AAS) [7] was adapted to various studies with optical emission spectrometry (OES) and mass spectrometry (MS) in metalloids determination such as As, Bi, Sb, Pb, Se, Te or Sn [8].

A modified cyclonic spray chamber, Multi–mode Sample Introduction System (MSIS) (Marathon Scientific, Ontario, Canada), is able to work in dual–mode i.e. plays a role of conventional spray chamber with pneumatic nebulizer (PN mode) and hydride generator (HG mode) simultaneously. McLaughlin and Brindle presented the first usage of the MSIS unit with inductively coupled plasma optical emission spectrometry (ICP–OES) as either a hydride generator or as a conventional spray chamber, separately or simultaneously [9]. Since then, the dual–mode of MSIS was used several times with different types of spectrometry i.e. ICP–OES [10–14], MIP–OES [15–17], ICP–MS [18] in determination of volatile hydride forming (e.g. As, Sb, Se, Sn) and non–hydride forming (e.g. Ca, Cu, Fe, Zn) elements. It is worth mentioning that above methods were used to determine elements in various sample types i.e. food products [10], leaves and branches [18], sediments and soils [12,15], agricultural samples [16], metallurgical samples [11], mineral water [17] and wastewater [13,14]. Nowadays (2020), the main weakness of the present research paper is the determination of total contents of elements. However, multi elemental speciation analyses were performed only with HPLC–ICP–MS. The method of the speciation analysis of As(III), As(V), Cr(VI), Mo(VI), Sb(III), Sb(V), Se(IV), Se(VI) and V(V) in leachates from cement-based materials is worth mentioning here as the most interesting example. Authors determined six element species, however as oxyanions only [19]. What is more, a lack of new methods for fast simultaneous determination of Fe species is surprising in comparison to metalloids (e.g. As, Sb, Se) and other metals (e.g. Al, Cr, Hg) [20,21].

In the literature, there are two significant studies with the usage of the MSIS unit as an interface between HPLC and optical emission spectrometry. Al–Assaf et al. used HPLC with MSIS as a post–column hydride generator coupled to ICP–OES and determined four arsenic species i.e. As(III), As(V), monomethylarsonate (MMA) and dimethylarsinate (DMA) in soils with satisfying limits of detection (LODs), 0.4 μg L^{-1} (As(III) and DMA) and 1.0 μg L^{-1} (As(V) and MMA). However, a long extraction of soils was necessary to obtain these results. Described sample preparation was a two–stage procedure: shaking for 24 h in 0.1 M phosphoric acid followed by shaking for 24 h extraction in 1.0 M sodium hydroxide solution [22]. Therefore, the usage of MSIS was limited to HG work mode. In turn, Barrientos et al. presented MSIS as a connector of ion–pair RP–HPLC and MIP–OES for determination of Se(IV) and Se(Met) in biofortified yeast [23]. In this case, the system was expanded by an additional post–column reaction loop which was required to oxidize organic selenium compounds. What is more, commercial available MIP–OES is unable to simultaneously determine the elements in conjunction with the use of a sequential optical system which is a Czerny–Turner monochromator. According to the published papers, no authors have used the potential of dual–mode the MSIS unit in simultaneous separation and detection of elements occurring in cationic, anionic and inert forms.

This study is a significant extension and a continuation of the research with the MSIS unit as an interface between HPLC and ICP–OES [24]. The novelty of this research is a performance of two different HPLC units coupled with the ICP–OES through the MSIS (dual–mode). Cation–exchange column (first HPLC unit) was employed and PCDA eluent was introduced in the conventional mode of MSIS (with pneumatic nebulizer). Simultaneously, anion–exchange column (second HPLC unit) was employed and eluent introduced with in–spray chamber hydride generation mode of the MSIS. Therefore, the first system was used to separate metals e.g. Fe(II) and Fe(III) instead of the second one which was able to volatile hydride forming elements e.g. As(III) and Se(IV). Moreover, no reducing, oxidizing or complexing agents were used post–column instead of published HPLC and IC solutions.

2. Materials and methods

2.1. Gases and reagents

High–pure argon (N–5.0, purity 99.999%), obtained from Linde (Poland), was employed as a plasma gas. All reagents were diluted by high–pure deionized water (≥18 MΩ cm resistivity) obtained from a Milli–Q water purification system (Millipore, USA).

Commercial standard solutions were obtained from Romil (England). Sodium arsenite, disodium hydroarsenate hepahydrate and cacodylic acid were obtained from Sigma–Aldrich (USA). Ferrous ammonium sulfate hexahydrate and ferric ammonium sulfate dodecahydrate were collected from Acros Organics (USA). Stock standard solutions of arsenic and iron (1000 mg L^{-1} in a single solution) were prepared by dissolving appropriate amounts of powder in water. Less concentrated standard solutions obtained by a dilution of the stock solutions were prepared daily. Stock standard solutions were stored in glass bottles at 4 °C in darkness.

Optimal HG reagents and phosphate buffer concentrations were chosen previously [24] and 1.0% (w/v) sodium tetrahydroborate ($NaBH_4$), were prepared daily, by dissolving appropriate amounts of powdered $NaBH_4$ (Sigma–Aldrich) in water and stabilized with 0.1% (w/v) NaOH (Merck). 5 M HCl solution were prepared from 30% HCl (Suprapur®, Merck). A phosphate buffer was prepared by mixing disodium hydrophosphate (Na_2HPO_4) and potassium dihydrophosphate ($KH_2PO_4 \cdot 2H_2O$) obtained from Merck. Appropriate amounts of powder reagents were dissolved and mixed to obtain the mobile phase solution, 25 mM $KH_2PO_4 \cdot 2H_2O$ and 2.5 mM Na_2HPO_4 adjusted to pH 6.0 ± 0.2. A PDCA eluent was prepared by mixing appropriate volumes of pyridine–2,6–dicarboxylic acid (PDCA) and formic acid (HCOOH) (Sigma–Aldrich), then appropriate amounts of potassium hydroxide (KOH) and potassium sulfate (K_2SO_4) (Merck) were dissolved and the solution was filled up with deionized water to the final volume. Final molar concentrations of PDCA, KOH, K_2SO_4 and HCOOH were 7.0, 66, 5.6 and 74 mM respectively and pH was fixed and adjusted to 4.2 ± 0.2.100 mM sodium sulfite (Merck) was obtained by dissolving appropriate amounts of powder (Na_2SO_3) in water and the solution was used to the periodic column condition.

2.2. Instrumentation

The hyphened technique, 2 HPLC–MSIS–ICP–OES with MSIS as

an interface is shown in Fig. 1. The first HPLC system was repeated [24] and constructed from a HPLC pump, Shimadzu LC–10AT (Shimadzu, Japan) and an anion–exchange HPLC column, Supelco LC–SAX1, 250 mm × 4.6 mm i.d., resin particle size 5 μm (Supelco, Germany). Mobile phase flow rate was isocratic at 1 mL min^{-1} and an injection volume (sample loop volume) was 200 μL. PEEK tubing, which was used to transfer the LC column eluent from the MSIS unit was inserted into a Tygon sleeve. The outlet of the anion–exchange HPLC column was connected with the tube which supplied HCl using T–shape connecter and these reagents were introduced both to vertical–placed inlet of the MSIS unit. The second HPLC system was constructed from a HPLC pump, Shimadzu LC–10AT (Shimadzu, Japan) and a cation–exchange HPLC column, Dionex IonPac CS5A, 250 mm × 4.0 mm i.d., resin particle size 5 μm (Thermo Fisher Scientific, USA). Mobile phase flow rate was isocratic at 1 mL min^{-1} and an injection volume (sample loop volume) was 200 μL. PEEK tubing, which was used to transfer the LC column eluent from the MSIS unit, was inserted into a Tygon sleeve. The outlet of the cation–exchange HPLC column was connected with the nebulizer sample channel. Worth mentioning is that cohesion of the introduced phase (eluent from the column) allowed a direct eluent introduction (peristaltic pump avoiding) to the MSIS unit by nebulizer and HG channel.

The MSIS unit (Marathon Scientific, Canada) was a hydride generation system and an interface between two HPLC units and ICP–OES. Due to dual–mode work, the MSIS was simultaneously a conventional spray chamber with pneumatic nebulizer and a hydride generator. The nebulizer provided post cation–exchange column solution and the HG process was possible due to inlets located vertically in the centre of this unit. HG reagents were delivered to the chamber, mixed at the top of the inlets and volatile hydrides were formed and carried with gas (argon) from the MSIS unit to ICP torch. The upper inlet of the unit was used to provide $NaBH_4$ solution. The lower inlet provided HCl solution and post anion–exchange column reagents (an eluent with sample solution). Additionally, the MSIS unit had a function of gas–liquid separator and due to this, the excess liquid was carried from the chamber using a peristaltic pump. The waste liquid flow rate was proportional to the sum of HG reagents flow rates.

The inductively coupled plasma optical emission spectrometer, Agilent 5110 ICP–OES (Agilent Technologies, USA), was used as a detector of the hyphenated system. The synchronous vertical dual view (SVDV) of the plasma was used in this study and allowed the axial and radial view analyses simultaneously. RF power was set up at 1450 W (maximum value). Nebulizer and auxiliary argon flow rates were 0.7 L min^{-1} and 1.0 L min^{-1} respectively. HG reagents were pumped continuously to the MSIS unit with flow rates established at 1 mL min^{-1} and the peristaltic pump speed set at 12 rpm. Echelle grading fixed optic was thermostated at 35 °C and a detector, VistaChip II with the Charge Coupled Device (CCD) was cooled to −40 °C using triple Peltier system. The analytical signal response (intensity) [cps] was read according to the time of analysis. Analytical wavelengths (emission lines) of elements were chosen according to available data, both literature and instrument software. All instrumental parameters for HPLC–HG–ICP–OES are shown in Table 1.

2.3. Sample preparation

Sample preparation procedure was repeated after Proch & Niedzielski [24]. Accurately weighted 1.00 (±0.01) g of a dry sample was placed in polyethylene test tube. 8 mL of 1 M orthophosphate acid (H_3PO_4) was added to each sample and the ultrasound assisted extraction was conducted for 30 min at ambient temperature. In the next step, samples were filtered using a paper filter, which had been washed with 200 mL of high–pure deionized water and 20 mL of phosphate buffer. Sample solutions were neutralized with a few drops of 15 M NaOH to obtain pH value in the range of 6.0–6.5 and filled up to the final volume of 10 mL. Samples were determined rapidly after preparation.

3. Results and discussion

3.1. Instruments optimization

The hyphenated system presented in this work is a simple modification of HPLC–HG(MSIS)–ICP–OES [24] due to the addition of a cation–exchange HPLC working independently of the

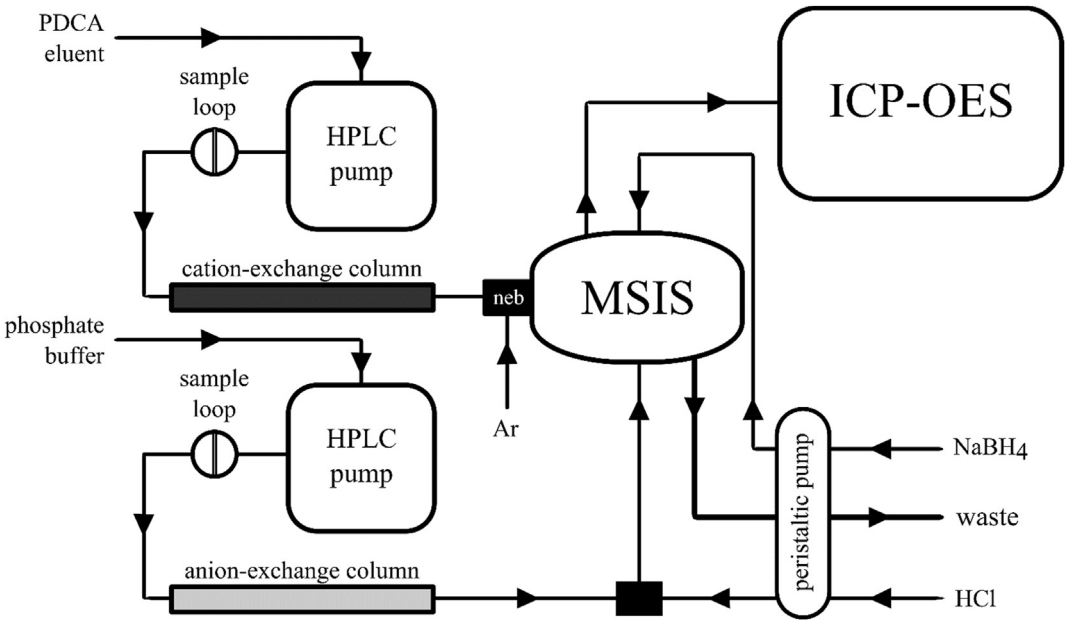

Fig. 1. General scheme of described technique, 2 HPLC–MSIS–ICP–OES.

Table 1
Experimental conditions for 2 HPLC–MSIS–ICP–OES.

HPLC conditions		
Pump	Shimadzu LC–10AT	Shimadzu LC–10AT
Column	Dionex IonPac CS5A, (250 mm × 4.0 mm i.d., 5 μm)	Supelco LC–SAX 1, (250 mm × 4.6 mm i.d., 5 μm)
Mobile phase composition	PDCA eluent, 7.0 mM pyridine–2,6–dicarboxylic acid (PDCA), 66 mM potassium hydroxide (KOH), 5.6 mM potassium sulfate (K_2SO_4), 74 mM formic acid (HCOOH)	Phosphate buffer, 2.5 mM disodium hydrophosphate (Na_2HPO_4), 25 mM potassium dihydrophosphate (KH_2PO_4 $2H_2O$)
pH	4.2 ± 0.2	6.0 ± 0.2
Mobile phase flow rate [mL min^{-1}]	1.0	1.0
Injection volume [mL]	0.2	0.2
MSIS parameters		
Work mode	dual–mode	
Sample channel	nebulizer (pneumatic)	hydride generation (lower inlet)
Hydride generation parameters		
$NaBH_4$ concentration [%, w/v]	n/a	1.0
NaOH concentration [%, v/v]	n/a	0.1
HCl concentration [mol L^{-1}]	n/a	5.0
$NaBH_4$ flow rate [mL min^{-1}]	n/a	1.0
HCl flow rate [mL min^{-1}]	n/a	1.0
ICP–OES conditions		
Spectrometer	ICP 5110 Dual–View	
RF generator [MHz]	27	
RF power [W]	1450	
Nebulizer gas flow rate [L min^{-1}]	0.7	
Plasma gas flow rate [L min^{-1}]	12	
Auxiliary gas flow rate [L min^{-1}]	1.0	
Peristaltic pump speed [rpm]	12	
Nebulizer/spray chamber type	pneumatic/MSIS	
Torch view	synchronous vertical dual view (SVDV)	
Analytical wavelengths [nm]	As 228.812, Cd 214.439, Co 238.892, Cu 327.395, Fe 234.350, Ge 209.426, Mn 257.610, Ni 231.604, Pb 220.353, Ru 240.272, Se 196.026, Sr 460.733, Tl 190.794, V 292.401, Zn 213.857	

n/a – not applicable.

anion–exchange HPLC. The outlet of additional column (cation–exchange, CS5A) was connected with a pneumatic nebulizer instead of Proch & Niedzielski, where it stayed blocked. Nevertheless, a nebulization process does not affect HG process which was reported repeatedly [9–11]. Moreover, elaborate optimization of MSIS (including HG reagents flow rates and concentrations) and ICP–OES (including RF and plasma gas flow rate) was conducted for As species determination before and these conditions were repeated [24]. Nebulizer and auxiliary gas flow rates were 0.7 and 1.0 L Ar min–1 respectively. Worth noting, SVDV was used instead of axial torch view (Table 1).

In the short optimization procedure of HPLC systems, mobile phase flow rates were investigated. In the range from 1.0 to 2.0 mL min^{-1} (per column), the optimal condition was 1.0 mL min^{-1}. It was mainly related to the limited volume and the structure of MSIS. The optimization procedure of the HPLC with SAX–1 were not conducted and optimal conditions were repeated [24] (Table 1). Due to lower mobile phase flow rate (1.0 mL min^{-1} instead of 2.0 mL min^{-1}) standard solutions contained 1000 μg L^{-1} of As(III), As(V) or DMA were carried out in one solution to redefine retention time [s] of these species. No significant changes were observed in peak shapes and heights for mentioned arsenic species.

The optimization procedure of the HPLC with CS5A column was conducted according to the application note and the literature. The concentration of PCDA eluent, 7.0 mM PDCA, 66 mM KOH, 5.6 mM K_2SO_4 and 74 mM HCOOH adjusted to pH 4.2, was repeated after Cardellicchio et al. [3] and Atanassova et al. [4]. It is notable that Chen et al. [5] conducted the composite optimization and optimal conditions were 10 mM PDCA, 33 mM KOH, 80 mM KCl and 37 mM HCOOH adjusted to pH 4. However, the increase of salt load on ICP (such as chlorides or sulfates) may cause several problems, including nebulizer clogging, ionization interferences, plasma instability and extinction, even torch damage [25]. According to this, other examples of phase based on PDCA avoid a salt addition and offered specific usage. In the literature, PDCA solutions were mixed with ammonium citrate to determine redox species of Cu, Fe and Mn [25]. To determine Fe(II) and Fe(III) in biological sample, PDCA with acetate buffer [26] or Tris–HAc and NH_4Ac were used [27]. To keep up correct results of Fe(II) and Fe(III), cation–exchange column was periodically conditioned with 100 mM sodium sulfite to eliminate any oxygen build–up on the column (in accordance with the product manual). The changes of retention time within longer time intervals (longer than a month) were observed during an analytical work. According to this, periodic controls were conducted with a single element form standard solutions to confirm respective retention times. Typical chromatograms of standard solution were presented in Fig. 2.

3.2. Analytical figures of merit

The quantification of 13 species of metals: Cd(II), Co(II), Cu(III), Fe(III), Fe(II), Mn(II), Ni(II), Pb(II), Ru(III), Sr(II), Tl(I), V(V), Zn(II) (cation–exchange column) with simultaneous quantification of 5 metalloids species: As(III), As(V), DMA, Ge(IV), Se(IV) (anion–exchange column) were employed. 16 investigated species obtained broad linear range of calibration curve (from LOQ to 10000 μg L^{-1}) due to up to 10–points calibration and acceptable coefficient of determination ($R^2 > 0.9900$). Calibration curves for As(V) and Sr(II) obtained R^2 values slightly below $R^2 > 0.9900$ and were 0.9891 and 0.9894 respectively. Calibration curves of Ge(IV) and V(V) were investigated in the ranges 1.00 and 5000 μg L^{-1} only. What is more, the aforementioned results were better than reported [5,25,28] and the method was able to work in broad range of concentration, from 10 to 10000 μg L^{-1}. Acceptable limits of detection (LOD<20.0 μg L^{-1}) were measured for investigated elements except 21.5, 24.4, 24.6 and 28.7 μg L^{-1} for Ru(III), Tl(I), Pb(II)

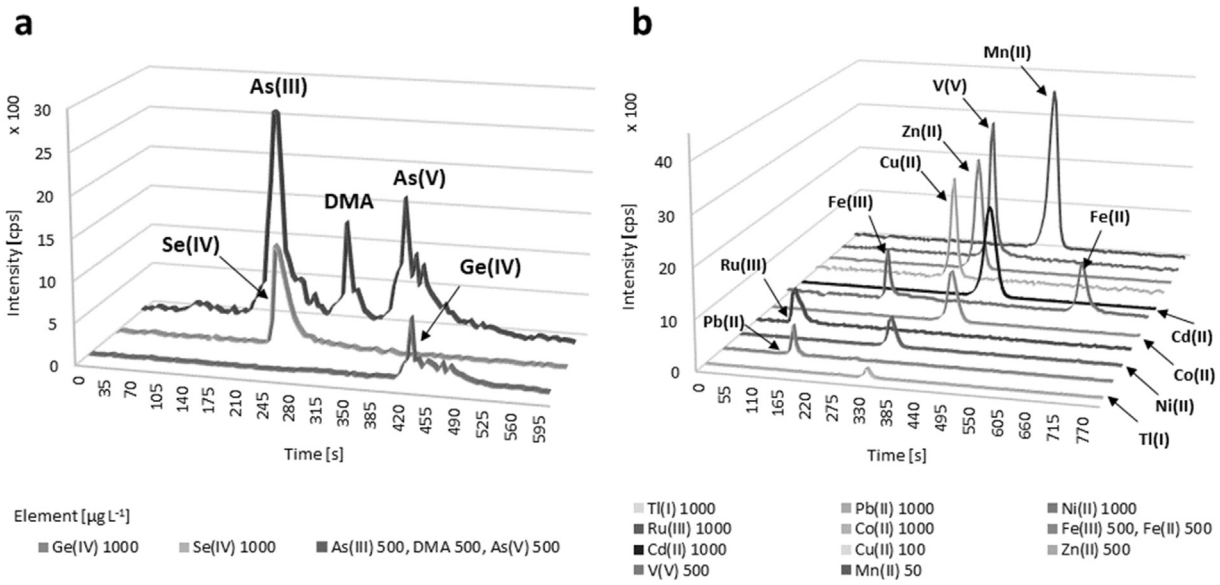

Fig. 2. Typical chromatograms of standard solutions obtained by 2 HPLC–MSIS–ICP–OES presenting separation of (a) anion–exchange chromatography (SAX–1) and (b) cation–exchange chromatography (CS5A) in experimental conditions.

and Sr(II) respectively. On one hand, measured LODs were slightly higher than reported. On the other hand, in the comparison with these methods, the system advantages were: more selectivity: IC–Vis [3], IC–CLD [5] and more multi elemental: HPLC–HG(MSIS)–ICP–OES [22], HPLC–HG(MSIS)–MIP–OES [23], SS–MSIS–MIP–OES [15], HPLC–ICP–MS [25]. Satisfactory precision (as RSD) [%] was measured for 17 species (RSD<20%) with Sr(II) as exception (RSD = 26% at 100 µg L^{-1}). High RSD of strontium is related to high LOD and LOQ values, 28.7 and 86.2 µg L^{-1}. This trend is observed for Tl(I) (RSD = 13% at 100 µg L^{-1}) whose LOD and LOQ was 24.4 and 73.2 µg L^{-1} respectively. Unfortunately, it was similar to investigated concentration in the precision measurement (100 µg L^{-1}).

Retention times of elements were in the range from 80 to 635 s for cation–exchange column (C5SA) and 190–425 s for anion–exchange column (SAX–1). Void time was 70 and 90 s for CS5A and SAX–1 respectively. Single–element chromatograms gave an information about significant peak resolution. Peak areas were proportional to the height in the investigated range for all investigated elements. Furthermore, in a view of asymmetry and peak shape variability (dispersion) only calculations of peak areas were used in samples determination. In the case of iron speciation analysis, retention times of Fe(II) and Fe(III) were measured at 630 and 230 s respectively. In the case of other elements, obtained results were much better in comparison with HPLC or IC systems based on the same column (C5SA) and mobile phase (PDCA buffer) [4,26,28]. On one hand, Chen et al. [5] obtained better retention times for iron species with Fe(II) elution within ca. 6 min. On the other hand, author confirmed that higher concertation of salt makes retention times shorten and used 80 mM KCl instead of 5.6 mM K_2SO_4 in this research. Retention times are marginally worse in comparison with the HPLC–IPC–MS [25], however, this system is more specific and redox species of Cu, Fe and Mn were determined only. As(III), As(V) and DMA obtained significant better peak resolution which may relate to a decrease of mobile phase flow rate in comparison with Proch & Niedzielski [24]. The response of As(III) was two times more intensive than signals of As(V) and DMA at the same standard solution. Contrarily, the similar signal disproportion of these arsenic species was observed in literature [29]. Complete data of analytical figures of merit and retention times were presented in Table 2.

There is a certified reference material (CRM), which allows to determine As(III), As(V) and DMA (ERM®–BC211) whereas there is a lack of reference materials for arsenic species in samples extracted by phosphoric acid [30]. What is more, the method was applied for a simultaneous determination of 15 elements, including Fe and As species separation in different sample matrix types. Therefore, the standard addition method was chosen for accuracy measurements. Standard solutions of each element were added in two concentrations (low and high) to the final extracts volumes of two different real samples, organic (P1) and inorganic (P2). Final concentrations of standards in sample solutions were established individually due to the range of calibration curves and calculated LOQs. Acceptable recoveries (80–120%) were presented for each sample matrix type. Complete data of standard addition recoveries were showed in Table 3.

3.3. Application

The applicability of the method 2 HPLC–MSIS–ICP–OES was presented with different sample matrix types. According to this, five groups of real samples were analysed: (A) post–glacial sediments from Spitsbergen, Svalbard (n = 8), (B) yerba mate *(Ilex paraguariensis)* available on the Polish market (n = 8), (C) soil samples located in the proximity of industry wastes disposal site (n = 5), (D) river sediments obtained from Mekong, Vietnam (n = 5) and (E) archaeological pottery (n = 6). Assuming high contamination level of metals and metalloids, samples were diluted respectively. The uncertainty for complete analytical process (including sample preparation) was at the level of 20%.

The first group contained environmental samples, i.e. post–glacial sediments from Spitsbergen, Svalbard (A1–A8). The results were presented in Table 4. From investigated elements, only Cd(II) was undetectable (<LOD) in all samples. Cu(II), Fe(II), Fe(III), Mn(II), Ru(III) and Sr(II) were found in all samples. According to the aim of the application, the discussion was focused on arsenic and iron speciation analyses results. Arsenic species were found above LODs in 7, 2 and 4 samples for As(III), DMA and As(V) respectively.

Table 2
Analytical figures of merit (n = 3, peak area).

	Column	Retention time [s]	R^2	LOD (as 3σ)		LOQ (as 3 LOD)		Linear range of calibration curve [μg L^{-1}]	Precision (as RSD) [%]
				[μg L^{-1}]	[μg kg^{-1}]	[μg L^{-1}]	[μg kg^{-1}]		
As(III)	SAX 1	190	0.9960	6.19	62.0	18.6	186	LOQ–10000	4.5 (at 100 μg L^{-1})
DMA	SAX 1	290	0.9942	11.9	119	35.8	358	LOQ–10000	8.3 (at 100 μg L^{-1})
As(V)	SAX 1	375	0.9891	10.2	102	30.7	307	LOQ–10000	7.5 (at 100 μg L^{-1})
Cd(II)	CS5A	430	0.9938	7.68	76.7	23.0	230	LOQ–10000	1.9 (at 100 μg L^{-1})
Co(II)	CS5A	400	0.9990	12.1	121	36.3	363	LOQ–10000	1.4 (at 100 μg L^{-1})
Cu(II)	CS5A	325	0.9992	3.79	38.0	11.4	114	LOQ–10000	3.8 (at 100 μg L^{-1})
Fe(II)	CS5A	655	0.9936	10.4	104	31.2	312	LOQ–10000	2.7 (at 100 μg L^{-1})
Fe(III)	CS5A	230	0.9906	13.4	134	40.3	403	LOQ–10000	4.2 (at 100 μg L^{-1})
Ge(IV)	SAX 1	425	0.9965	8.45	84.3	25.3	253	LOQ–5000	11 (at 500 μg L^{-1})
Mn(II)	CS5A	490	0.9949	5.90	59.0	17.7	177	LOQ–10000	2.1 (at 100 μg L^{-1})
Ni(II)	CS5A	325	0.9991	11.2	112	33.5	335	LOQ–10000	0.9 (at 100 μg L^{-1})
Pb(II)	CS5A	150	0.9966	24.6	246	73.7	737	LOQ–10000	6.9 (at 100 μg L^{-1})
Ru(III)	CS5A	80	0.9992	21.5	215	64.5	6450	LOQ–10000	11 (at 500 μg L^{-1})
Se(IV)	SAX 1	215	0.9994	2.67	26.7	8.02	80.2	LOQ–10000	9.6 (at 100 μg L^{-1})
Sr(II)	CS5A	635	0.9894	28.7	287	86.2	862	LOQ–10000	26 (at 100 μg L^{-1})
Tl(I)	CS5A	335	0.9940	24.4	244	73.2	732	LOQ–10000	13 (at 100 μg L^{-1})
V(V)	CS5A	365	0.9954	2.09	20.9	6.27	62.7	LOQ–5000	5.9 (at 50.0 μg L^{-1})
Zn(II)	CS5A	355	0.9992	9.94	99.3	29.8	298	LOQ–10000	2.8 (at 100 μg L^{-1})

LOD– limit of detection: instrumental [μg L^{-1}] and method [μg kg^{-1}] (including sample preparation procedure); LOQ– limit of quantification: instrumental [μg L^{-1}] and method [μg kg^{-1}]; RSD – relative standard deviation.

As(III) was detected more commonly but in the lowest content for three arsenic species, in the range from 1.81 to 2.39 (±0.20 as ± SD) mg kg^{-1} instead of As(V) was found in the maximum content in four samples, in the range from 2.52 to 4.18 (±0.61) mg kg^{-1}. Moreover, the ratio of inorganic As species, As(ratio) = As(V)÷As(III), was calculated for 4 samples and contained in the narrow range, from 1.2 to 2.3 (median = 1.6). DMA was determined in two samples, 2.19 (A6) and 3.46 (A8) mg kg^{-1} respectively. Iron species were found in all samples (n = 8) in wide ranges, 161–2351 (±817) and 1736–8446 (±2284) mg kg^{-1} for Fe(II) and Fe(III) respectively. Fe(sum), i.e. Fe(II)+Fe(III), was calculated, 2528–8616 (±2076) mg kg^{-1} and results were comparable to arctic sediments from Svalbard [31] or to similar sample matrix types [32,33]. Additionally, Fe(ratio), i.e. Fe(III)÷Fe(II), was calculated. On one hand, ratios of Fe(III) to Fe(II) were contained in the wide range, from 1.7 to 52 (median = 4.5). On the other hand, the dominance of Fe(III) was observed in the whole population (n = 8). It is surprising that pairs of samples showed a similarity in Fe(ratio) i.e. 6.6, 6.5 (A1–A2), 2.5, 2.2 (A3–A4), 1.8, 1.7 (A5–A6) and 52, 50 (A7–A8). Additionally, it should be mentioned that all real samples (A–E) were chosen randomly. However, the Fe(ratio) similarity might be significant as an environmental marker and its measurement could be a new routine part of environmental analyses. Occurring of As(III) only along with low Fe(ratio), might suggest that these samples came from reducing environment e.g. anaerobic conditions (A1–A3). The domination of Fe(III), high Fe(ratio) and high levels of As(V) (rarely DMA) might suggest the oxidizing environment (A7–A8). Low Fe(ratio), <2.2, along with high As(ratio), >1.5, would suggest that samples came from mixed environment (periodically or in moderate aerobic conditions) (A4–A6). Results for other detected elements such as Cu, Mn, Ni, Pb, Sr, V and Zn were comparable with [31–33].

The second group consisted of food samples representing by yerba mate *(Ilex paraguariensis)* samples (B1–B8), available on the Polish market. The results were presented in Table 5. In the case of yerba mate tea, As, Cd and Pb contents are monitored regularly. The ANVISA Resolution RDC No. 42 of August 29, 2013, which internalizes the MERCOSUL Technical Regulation on Maximum Limits of Inorganic Contaminants in Food in Brazil, recommends the following maximum limits in teas, herbs and other vegetables used for infusions: 0.4 mg kg^{-1} (Cd) and 0.6 mg kg^{-1} (As and Pb) [34,35]. From investigated elements, As(III), DMA, Cd(II), Co(II), Ge(IV), Ru(III), Tl(I), V(V) were found below limit of quantification (<LOQ) in all samples. Cu(II), Fe(III), Mn(II), Ni(II) and Sr(II) were found in all samples. Determination of As species has not been performed on yerba mate *(Ilex paraguariensis)* yet expects the introduction [24]. From investigated species, only As(V) was determined in three samples. Results were slightly above LOQ, 0.31–0.33 (±0.01) mg kg^{-1}. Nevertheless, measured concentrations of As species were 4–5 times higher than As total concentration in the literature [34–38]. Lead was found in sample B8 only, however, the content was 2.6 times higher (1.56 mg kg^{-1}) according to recommended limit (0.6 mg kg^{-1}) [34]. Exceeding the Pb limit was reported by Ref. [38]. In the case of iron species, Fe(III) was found in all samples (n = 8) in the range from 1.33 to 19.1 (±6.97) mg kg^{-1}. Fe(II) was determined in 4 samples, 3.07–7.05 (±1.20) mg kg^{-1}. For these samples, Fe(ratio) was contained in the narrow range, 2.2–3.0 (median = 2.8). The dominance of Fe(III) was observed in the whole population and it could confirm the implication of the oxidizing conditions of the production process of yerba mate tea. Results for the other detected elements such as Cu, Fe, Mn, Ni, Sr and Zn were comparable with the literature [36,37]. In the case of Se(IV), results were 3–4 times higher, 0.37–0.42 mg kg^{-1} than reported before [39].

The third group was represented by soil samples located in the proximity of industry wastes disposal site (C1–C5). Results were shown in Table 6. From investigated elements, only Ge(IV) was undetectable (<LOD) in all samples. As(III), As(V), Cu(II), Fe(II), Fe(III), Mn(II), Ni(II), Ru(III), Sr(II) and V(V) were found above LODs in all samples (n = 8). In the opposition to Proch & Niedzielski [24], the total content of As species was significantly lower, 3.81–20.3 (±6.08) mg kg^{-1}. In the literature, similar results of arsenic were found in soils from metallurgical site (3.19–9.16 mg kg^{-1}), mining site (17.4–50.0 mg kg^{-1}) [40], proximity of mining area (≤44.4 mg kg^{-1}) [41]. As(III) was detected in the narrow range, 1.70–4.32 (±0.93) mg kg^{-1} instead of As(V), 2.11–10.4 (±3.17) mg kg^{-1}. What is worthy of mention is that the ratios of As(V) to As(III) were significantly varied, 0.6–2.5 (median = 1.7) however the dominance of As(III) was observed in C1 only. DMA was detected in C4 but only because the content was the highest in the sample, 8.83 mg kg^{-1}, same as As(sum), 20.3 mg kg^{-1}. Iron species were found in all samples (n = 5), 7.02–89.7(±31.7) and 54.2–1906

Table 3
Recovery at the addition of standard solution (n = 3, peak area).

	P1			P2		
	Added [μg L^{-1}]	Found [μg L^{-1}]	Recovery [%]	Added [μg L^{-1}]	Found [μg L^{-1}]	Recovery [%]
As(III)	0.0	<18.6	–	0.0	<18.6	–
	100	92 ± 4	92 ± 4	100	101 ± 4	101 ± 4
	500	509 ± 22	102 ± 4	500	522 ± 22	104 ± 4
DMA	0.0	<35.8	–	0.0	<35.8	–
	100	90 ± 7	90 ± 7	100	82 ± 6	82 ± 6
	500	486 ± 38	97 ± 8	500	471 ± 37	94 ± 7
As(V)	0.0	<30.7	–	0.0	<30.7	–
	100	89 ± 6	89 ± 6	100	101 ± 7	101 ± 7
	500	497 ± 35	99 ± 7	500	490 ± 35	98 ± 7
Cd(II)	0.0	<23.0	–	0.0	<23.0	–
	1000	1190 ± 21	119 ± 2	1000	1062 ± 19	106 ± 2
	5000	4394 ± 79	88 ± 2	5000	4092 ± 74	82 ± 1
Co(II)	0.0	<36.3	–	0.0	<36.3	–
	1000	1055 ± 14	106 ± 1±1	1000	1052 ± 14	105 ± 1
	5000	4305 ± 58	86 ± 1	5000	4143 ± 55	83 ± 1
Cu(II)	0.0	32 ± 1	–	0.0	<11.4	–
	1000	996 ± 36	96 ± 3	1000	803 ± 29	80 ± 3
	5000	5419 ± 195	108 ± 4	5000	4067 ± 146	81 ± 3
Fe(II)	0.0	<31.2	–	0.0	<31.2	–
	500	484 ± 12	97 ± 2	500	440 ± 11	88 ± 2
	2500	2415 ± 62	97 ± 2	2500	2915 ± 75	117 ± 3
Fe(III)	0.0	<40.3	–	0.0	4167 ± 173	–
	500	478 ± 19	96 ± 4	500	4698 ± 186	106 ± 4
	2500	2459 ± 97	98 ± 4	2500	6818 ± 269	106 ± 4
Ge(IV)	0.0	<25.3	–	0.0	<25.3	–
	1000	496 ± 51	99 ± 10	1000	1069 ± 109	107 ± 11
	5000	2300 ± 235	92 ± 9	5000	4041 ± 412	81 ± 8
Mn(II)	0.0	506 ± 11	–	0.0	3033 ± 65	–
	1000	1504 ± 31	100 ± 2	1000	4117 ± 84	108 ± 2
	5000	4635 ± 94	83 ± 2	5000	8778 ± 179	115 ± 2
Ni(II)	0.0	<33.5	–	0.0	<33.5	–
	1000	1075 ± 10	108 ± 1106±1	1000	1058 ± 10	105 ± 1
	5000	4436 ± 40	88 ± 1	5000	4897 ± 44	98 ± 1
Pb(II)	0.0	<73.7	–	0.0	<73.7	–
	1000	926 ± 61	93 ± 6	1000	1159 ± 76	116 ± 8
	5000	5938 ± 391	119 ± 8	5000	5710 ± 376	114 ± 8
Ru(III)	0.0	162 ± 18	–	0.0	212 ± 23	–
	1000	1010 ± 106	85 ± 9	1000	1366 ± 143	115 ± 12
	5000	4584 ± 481	88 ± 9	5000	4304 ± 452	82 ± 9
Se(IV)	0.0	<8.02	–	0.0	<8.02	–
	100	114 ± 10	114 ± 10	100	96 ± 9	96 ± 9
	500	593 ± 54	119 ± 11	500	602 ± 55	120 ± 11
Sr(II)	0.0	294 ± 75	–	0.0	292 ± 75	–
	1000	1339 ± 325	104 ± 25	1000	1316 ± 319	102 ± 25
	5000	5797 ± 1406	110 ± 27	5000	5710 ± 1385	108 ± 26
Tl(I)	0.0	<73.2	–	0.0	<73.2	–
	1000	1036 ± 132	104 ± 13	1000	1030 ± 131	103 ± 13
	5000	5538 ± 703	111 ± 14	5000	5236 ± 665	105 ± 13
V(V)	0.0	<6.28	–	0.0	<6.28413 ± 23	–
	500	543 ± 30	108 ± 6	500	2310 ± 129	83 ± 4
	2500	2326 ± 130	93 ± 5	2500		92 ± 5
Zn(II)	0.0	557 ± 15	–	0.0	729 ± 20	–
	1000	1430 ± 38	87 ± 2	1000	1561 ± 41	83 ± 2
	5000	5505 ± 145	99 ± 3	5000	5971 ± 158	105 ± 3

<xx.x–– below limit of quantification.

(±747) mg kg^{-1} for Fe(II) and Fe(III) respectively. Worth noticing, Fe(III) content was contained in significantly wide range. Fe(sum) was in the range from 61.2 (C1) to 1944 (C4) (±770) mg kg^{-1}. Even though, ratios of Fe(III) to Fe(II) were contained in the wide range, from 7.7 to 71 (median = 17) the substantial domination of Fe(III) was observed in the whole population. Extremely varied condition (aerobic, acidity etc.) were expected in the case of soils located in the proximity of industry wastes disposal site. Due to this, valuable data obtained from As and Fe ratios were questionable (C2–C5). However, As(ratio) < 1.0 and the lowest Fe(ratio) clearly suggested the reducing environment (C1). Results for other detected elements were comparable to a similar sample type matrix with the literature [41], however Se(IV) results, 0.51–0.67 mg kg^{-1}, were 3–4 times lower than reported [15].

The fourth group contained environmental samples, i.e. river sediments from Mekong, Vietnam (D1–D5). Results were shown in Table 7. From investigated elements, only Cd(II), Ru(III) and Tl(I) were found below limit of detection (<LOD) in all samples. Only Cu(II), Fe(III), Ni(II) and Sr(II) were found in all samples. As(III) and As(V) were found above LODs in 3 of 5 samples in the ranges, 1.81 to 3.19 (±0.63) and 2.46 to 5.45 (±1.16) mg kg^{-1}. The ratios of As(V) to As(III) were calculated for two samples only and contained within the narrow range, from 1.5 (D1) to 1.7 (D5). Recently, transformation of As species in deep–sea sediments was reported [42] and results of As(III) and As(V) concentrations and As(ratio) were comparable. However, some authors reported high As

Table 4
Quantification of 18 element species by 2 HPLC–MSIS–ICP–OES for 8 real samples of post–glacial sediments (Spitsbergen, Svalbard) (peak area) [mg kg^{-1}].

	A1	A2	A3	A4	A5	A6	A7	A8
As(III)	1.81 ± 0.36	2.39 ± 0.48	<0.19	1.81 ± 0.36	1.86 ± 0.37	2.17 ± 0.43	1.95 ± 0.39	1.95 ± 0.39
DMA	<0.36	<0.36	<0.36	<0.36	<0.36	2.19 ± 0.44	<0.36	3.46 ± 0.69
As(V)	<0.31	<0.31	<0.31	2.96 ± 0.59	4.18 ± 0.84	2.52 ± 0.50	3.19 ± 0.64	<0.31
As(sum)	1.81 ± 0.36	2.39 ± 0.48	–	4.78 ± 0.96	6.04 ± 1.21	6.89 ± 1.38	5.13 ± 1.03	5.40 ± 1.08
As(ratio)	–	–	–	1.6	2.3	1.2	1.6	–
Cd(II)	<0.23	<0.23	<0.23	<0.23	<0.23	<0.23	<0.23	<0.23
Co(II)	<0.36	<0.36	<0.36	<0.36	3.68 ± 0.74	<0.36	<0.36	<0.36
Cu(II)	19.2 ± 3.8	73.2 ± 14.6	14.1 ± 2.8	15.9 ± 3.2	403 ± 81	11.1 ± 2.2	15.3 ± 3.1	23.9 ± 4.8
Fe(II)	411 ± 82	710 ± 142	1925 ± 385	792 ± 158	1901 ± 380	2351 ± 470	161 ± 32	170 ± 34
Fe(III)	2705 ± 541	4620 ± 924	4800 ± 960	1736 ± 347	3514 ± 703	3979 ± 796	8309 ± 1662	8446 ± 1689
Fe(sum)	3115 ± 623	5329 ± 1066	6725 ± 1345	2528 ± 506	5415 ± 1083	6331 ± 1266	8471 ± 1694	8616 ± 1723
Fe(ratio)	6.6	6.5	2.5	2.2	1.8	1.7	52	50
Ge(IV)	<0.25	<0.25	<0.25	<0.25	<0.25	<0.25	2.29 ± 0.46	<0.25
Mn(II)	172 ± 34	316 ± 63	316 ± 63	157 ± 31	243 ± 49	365 ± 73	441 ± 88	395 ± 79
Ni(II)	<0.34	<0.34	5.63 ± 1.13	<0.34	<0.34	<0.34	<0.34	6.49 ± 1.30
Pb(II)	6.48 ± 1.30	<0.74	<0.74	<0.74	<0.74	<0.74	4.28 ± 0.86	<0.74
Ru(III)	10.6 ± 2.1	12.3 ± 2.5	13.1 ± 2.6	11.3 ± 2.3	13.6 ± 2.7	11.6 ± 2.3	12.6 ± 2.5	14.3 ± 2.9
Se(IV)	1.25 ± 0.25	1.04 ± 0.21	<0.08	<0.08	0.64 ± 0.13	1.25 ± 0.25	0.64 ± 0.13	<0.08
Sr(II)	697 ± 139	685 ± 137	610 ± 122	627 ± 125	764 ± 153	701 ± 140	718 ± 144	760 ± 152
Tl(I)	<0.73	3.32 ± 0.66	<0.73	<0.73	<0.73	<0.73	1.66 ± 0.33	<0.73
V(V)	2.60 ± 0.52	2.50 ± 0.50	2.63 ± 0.53	2.65 ± 0.53	<0.06	<0.06	<0.06	<0.06
Zn(II)	<0.30	38.9 ± 7.8	40.5 ± 8.1	<0.30	51.8 ± 10.4	49.6 ± 9.9	43.2 ± 8.6	60.3 ± 12.1

<x.xx–– below limit of quantification; , As(sum) = As(III)+As(V)+DMA, As(ratio) = As(V)÷As(III), Fe(sum) = Fe(II)+Fe(III), Fe(ratio) = Fe(III)÷Fe(II).

Table 5
Quantification of 18 element species by 2 HPLC–MSIS–ICP–OES for 8 real samples of yerba mate (*Ilex paraguariensis*) obtained from Polish market distribution (peak area) [mg kg^{-1}].

	B1	B2	B3	B4	B5	B6	B7	B8
As(III)	<0.19	<0.19	<0.19	<0.19	<0.19	<0.19	<0.19	<0.19
DMA	<0.36	<0.36	<0.36	<0.36	<0.36	<0.36	<0.36	<0.36
As(V)	0.33 ± 0.07	<0.31	<0.31	<0.31	0.33 ± 0.07	0.31 ± 0.06	<0.31	<0.31
As(sum)	0.33 ± 0.07	–	–	–	0.33 ± 0.07	0.31 ± 0.06	–	–
As(ratio)	–	–	–	–	–	–	–	–
Cd(II)	<0.23	<0.23	<0.23	<0.23	<0.23	<0.23	<0.23	<0.23
Co(II)	<0.36	<0.36	<0.36	<0.36	<0.36	<0.36	<0.36	<0.36
Cu(II)	5.42 ± 1.08	1.07 ± 0.21	0.55 ± 0.11	8.66 ± 1.73	3.43 ± 0.69	1.66 ± 0.33	1.95 ± 0.39	3.25 ± 0.65
Fe(II)	7.05 ± 1.41	<0.36	<0.36	6.96 ± 1.39	5.80 ± 1.16	<0.36	<0.36	3.07 ± 0.61
Fe(III)	15.4 ± 3.1	4.99 ± 1.00	1.62 ± 0.32	19.1 ± 3.8	16.8 ± 3.4	1.33 ± 0.27	1.47 ± 0.29	9.10 ± 1.82
Fe(sum)	22.4 ± 4.5	4.99 ± 1.00	1.62 ± 0.32	26.0 ± 5.2	22.6 ± 4.5	1.33 ± 0.27	1.47 ± 0.29	12.2 ± 2.4
Fe(ratio)	2.2	–	–	2.7	2.9	–	–	3.0
Ge(IV)	<0.25	<0.25	<0.25	<0.25	<0.25	<0.25	<0.25	<0.25
Mn(II)	525 ± 105	155 ± 31	37.2 ± 7.4	1048 ± 210	922 ± 184	10.9 ± 2.2	12.1 ± 2.4	295 ± 59
Ni(II)	5.42 ± 1.08	1.30 ± 0.26	1.30 ± 0.26	5.25 ± 1.05	4.05 ± 0.81	2.67 ± 0.53	1.64 ± 0.33	6.15 ± 1.23
Pb(II)	<0.74	<0.74	<0.74	<0.74	<0.74	<0.74	<0.74	1.56 ± 0.31
Ru(III)	<0.65	<0.65	<0.65	<0.65	<0.65	<0.65	<0.65	<0.65
Se(IV)	0.37 ± 0.07	<0.08	0.42 ± 0.08	0.37 ± 0.07	0.37 ± 0.07	<0.08	0.42 ± 0.08	<0.08
Sr(II)	29.1 ± 5.8	25.7 ± 5.1	23.5 ± 4.7	38.3 ± 7.7	35.5 ± 7.1	25.4 ± 5.1	24.4 ± 4.9	20.2 ± 4.0
Tl(I)	<0.73	<0.73	<0.73	<0.73	<0.73	<0.73	<0.73	<0.73
V(V)	<0.06	<0.06	<0.06	<0.06	<0.06	<0.06	<0.06	<0.06
Zn(II)	16.9 ± 3.4	4.92 ± 0.98	<0.57	44.8 ± 9.0	30.5 ± 6.1	<0.57	<0.57	46.5 ± 9.3

<x.xx–– below limit of quantification; , As(sum) = As(III)+As(V)+DMA, As(ratio) = As(V)÷As(III), Fe(sum) = Fe(II)+Fe(III), Fe(ratio) = Fe(III)÷Fe(II).

contaminations of river sediments [43,44]. DMA was determined in sample D5 only and the highest concentrations of three As species were found in order, As(III)<DMA < As(V) (D5). What is more, the dominance of inorganic arsenic species in river sediments from Vietnam was reported before [45]. Fe(II) and Fe(III) were found in 4 and 5 samples respectively. Fe(II) was found in narrow range, 18.2–52.2 (±13.6), instead of Fe(III), 21.7–3169 (±1147) mg kg^{-1}. Additionally, calculated Fe(sum) results, 21.7–3222 (±1161) mg kg^{-1} were comparable with the literature [44,46]. Although ratios of Fe(III) to Fe(II) were found in the significant wide range, from 3.2 to 67 (median = 50), substantial dominance (D1–D3) or dominance (D4–D5) of Fe(III) were observed. Fe ratios were comparable with different river sediments from Vietnam [45]. Other element contents were similar (Pb, Zn) or slightly lower (Cu, Cd, Ni) in comparison to the literature [44,46]. Undetectable Cd and low Pb contents in all samples may suggest low mobility of these elements, what was confirmed using a sequential extraction [46].

The fifth and last application group was represented by samples of archaeological pottery i.e. potshards (n = 6). Results were shown in Table 8. From investigated elements, only DMA, Cd(II), Co(II) and Ge(IV) were undetectable (<LOD) in all samples. Only As(III), Cu(II), Fe(II), Fe(III), Ru(III), Se(IV) and Sr(II) were found in all samples. As(III) and As(V) were detected in narrow ranges, 1.81–2.35 (±0.18) and 2.41–3.41 (±0.36) mg kg^{-1} respectively. Calculated ratios of As(V) to As(III) were contained in the narrow range, 1.0–1.6 (median = 1.4) with slight dominance of As(V). Arsenic contents were lower than reported in potshards [47] and clay used to produce archaeological pottery [47,48]. In the case of iron speciation, Fe(II) was found in narrow range, 115–1108 (±360), instead of Fe(III), 227–17989 (±5971) mg kg^{-1}. Fe(sum) results, 344–18176

Table 6
Quantification of 18 element species by 2 HPLC–MSIS–ICP–OES for 5 real samples of soil located in the proximity of industry wastes disposal site (peak area), [mg kg^{-1}].

	C1	C2	C3	C4	C5
As(III)	3.42 ± 0.68	3.24 ± 0.65	4.17 ± 0.83	4.32 ± 0.86	1.70 ± 0.34
DMA	<0.36	<0.36	<0.36	8.83 ± 1.77	<0.36
As(V)	2.11 ± 0.42	5.74 ± 1.15	10.4 ± 2.1	7.16 ± 1.43	2.11 ± 0.42
As(sum)	5.53 ± 1.11	8.98 ± 1.80	14.6 ± 2.9	20.3 ± 4.1	3.81 ± 0.76
As(ratio)	0.6	1.8	2.5	1.7	1.2
Cd(II)	<0.23	1.76 ± 0.35	<0.23	<0.23	4.34 ± 0.87
Co(II)	<0.36	11.1 ± 2.2	<0.36	11.5 ± 2.3	<0.36
Cu(II)	181 ± 36	2468 ± 494	82.9 ± 16.6	1339 ± 268	81.2 ± 16.2
Fe(II)	7.02 ± 1.40	89.7 ± 17.9	7.37 ± 1.47	38.5 ± 7.7	10.9 ± 2.2
Fe(III)	54.2 ± 10.8	1491 ± 298	56.7 ± 11.3	1906 ± 381	779 ± 156
Fe(sum)	61.2 ± 12.2	1581 ± 316	64.1 ± 12.8	1944 ± 389	790 ± 158.
Fe(ratio)	7.7	17	7.7	50	71
Ge(IV)	<0.25	<0.25	<0.25	<0.25	<0.25
Mn(II)	25.6 ± 5.12	1080 ± 216	42.9 ± 8.6	1616 ± 323	181 ± 36
Ni(II)	<0.34	26.6 ± 5.3	<0.34	7.41 ± 1.48	2.25 ± 0.45
Pb(II)	21.0 ± 4.20	418 ± 84	<0.74	66.0 ± 13.2	6.24 ± 1.25
Ru(III)	9.87 ± 1.97	8.88 ± 1.78	11.6 ± 2.3	10.1 ± 2.0	10.5 ± 2.1
Se(IV)	0.67 ± 0.13	0.67 ± 0.13	<0.08	<0.08	0.51 ± 0.10
Sr(II)	47.8 ± 9.56	116 ± 23	47.8 ± 9.6	104 ± 21	55.9 ± 11.2
Tl(I)	<0.73	<0.73	<0.73	3.23 ± 0.65	5.51 ± 1.10
V(V)	1.98 ± 0.40	3.07 ± 0.61	1.92 ± 0.38	3.65 ± 0.73	3.54 ± 0.71
Zn(II)	2.00 ± 0.40	86.5 ± 17.3	<0.57	30.3 ± 6.1	18.6 ± 3.7

<x.xx– – below limit of quantification; , As(sum) = As(III)+As(V)+DMA, As(ratio) = As(V)÷As(III), Fe(sum) = Fe(II)+Fe(III), Fe(ratio) = Fe(III)÷Fe(II).

Table 7
Quantification of 18 element species by 2 HPLC–MSIS–ICP–OES for 5 real samples of river sediments (Mekong, Vietnam) (peak area), [mg kg^{-1}].

	D1	D2	D3	D4	D5
As(III)	1.81 ± 0.36	1.88 ± 0.38	<0.19	<0.19	3.19 ± 0.64
DMA	<0.36	<0.36	<0.36	<0.36	4.52 ± 0.90
As(V)	2.64 ± 0.53	<0.31	<0.31	4.39 ± 0.88	5.45 ± 1.09
As(sum)	4.45 ± 0.89	1.88 ± 0.38	–	4.39 ± 0.88	13.2 ± 2.6
As(ratio)	1.5	–	–	–	1.7
Cd(II)	<0.23	<0.23	<0.23	<0.23	<0.23
Co(II)	<0.36	3.52 ± 0.70	<0.36	5.11 ± 1.02	<0.36
Cu(II)	10.1 ± 2.0	3.06 ± 0.61	7.15 ± 1.43	<0.23	<0.23
Fe(II)	18.2 ± 3.6	20.5 ± 4.1	52.2 ± 10.4	26.1 ± 5.2	<0.36
Fe(III)	1216 ± 243	793 ± 159	3169 ± 634	84.4 ± 16.9	21.7 ± 4.3
Fe(sum)	1234 ± 247	814 ± 163	3222 ± 644	111 ± 22	21.7 ± 4.3
Fe(ratio)	67	39	61	3.2	–
Ge(IV)	2.54 ± 0.51	<0.25	<0.25	<0.25	<0.25
Mn(II)	244 ± 49	62.9 ± 12.6	649 ± 130	<0.18	<0.18
Ni(II)	3.28 ± 0.66	3.63 ± 0.73	5.19 ± 1.04	5.19 ± 1.04	8.62 ± 1.72
Pb(II)	9.05 ± 1.81	<0.74	<0.74	<0.74	<0.74
Ru(III)	<0.65	<0.65	<0.65	<0.65	<0.65
Se(IV)	1.16 ± 0.23	0.84 ± 0.17	<0.08	<0.08	<0.08
Sr(II)	47.6 ± 9.5	47.2 ± 9.4	277 ± 55	96.4 ± 19.3	89.5 ± 17.9
Tl(I)	<0.73	<0.73	<0.73	<0.73	<0.73
V(V)	<0.06	<0.06	6.63 ± 1.33	5.37 ± 1.07	<0.06
Zn(II)	54.8 ± 11.0	4.18 ± 0.84	31.3 ± 6.3	<0.30	<0.30

<x.xx– – below limit of quantification; , As(sum) = As(III)+As(V)+DMA, As(ratio) = As(V)÷As(III), Fe(sum) = Fe(II)+Fe(III), Fe(ratio) = Fe(III)÷Fe(II).

(±5967) mg kg^{-1} were comparable with the literature [49,50]. Although ratios of Fe(III) to Fe(II) were found in the significant wide range, from 1.9 to 96 (median = 25), dominance (1, 4, 6) or substantial dominance (2, 3, 5) of Fe(III) were observed. Other element contents were varied in comparison with the literature, e.g. slightly lower [49] or similar [50,51] and it was connected with a sample preparation procedure.

3.4. Qualitative speciation analysis

The method application, except wide applicability in quantitative speciation analysis, showed other possibilities in separation and detection of unknown element species. Except for investigated element species, significant signals were observed in Mn, Cu, Fe and Zn chromatograms in different sample matrix types. Few elements species (peaks) were characterized as definite element species according to the literature.

Six significant signal responses of manganese species were observed in chromatogram (grey) of soil samples located in the proximity of industry wastes disposal site (sample C2) and chromatogram (black) of Mn(II) standard solution, 2.500 mg L^{-1}, was added in comparison (Fig. 3). At the figure, unknown manganese species were labelled as Mn1–Mn5 and two resolutions were presented (a, b) according to intensity [cps]. Three species, including Mn(II), were determined with high intensity (>5000 cps) and these signal responses reached the maximum at 225 s (Mn1), 480 s [Mn(II)] and 550 s (Mn2). It should be noted that Mn(II) and Mn2 were not separated efficiently under this chromatographic conditions however both signal responses reached high intensity (>40000 cps). What is more, three additional Mn species, (Mn3–Mn5)) were observed in bigger resolution (Fig. 3b). Each peak (Mn3– Mn5)was spike and symmetric although Mn4and Mn5 were overlaid slightly with peaks of Mn1 and Mn(II) respectively. These results may suggest that Mn4 and Mn5 are redox forms of Mn1 and Mn(II). Retention times were measured at 25 s (Mn3, at void time), 165 s (Mn4), 420 s (Mn5) however the measured intensity [cps] were much lower (Mn5, <2000 cps and Mn3, Mn4, <1000 cps) in comparison with peaks of Mn(II), Mn1 andMn2 (Fig. 3b). According to the literature, the species identification was attempted. On one hand, retention time of Mn1 was comparable to Mn(III), obtained with similar chromatographic system [25]. On the other hand, manganese exists in two main forms: Mn(II) and Mn(IV), in an aquatic environment. Mn(III) and the highest oxidation state, Mn(VII), are difficult to find in the natural environment [52]. In the case of soils located in the proximity of industry wastes disposal site, the natural balance is disturbed. Due to this, Mn4 could be a signal response of Mn(IV) and Mn3 (at void time) could be a signal response of Mn(VII) occurring as an anion (MnO_4^-) [53]. Nevertheless, there is a lack of the hyphenated technique to determine Mn(II), Mn(III), Mn(IV) and Mn(VII) after HPLC separation in one run. As there are no reference methods, above description is slightly questionable.

Other significant contents of manganese species were observed in different sample matrix types: (a) post–glacial sediment (sample A5) and (b) yerba mate *(Ilex paraguariensis)* (sample B3). The data (grey) and Mn standard solution, 0.050 mg L^{-1}, (black) were presented in Fig. 4. Unknown manganese species were constantly labelled (Mn6–Mn10) to easily distinguish data from Figs. 3 and 4. In the (a) case, Mn chromatograms (grey) showed significant variation of signal response (intensity) (Fig. 4a). Due to this, four unknown Mn species (Mn6– Mn9) are found at 90 s (Mn6), 135 s (Mn7), 305 s (Mn8), 390 s (Mn9) and obtained significant peak resolution and symmetry. Nevertheless, intensity [cps] were much lower (<400 cps). The maximum intensity signal (>5000 cps) was detected for Mn(II) at 495 s. In the (b) case, Mn chromatograms presented the least variation in signal response (intensity) and two Mn species peaks were observed (Fig. 4b). Retention times were 190 s (Mn10) and 490 s [Mn(II)] and obtained signal responses were varied i.e. Mn(II) (ca. 19000 cps) was twenty time more intensive than Mn10 (<400 cps). Worth mentioning, retention time of Mn10 was similar to Mn1 (Fig. 3). According to the above and the literature, Mn10 could be Mn(IV) occurring commonly in natural environment [52]. Moreover, retention time of Mn9 was similar to Mn5 (Fig. 3) however a lack of literature references prevents the species identification. Although most of measured signal response stayed unidentifiable, up to six Mn species could be detected under these operating conditions. A composite optimization of the system

Table 8
Quantification of 18 element species by 2 HPLC–MSIS–ICP–OES for 6 real samples of archaeological pottery (peak area) [mg kg^{-1}].

	E1	E2	E3	E4	E5	E6
As(III)	2.35 ± 0.47	2.13 ± 0.43	1.81 ± 0.36	1.90 ± 0.38	2.13 ± 0.43	2.17 ± 0.43
DMA	<0.36	<0.36	<0.36	<0.36	<0.36	<0.36
As(V)	2.41 ± 0.48	2.52 ± 0.50	2.52 ± 0.50	2.63 ± 0.53	<0.31	3.41 ± 0.68
As(sum)	4.76 ± 0.95	4.65 ± 0.93	4.33 ± 0.87	4.53 ± 0.91	2.13 ± 0.43	5.58 ± 1.12
As(ratio)	1.0	1.2	1.4	1.4	–	1.6
Cd(II)	<0.23	<0.23	<0.23	<0.23	<0.23	<0.23
Co(II)	<0.36	<0.36	<0.36	<0.36	<0.36	<0.36
Cu(II)	40.5 ± 8.1	11.5 ± 2.3	10.5 ± 2.1	12.5 ± 2.5	6.84 ± 1.37	<0.11
Fe(II)	115 ± 23	187 ± 37	176 ± 35	1108 ± 222	133 ± 27	117 ± 23
Fe(III)	738 ± 148	17989 ± 3598	9102 ± 1820	5001 ± 1000	5904 ± 1181	227 ± 45
Fe(sum)	853 ± 171	18176 ± 3635	9278 ± 1856	6109 ± 1222	6037 ± 1207	344 ± 69
Fe(ratio)	6.4	96	52	4.5	44	1.9
Ge(IV)	<0.25	<0.25	<0.25	<0.25	<0.25	<0.25
Mn(II)	<0.18	248 ± 50	263 ± 53	741 ± 148	<0.18	<0.18
Ni(II)	<0.34	<0.34	5.63 ± 1.13	4.77 ± 0.95	6.49 ± 1.30	<0.34
Pb(II)	3.84 ± 0.77	<0.74	<0.74	<0.74	<0.74	<0.74
Ru(III)	13.8 ± 2.8	14.8 ± 3.0	15.5 ± 3.1	15.5 ± 3.1	14.8 ± 3.0	16.8 ± 3.4
Se(IV)	0.84 ± 0.17	1.25 ± 0.25	0.84 ± 0.17	2.27 ± 0.45	2.27 ± 0.45	1.45 ± 0.29
Sr(II)	670 ± 134	737 ± 147	664 ± 133	698 ± 140	656 ± 131	623 ± 125
Tl(I)	<0.73	<0.73	2.75 ± 0.55	<0.73	3.89 ± 0.78	4.46 ± 0.89
V(V)	<0.06	4.70 ± 0.94	3.24 ± 0.65	3.93 ± 0.79	3.76 ± 0.75	<0.06
Zn(II)	<0.30	96.7 ± 19.3	60.3 ± 12.1	227 ± 45	48.0 ± 9.6	<0.30

<x.xx–– below limit of quantification; , As(sum) = As(III)+As(V)+DMA, As(ratio) = As(V)÷As(III), Fe(sum) = Fe(II)+Fe(III), Fe(ratio) = Fe(III)÷Fe(II).

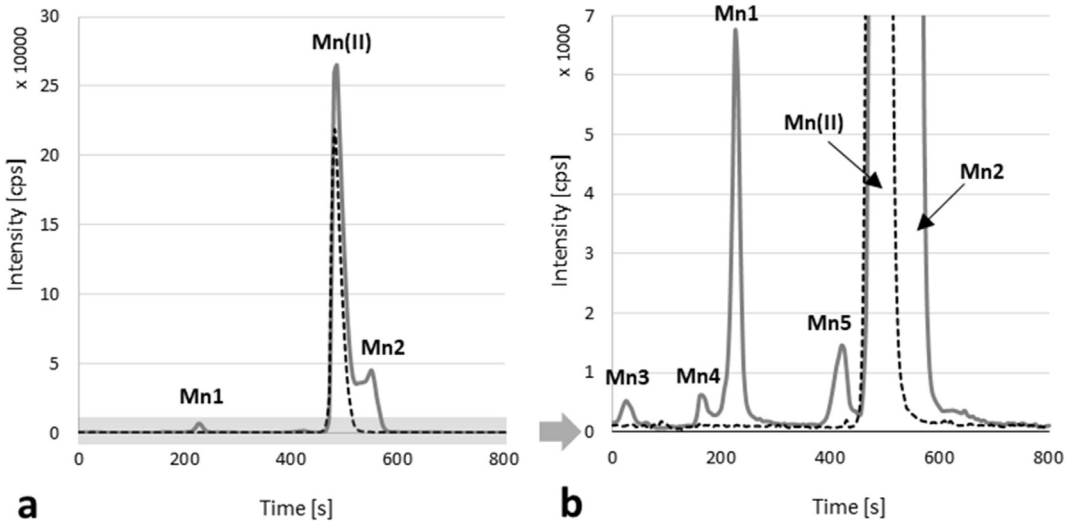

Fig. 3. Qualitative analysis of manganese species by 2 HPLC–MSIS–ICP–OES: (a–b) soil located in the proximity of industry wastes disposal site (grey) and Mn(II) standard solution, 2.500 mg L^{-1} (black). Unknown manganese species were labelled as Mn1–Mn5 – identification details in text.

would carry out better results in identification and quantification of Mn species. This research presents an interesting direction of the method developing due to six Mn species which were able to determine in three sample matrix types, both inorganic (A, C) and organic (B).

Chromatograms of Cu species (grey) were presented in Fig. 5 and possibilities of the system in copper speciation analysis were presented with two sample matrix types: (a) soil located in the proximity of industry wastes disposal site (sample C2) and (b) yerba mate *(Ilex paraguariensis)* (sample B5). In comparison, chromatograms of Cu standard solution (black), 10.000 mg L^{-1} (a) and 0.050 mg L^{-1} (b) were added. Unknown copper species were labelled as Cu1–Cu3. Two (a) and three (b) signal responses were observed, including Cu(II) found at 325 s. According to the literature, Cu species identification was attempted. On the one hand, retention time of Cu1 (205 s) and Cu2 (245 s) were comparable to Cu(I), obtained with similar chromatographic system [25]. On the other hand, the eluent was the mixture of PDCA and ammonium citrate without a neutral salt addition. In the case of (b), there was additional signal response at 295 s (Cu3) however overlaid with signal response of Cu(II). It could be a kind of copper organic complex (e.g. copper metallothioneins, Cu–MTs) [54]. Unfortunately, there is no reference method of Cu species separation, especially Cu organic complexes, by HPLC hyphened with specific detectors e.g. spectrometers. In comparison with other metals (alkali, transition and precious) and rare earth elements (REEs), the surprising lack of the method to determine Cu species was shown in the review recently [55]. In opposite of the above Mn speciation analysis, most of the measured signal responses stayed identifiable. However, only three Cu species could be detected under these operating conditions. Nevertheless, a composite system optimization could carry out better results of Cu species identification and quantification.

Although Fe(II) and Fe(III) are quantified by this method, other

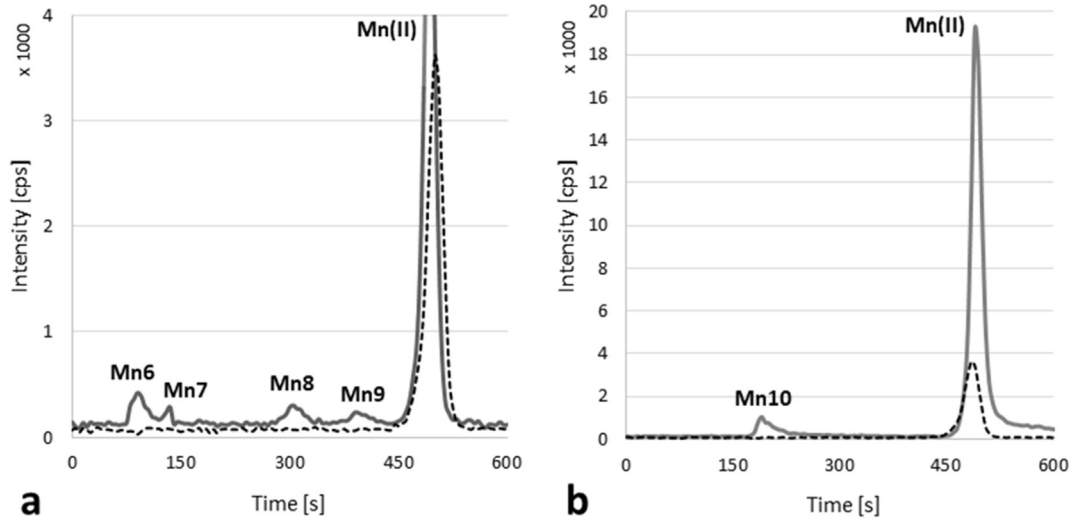

Fig. 4. Qualitative analysis of manganese species by 2 HPLC–MSIS–ICP–OES: (a) yerba mate (*Ilex paraguariensis*) (grey) and Mn(II) standard solution, 0.050 mg L^{-1} (black); (b) post–glacial sediment (Spitsbergen, Svalbard) (grey) and Mn(II) standard 0.050 mg L^{-1} (black). Unknown manganese species were labelled as Mn6–Mn10 – identification details in text.

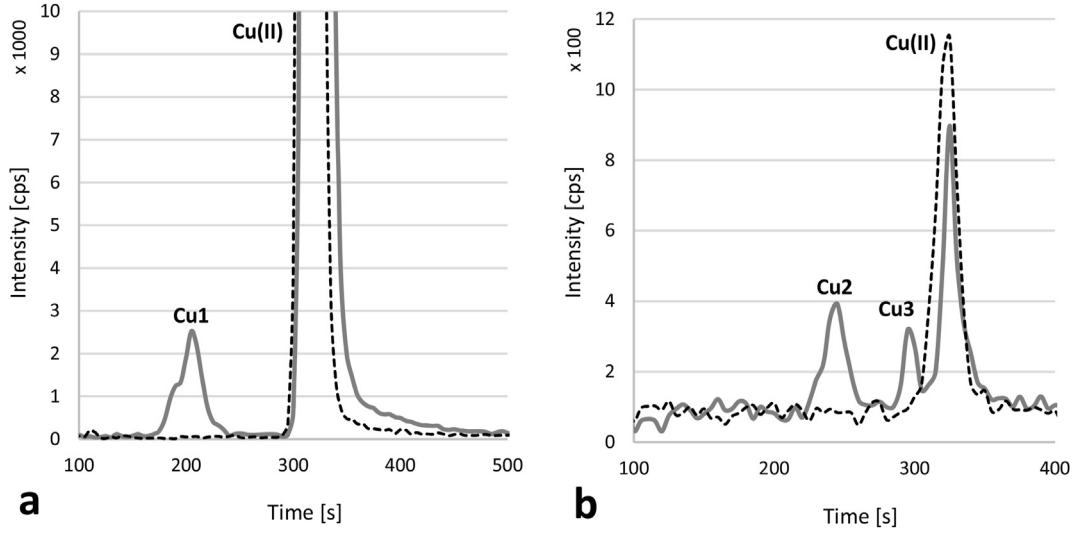

Fig. 5. Qualitative analysis of copper species by 2 HPLC–MSIS–ICP–OES: (a) soil located in the proximity of industry wastes disposal site (grey) and Cu(II) standard solution, 10.000 mg L^{-1} (black); (b) yerba mate (*Ilex paraguariensis*) (grey) and Cu(II) standard solution, 0.050 mg L^{-1} (black). Unknown copper species were labelled as Cu1–Cu3 – identification details in text.

significant variations of Fe signal response (intensity) were observed for two sample matrix types: (a) post–glacial sediment (Spitsbergen, Svalbard) (sample A5) and (b) river sediment (Mekong, Vietnam) (sample D3). Results with chromatograms of Fe(II)+ Fe(III) standard solution, 1.000 + 1.000 [mg L^{-1}] (black) were presented in Fig. 6. Besides of Fe(II) and Fe(III) found at 650–660 and 230–235 [s] respectively, interesting variations of signal response (intensity) were observed in samples (a–b). According to this, unknown iron species were labelled as Fe1–Fe3. Two areas (Fe1–Fe2) were distinguished in the range from 0 to 230 s. In the first area (Fe1), two (a) or three (b) peaks were contained in the range from 35 to 120 s with maximum signal of intensity [cps] at 50–70 s. In the second area (Fe2), two (b) or three (a) peaks were detected from 125 to 195 s with maximum signal response [cps] at 165–175 s. According to the literature, the identification of unknown Fe species was attempted, however, no sufficient data was found. There is an example of natural occurring Fe–based organic complexes (e.g. siderophores, which came from bacteria) in salt–march sediments [56] or marine environment [57]. Due to this, Fe1 could contain inert Fe organic complexes due to early elution and Fe2 could contain ionic Fe organic complexes. Moreover, the ratio of signals between these areas (Fe1–Fe2) and chromatogram shapes could be defined as a fingerprint. However, this separation could be extensive and each peak area came from single form complex. A composite optimization could specify the system to identity iron organic species, such as Fe–DTPA (i.e. Fe complexed with diethylenetriaminepentaacetic acid), which presence of a significant level in natural environment may suggest fertilizer contamination [58]. In the (b), Fe3 was observed at 375 s however it was overlaid with Fe(III) signal response. Fe3 could be another example of unknown Fe complex, co–eluting nearly with Fe(III) but at the same time the high level of Fe(III) in sample (D3) could suggest that peak 5 is “a tail” of Fe(III) signal response.

Two Zn species were found in two samples (C1–C2) of soil

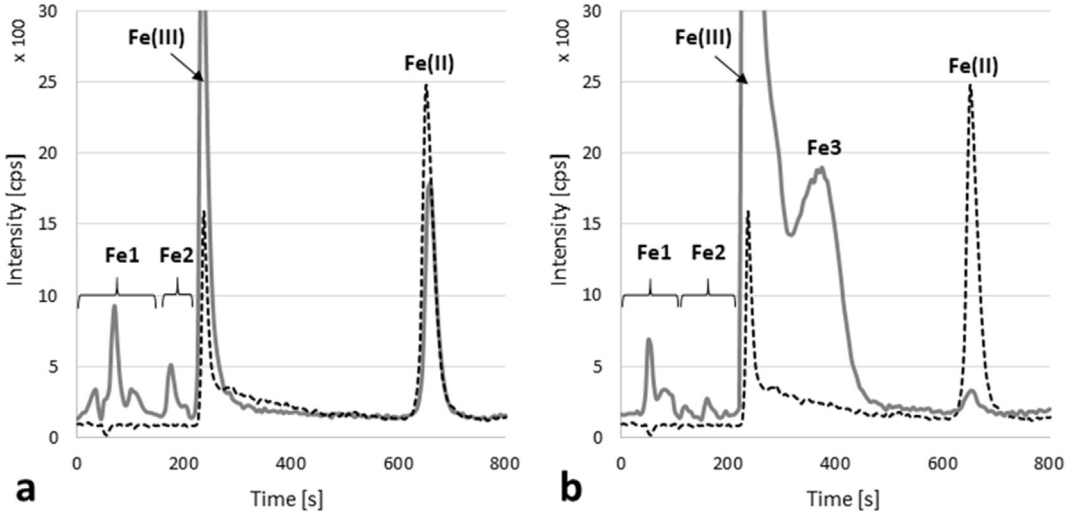

Fig. 6. Qualitative analysis of iron species by 2 HPLC–MSIS–ICP–OES: (a) post–glacial sediment (Spitsbergen, Svalbard) (grey) and Fe(II)+ Fe(III) standard solution, 1.000 + 1.000 [mg L^{-1}] (black); (b) river sediment (Mekong, Vietnam) (grey) and Fe(II)+ Fe(III) standard solution, 1.000 + 1.000 [mg L^{-1}] (black). Unknown iron species were labelled as Fe1–Fe3 – identification details in text.

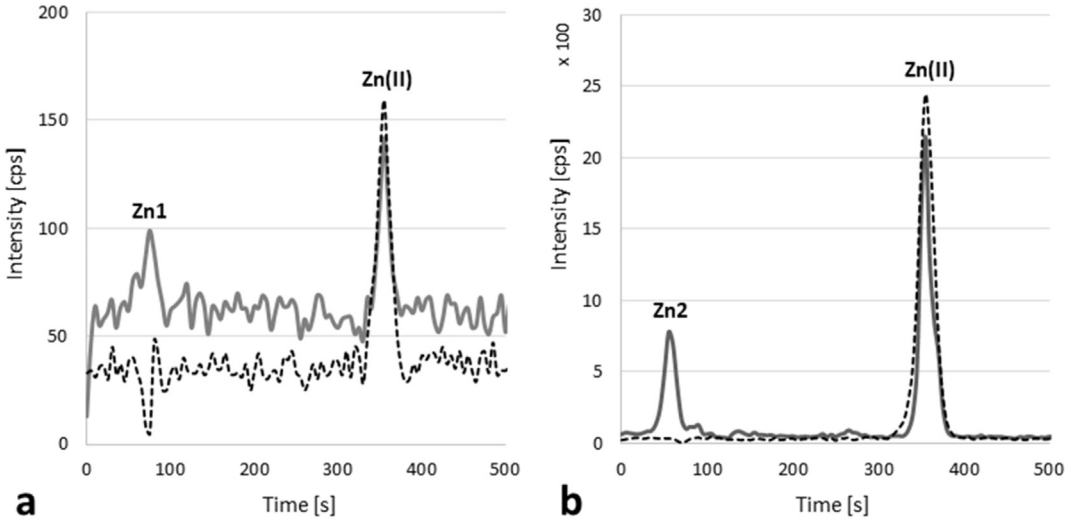

Fig. 7. Qualitative analysis of zinc species by 2 HPLC–MSIS–ICP–OES in two samples of soil located in the proximity of industry wastes disposal site: (a) sample C1 (grey) and Zn(II) standard solution, 0.010 mg L^{-1} (black); (b) sample C2 (grey) and Zn(II) standard solution, 0.500 mg L^{-1} (black). Unknown zinc species were labelled as Zn1–Zn2 – identification details in text.

located in the proximity of industry wastes disposal site. The following chromatograms were presented (Fig. 7): (a) sample C1 (grey) and Zn(II) standard solution, 0.010 mg L^{-1} (black); (b) sample C2 (grey) and Zn(II) standard solution, 0.500 mg L^{-1} (black). Unknown iron species were labelled as Zn1–Zn2. Two signal responses were observed, including Zn(II) found at 355 s. According to the literature, Zn species identification was attempted. On one hand, Zn1 and Zn2 could be volatile species of Zn [59] due to early elution i.e. 50 s (Zn1) and 70 s (Zn2). On the other hand, signal response gained maximum [cps] at the time which was corresponding to void time of the whole system, 70 s (CS5A) and 90 s (SAX–1). Furthermore, authors reported high efficiently of Zn hydrides forming e.g. 75% (by HG–AAS) [60] and ≥95% (HG–ICP–OES) [59] in comparison with conventional nebulization. These percentages are significantly higher in comparison with investigated transition metals including precious, i.e. Cd (50%), 8% (Ag), Cu (4%), 0.6% (Au) [60] or Ag, Cu, Pd (1%) [61]. Authors expected that volatile species of Zn generate unstable ZnH_2 which decomposes rapidly to Zn0 (g) as it was reported for Cd [62] or Ag [61]. However, CVG efficiently values of Ag and Cd were varied significantly. Even though Smichowski et al. reported that no Zn0 was observed and no monoatomic Zn was generated by reaction of $NaBH_4$ and Zn acidified solution [59], authors stayed unclearly the identification of volatile Zn species. According to this, it is equally probable that Zn1 could contain inert Zn organic complexes due to early elution (e.g. zinc metallothioneins, Zn–MTs). Unfortunately, there is no reference method of Zn species separation, especially hyphenated techniques. Nevertheless, the assessment of efficiency of CVG is a difficult parameter to estimate when using ICP–OES or ICP–MS and values from bibliography are very different [63].

4. Conclusions

The MSIS unit was applied as an interface between two HPLC

systems and ICP–OES and simultaneous quantification of 18 element species under uniform conditions were performed. The applicability of the method was performed in speciation analyses of real samples: (A) post–glacial sediments (Spitsbergen, Svalbard), (B) yerba mate *(Ilex paraguariensis)*, (C) soil samples located in the proximity of industry wastes disposal site, (D) river sediments (Mekong, Vietnam) and (E) archaeological pottery. Considerably wide applicability, broad linear range of calibration curves, and high accuracy compensated slightly high LODs. Moreover, the method was relatively fast and allowed to separate and determine species within 700 s of a single analysis.

Due to detection of unknown Cu, Fe, Mn and Zn in different sample matrix types, inorganic (A, C, D) and organic (B) both, an interesting direction to develop the method was presented. A composite optimization of the 2 HPLC–MSIS–ICP–OES could lead to more sophisticated analytical methods. Indisputable novelty was simultaneous application of two columns (cation– and anion–exchange), which were coupled to the specific detector (ICP–OES) through the MSIS unit working in dual–mode. According to the above, the system is easy to replace parts, such as column types and mobile phases. The MSIS unit could be placed between various types of chromatography and spectrometry however the most efficient usage of its dual–mode was possible with ICP type spectrometers, OES and MS both. The limitation could be the MSIS construction, which allows to apply one channel to generate volatile hydrides only. An alternative could be HG substitution with CVG techniques.

In the literature, surprising lack of the hyphenated technique for determination of metal species e.g. Cu, Fe, Mn, were found instead of presented possibilities in simultaneous separation of Cu, Mn, Fe and Zn species. According to this, there are no reference methods and conducted species identification is quite questionable. Nevertheless, possibilities of 2 HPLC–MSIS–ICP–OES distinguish the method from all of reported recently in a significant way.

CRediT authorship contribution statement

Jędrzej Proch: Conceptualization, Investigation, Methodology, Data curation, Funding acquisition, Validation, Writing - original draft, Writing - review & editing. **Przemysław Niedzielski:** Conceptualization, Investigation, Methodology, Formal analysis, Writing - original draft, Writing - review & editing.

Declaration of competing interest

The authors declare that they have no known competing financial interests or personal relationships that could have appeared to influence the work reported in this paper.

Acknowledgments

The work was supported by grant no. POWR.03.02.00–00–I026/16 co–financed by the European Union through the European Social Fund under the Operational Program Knowledge Education Development.

References

[1] T. Guerin, A. Astruc, M. Astruc, Speciation of arsenic and selenium compounds by HPLC hyphenated to specific detectors: a review of the main separation techniques, Talanta 50 (1) (1999) 1–24, https://doi.org/10.1016/s0039–9140(99)00140–x.
[2] P. Janvion, S. Motellier, H. Pitsch, Ion–exchange mechanisms of some transition metals on a mixed–bed resin with a complexing eluent, J. Chromatogr. A 715 (1) (1995) 105–115, https://doi.org/10.1016/0021–9673(95)00576–9.
[3] N. Cardellicchio, P. Ragone, S. Cavalli, J. Riviello, Use of ion chromatography for the determination of transition metals in the control of sewage–treatment–plant and related waters, J. Chromatogr. A 770 (1–2) (1997) 185–193, https://doi.org/10.1016/s0021–9673(97)00086–1.
[4] A. Atanassova, R. Lam, D. Zamble, A high–performance liquid chromatography method for determining transition metal content in proteins, Anal. Biochem. 335 (1) (2004) 103–111, https://doi.org/10.1016/j.ab.2004.08.013.
[5] Y. Chen, Y. Jian, K. Chiu, H. Yak, Simultaneous speciation of iron(II) and iron(III) by ion chromatography with chemiluminescence detection, Anal. Sci. 28 (8) (2012) 795–799, https://doi.org/10.2116/analsci.28.795.
[6] M. Ślachciński, Recent achievements in sample introduction systems for use in chemical vapor generation plasma optical emission and mass spectrometry: from macro– to microanalytics, Appl. Spectrosc. Rev. 49 (4) (2013) 271–321, https://doi.org/10.1080/05704928.2013.823547.
[7] W. Holak, Gas–sampling technique for arsenic determination by atomic absorption spectrophotometry, Anal. Chem. 41 (12) (1969) 1712–1713, https://doi.org/10.1021/ac60281a025.
[8] P. Pohl, Hydride generation – recent advances in atomic emission spectrometry, Trac. Trends Anal. Chem. 23 (2) (2004) 87–101, https://doi.org/10.1016/s0165–9936(04)00306–1.
[9] R. McLaughlin, I. Brindle, A new sample introduction system for atomic spectrometry combining vapour generation and nebulization capacities, J. Anal. At. Spectrom. 17 (11) (2002) 1540–1548, https://doi.org/10.1039/b208011g.
[10] A. Asfaw, G. Wibetoe, Simultaneous determination of hydride (Se) and non–hydride–forming (Ca, Mg, K, P, S and Zn) elements in various beverages (beer, coffee, and milk), with minimum sample preparation, by ICP–AES and use of a dual–mode sample–introduction system, Anal. Bioanal. Chem. 382 (1) (2005) 173–179, https://doi.org/10.1007/s00216–005–3188–2.
[11] H. Wiltsche, I. Brenner, K. Prattes, G. Knapp, Characterization of a multimode sample introduction system (MSIS) for multielement analysis of trace elements in high alloy steels and nickel alloys using axially viewed hydride generation ICP–AES, J. Anal. At. Spectrom. 23 (9) (2008) 1253, https://doi.org/10.1039/b803943g.
[12] A. Asfaw, D. Beauchemin, Combination of a multimode sample introduction system with a pre–evaporation tube to improve multi–element analysis by ICP–OES, J. Anal. At. Spectrom. 27 (1) (2012) 80–91, https://doi.org/10.1039/c1ja10224a.
[13] A. Fuentes–Cid, J. Villanueva–Alonso, E. Peña–Vázquez, P. Bermejo–Barrera, Comparison of two lab–made spray chambers based on MSIS™ for simultaneous metal determination using vapor generation–inductively coupled plasma optical emission spectroscopy, Anal. Chim. Acta 749 (2012) 36–43, https://doi.org/10.1016/j.aca.2012.08.001.
[14] T.K. Anderlini, D. Beauchemin, Improvements to the analytical performance of inductively coupled plasma optical emission spectrometry by coupling a multi-mode sample introduction system to an infrared heated preevaporation tube, J. Anal. At. Spectrom. 33 (2018) 1068.
[15] H. Matusiewicz, M. Ślachciński, Simultaneous determination of hydride forming (As, Bi, Ge, Sb, Se, Sn) and Hg and non–hydride forming (Ca, Fe, Mg, Mn, Zn) elements in sonicate slurries of analytical samples by microwave induced plasma optical emission spectrometry with dual–mode sample introduction system, Microchem. J. 86 (1) (2007) 102–111, https://doi.org/10.1016/j.microc.2006.12.002.
[16] R. Machado, C. Amaral, J. Nóbrega, A. Araujo Nogueira, Multielemental determination of as, Bi, Ge, Sb, and Sn in agricultural samples using hydride generation coupled to microwave–induced plasma optical emission spectrometry, J. Agric. Food Chem. 65 (23) (2017) 4839–4842, https://doi.org/10.1021/acs.jafc.7b01448.
[17] I. Mikheev, E. Karpukhina, L. Usol'tseva, T. Samarina, D. Volkov, M. Proskurnin, Application of microwave plasma atomic emission spectrometry and hydride generation for determination of arsenic and selenium in mineral water, Inorg. Mater. 53 (14) (2017) 1422–1426, https://doi.org/10.1134/s0020168517140126.
[18] A. Asfaw, G. Wibetoe, Dual mode sample introduction for multi–element determination by ICP–MS: the optimization and use of a method based on simultaneous introduction of vapor formed by NaBH4 reaction and aerosol from the nebulizer, J. Anal. At. Spectrom. 21 (10) (2006) 1027, https://doi.org/10.1039/b604116g.
[19] M. Mulugeta, G. Wibetoe, C. Engelsen, W. Lund, Optimization of an anion-exchange high performance liquid chromatography-inductively coupled plasma-mass spectrometric method for the speciation analysis of oxyanion-forming metals and metalloids in leachates from cement-based materials, J. Chromatogr. A 1217 (40) (2010) 6186–6194, https://doi.org/10.1016/j.chroma.2010.07.082.
[20] R. Michalski, M. Jabłonska, S. Szopa, A. Łyko, Application of ion chromatography with ICP–MS or MS detection to the determination of selected halides and metal/metalloids species, Crit. Rev. Anal. Chem. 41 (2) (2011) 133–150, https://doi.org/10.1080/10408347.2011.559438.
[21] M. Grotti, A. Terol, J. Todolí, Speciation analysis by small–bore HPLC coupled to ICP–MS, Trac. Trends Anal. Chem. 61 (2014) 92–106, https://doi.org/10.1016/j.trac.2014.06.009.
[22] K. Al–Assaf, J. Tyson, P. Uden, Determination of four arsenic species in soil by sequential extraction and high performance liquid chromatography with post–column hydride generation and inductively coupled plasma optical emission spectrometry detection, J. Anal. At. Spectrom. 24 (4) (2009) 376, https://doi.org/10.1039/b820300h.
[23] E. Barrientos, K. Wrobel, J. Torres Guzman, A. Corrales Escobosa, K. Wrobel,

Determination of SeMet and Se(iv) in biofortified yeast by ion–pair reversed phase liquid chromatography–hydride generation–microwave induced nitrogen plasma atomic emission spectrometry (HPLC–HG–MP–AES), J. Anal. At. Spectrom. 31 (1) (2016) 203–211, https://doi.org/10.1039/c5ja00276a.
[24] J. Proch, P. Niedzielski, In–spray chamber hydride generation by multi–mode sample introduction system (MSIS) as an interface in the hyphenated system of high performance liquid chromatography and inductivity coupled plasma optical emission spectrometry (HPLC/HG–ICP–OES) in arsenic species determination, Talanta 208 (2020) 120395, https://doi.org/10.1016/j.talanta.2019.120395.
[25] N. Solovyev, M. Vinceti, P. Grill, J. Mandrioli, B. Michalke, Redox speciation of iron, manganese, and copper in cerebrospinal fluid by strong cation exchange chromatography – sector field inductively coupled plasma mass spectrometry, Anal. Chim. Acta 973 (2017) 25–33, https://doi.org/10.1016/j.aca.2017.03.040.
[26] Y. Kim, H. Chung, H. Kong, D. Choi, D. Cho, The application of Ion chromatographic method for bioavailability and stability test of iron preparations, Arch Pharm. Res. (Seoul) 22 (3) (1999) 288–293, https://doi.org/10.1007/bf02976364.
[27] K. Fernsebner, J. Zorn, B. Kanawati, A. Walker, B. Michalke, Manganese leads to an increase in markers of oxidative stress as well as to a shift in the ratio of Fe(ii)/(iii) in rat brain tissue, Metall 6 (4) (2014) 921, https://doi.org/10.1039/c4mt00022f.
[28] N. Cardellicchio, S. Cavalli, P. Ragone, J. Riviello, New strategies for determination of transition metals by complexation ion–exchange chromatography and post column reaction, J. Chromatogr. A 847 (1–2) (1999) 251–259, https://doi.org/10.1016/s0021–9673(99)00426–4.
[29] M. Welna, A. Szymczycha–Madeja, P. Pohl, Critical evaluation of strategies for single and simultaneous determinations of As, Bi, Sb and Se by hydride generation inductively coupled plasma optical emission spectrometry, Talanta 167 (2017) 217–226, https://doi.org/10.1016/j.talanta.2017.01.029.
[30] S. Budzyńska, Z. Magdziak, P. Goliński, P. Niedzielski, M. Mleczek, Arsenic forms in phytoextraction of this metalloid in organs of 2–year–old Acer platanoides seedlings, Environ. Sci. Pollut. Control Ser. 25 (27) (2018) 27260–27273.
[31] S. Choudhary, G. Nayak, N. Khare, Source, mobility, and bioavailability of metals in fjord sediments of Krossfjord–Kongsfjord system, Arctic, Svalbard, Environ. Sci. Pollut. Control Ser. (2020), https://doi.org/10.1007/s11356–020–07879–1.
[32] G. Heltai, Z. Győri, I. Fekete, G. Halász, K. Kovács, A. Takács, et al., Longterm study of transformation of potentially toxic element pollution in soil/water/sediment system by means of fractionation with sequential extraction procedures, Microchem. J. 136 (2018) 85–93, https://doi.org/10.1016/j.microc.2017.01.026.
[33] P. Niedzielski, L. Kozak, M. Wachelka, K. Jakubowski, J. Wybieralska, The microwave induced plasma with optical emission spectrometry (MIP–OES) in 23 elements determination in geological samples, Talanta 132 (2015) 591–599, https://doi.org/10.1016/j.talanta.2014.10.009.
[34] MERCOSUL, Regulamento técnico mercosul sobre limites máximos de contaminantes inorgânicos em alimentos (REVOGAÇÃO DAS RES. GMC N° 102/94 e N°35/96), in: MERCOSUL, 2013, pp. 1–18. N° 12/11.
[35] L. Santos, S. Vicentini Neto, G. Iozzi, S. Jacob, Arsenic, cadmium and lead concentrations in Yerba mate commercialized in Southern Brazil by inductively coupled plasma mass spectrometry, Ciência Rural. 47 (12) (2017), https://doi.org/10.1590/0103–8478cr20170202.
[36] D. Pozebon, V. Dressler, M. Marcelo, T. de Oliveira, M. Ferrão, Toxic and nutrient elements in yerba mate (Ilex paraguariensis), Food Addit. Contam. B 8 (3) (2015) 215–220, https://doi.org/10.1080/19393210.2015.1053420.
[37] M. Marcelo, C. Martins, D. Pozebon, V. Dressler, M. Ferrão, Classification of yerba mate (Ilex paraguariensis) according to the country of origin based on element concentrations, Microchem. J. 117 (2014) 164–171, https://doi.org/10.1016/j.microc.2014.06.027.
[38] R. Pardinho, P. Dalla Vecchia, A. Mendes, C. Bizzi, P. Mello, F. Duarte, E. Flores, Determination of toxic elements in yerba mate by ICP–MS after diluted acid digestion under O2 pressure, Food Chem. 263 (2018) 37–41, https://doi.org/10.1016/j.foodchem.2018.04.112.
[39] L. Escudero, P. Pacheco, J. Gasquez, J. Salonia, Development of a FI–HG–ICP–OES solid phase preconcentration system for inorganic selenium speciation in Argentinean beverages, Food Chem. 169 (2015) 73–79, https://doi.org/10.1016/j.foodchem.2014.07.127.
[40] J. Gál, A. Hursthouse, S. Cuthbert, Chemical availability of arsenic and antimony in industrial soils, Environ. Chem. Lett. 3 (4) (2005) 149–153, https://doi.org/10.1007/s10311–005–0022–1.
[41] H. Yang, M. He, Distribution and speciation of selenium, antimony, and arsenic in soils and sediments around the area of xikuangshan (China), Clean 44 (11) (2016) 1538–1546.
[42] H. Masuda, H. Yoshinishi, S. Fuchida, T. Toki, E. Even, Vertical profiles of arsenic and arsenic species transformations in deep–sea sediment, Nankai Trough, offshore Japan, Progress in Earth and Planetary Science 6 (1) (2019), https://doi.org/10.1186/s40645–019–0269–y.
[43] L. Gómez, J. Ariza, D. Sánchez–Rodas, I. Giráldez, Selective extraction of iron oxide associated arsenic species from sediments for speciation with coupled HPLC–HG–AAS, J. Anal. At. Spectrom. 13 (12) (1998) 1375–1379, https://doi.org/10.1039/a806111d.
[44] J. Wang, J. Song, R. Xie, Y. Li, M. Xu, J. Lu, et al., Source identification of heavy metals in surface sediments from a river in Anhui, China, Environ. Forensics (2020) 1–9, https://doi.org/10.1080/15275922.2020.1728439.
[45] D. Postma, S. Jessen, N. Hue, M. Duc, C. Koch, P. Viet, et al., Mobilization of arsenic and iron from Red River floodplain sediments, Vietnam, Geochem. Cosmochim. Acta 74 (12) (2010) 3367–3381, https://doi.org/10.1016/j.gca.2010.03.024.
[46] F. Howari, K. Banat, Assessment of Fe, Zn, Cd, Hg, and Pb in the Jordan and yarmouk river sediments in relation to their physicochemical properties and sequential extraction characterization, Water, Air, Soil Pollut. 132 (1/2) (2001) 43–59, https://doi.org/10.1023/a:1012062814873.
[47] V. Kilikoglou, Y. Maniatis, A. Grimanis, The effect of purification and firing of clays on trace element provenance studies, Archaeometry 30 (1) (1988) 37–46, https://doi.org/10.1111/j.1475–4754.1988.tb00433.x.
[48] G. Christidis, C. Shriner, H. Murray, An integrated methodological approach for source–clay determination of ancient ceramics: the case of aegina island, Greece, Clay Clay Miner. 62 (6) (2014) 447–469, https://doi.org/10.1346/ccmn.2014.0620601.
[49] H. Hatcher, M. Tite, J. Walsh, A comparison of inductively–coupled plasma emission spectrometry and atomic absorption spectrometry analysis on standard reference silicate materials and ceramics, Archaeometry 37 (1) (1995) 83–94, https://doi.org/10.1111/j.1475–4754.1995.tb00728.x.
[50] B. Li, J. Zhao, K. Collerson, A. Greig, Application of ICP–MS trace element analysis in study of ancient Chinese ceramics, Chin. Sci. Bull. 48 (12) (2003) 1219–1224, https://doi.org/10.1007/bf03183941.
[51] P. Fermo, E. Delnevo, M. Lasagni, S. Polla, M. de Vos, Application of chemical and chemometric analytical techniques to the study of ancient ceramics from Dougga (Tunisia), Microchem. J. 88 (2) (2008) 150–159, https://doi.org/10.1016/j.microc.2007.11.012.
[52] M. Jabłońska–Czapla, Manganese and its speciation in environmental samples using hyphenated techniques: a review, Journal of Elementology 4 (2015), https://doi.org/10.5601/jelem.2014.19.4.787, 2015.
[53] E. Grygo–Szymanko, A. Tobiasz, N. Miliszkiewicz, D. Dudek–Adamska, S. Walas, Evaluation of manganese(II) and manganese(VII) speciation in water samples by ion pair high–performance liquid chromatography–inductively coupled plasma mass spectrometry, Anal. Lett. 50 (13) (2017) 2147–2160, https://doi.org/10.1080/00032719.2016.1267185.
[54] M. Montes–Bayon, D. Pröfrock, A. Sanz–Medel, A. Prange, Direct comparison of capillary electrophoresis and capillary liquid chromatography hyphenated to collision–cell inductively coupled plasma mass spectrometry for the investigation of Cd–, Cu– and Zn–containing metalloproteins, J. Chromatogr. A 1114 (1) (2006) 138–144, https://doi.org/10.1016/j.chroma.2006.02.028.
[55] R. Clough, C. Harrington, S. Hill, Y. Madrid, J. Tyson, Atomic Spectrometry Update: review of advances in elemental speciation, J. Anal. At. Spectrom. 33 (7) (2018) 1103–1149, https://doi.org/10.1039/c8ja90025.
[56] G. Luther, J. Kostka, T. Church, B. Sulzberger, W. Stumm, Seasonal iron cycling in the salt–marsh sedimentary environment: the importance of ligand complexes with Fe(II) and Fe(III) in the dissolution of Fe(III) minerals and pyrite, respectively, Mar. Chem. 40 (1–2) (1992) 81–103, https://doi.org/10.1016/0304–4203(92)90049–g.
[57] M. Gledhill, K. Buck, The organic complexation of iron in the marine environment: a review, Front. Microbiol. 3 (2012), https://doi.org/10.3389/fmicb.2012.00069.
[58] M. Sillanpää, Environmental fate of EDTA and DTPA, Rev. Environ. Contam. Toxicol. (1997) 85–111, https://doi.org/10.1007/978–1–4612–1964–4_3.
[59] P. Smichowski, S. Farías, S. Pérez Arisnabarreta, Chemical vapour generation of transition metal volatile species for analytical purposes: determination of Zn by inductively coupled plasma–optical emission spectrometry, The Analyst 128 (6) (2003) 779–785, https://doi.org/10.1039/b212844f.
[60] A. Luna, R. Sturgeon, R. de Campos, Chemical vapor generation: atomic absorption by Ag, Au, Cu, and Zn following reduction of aquo ions with sodium tetrahydroborate(III), Anal. Chem. 72 (15) (2000) 3523–3531, https://doi.org/10.1021/ac000221n.
[61] N. Panichev, R. Sturgeon, Atomic absorption by free atoms in solution following chemical reduction from the ionic state, Anal. Chem. 70 (9) (1998) 1670–1676, https://doi.org/10.1021/ac980032t.
[62] A. Sanz–Medel, M.C. Valdes–Hevia y Temprano, N. Bordel Garcia, M.R. Fernandez de la Campa, Generation of cadmium atoms at room temperature using vesicles and its application to cadmium determination by cold vapor atomic spectrometry, Anal. Chem. 67 (13) (1995) 2216–2223, https://doi.org/10.1021/ac00109a048.
[63] E. Peña–Vázquez, J. Villanueva–Alonso, P. Bermejo–Barrera, Optimization of a vapour generation method for metal determination using ICP–OES, J. Anal. At. Spectrom. 22 (6) (2007) 642–649, https://doi.org/10.1039/b618652a.

foods

MDPI

Article

Elemental and Speciation Analyses of Different Brands of Yerba Mate (*Ilex paraguariensis*)

Jędrzej Proch, Aleksandra Orłowska and Przemysław Niedzielski *

Department of Analytical Chemistry, Faculty of Chemistry, Adam Mickiewicz University, Uniwersytetu Poznańskiego 8, 61-614 Poznań, Poland; jedrzej.proch@amu.edu.pl (J.P.); aleksandra.orlowska@amu.edu.pl (A.O.)
* Correspondence: pnied@amu.edu.pl

Abstract: In this work, a methodology for determination of As(III), As(V), dimethylarsinic acid (DMA), Fe(II) and Fe(III) in fifty-eight samples (forty-nine products of thirteen brands from three countries) commercial yerba mate *(Ilex paraguariensis)* was performed. The hyphenated high performance liquid chromatography inductively coupled plasma optical emission spectrometry (HPLC-ICP OES) technique was used. Arsenic was determined below the quantification limit in 38 samples of yerba mate. As(III) was found at the level 0.09 and 0.08 mg kg^{-1}. The As(V) content was in the range: 0.21 to 0.28 mg kg^{-1}. The content of DMA was found the highest of the three arsenic species in the range: 0.21 to 0.47 mg kg^{-1}. The content of Fe(II) and Fe(III) was found in the range: 0.61 to 15.4 mg kg^{-1} and 0.66 to 43.1 mg kg^{-1}, respectively and the dominance of Fe(III) was observed. Moreover, total and extractable content of 16 elements were determined. The results have been subjected to statistical analysis in order to establish relationships between samples of the same origin (country), kind (type) and composition (purity).

Keywords: yerba mate *(Ilex paraguariensis)*; speciation analysis; essential trace elements; potentially toxic elements; hyphenated systems; ICP OES

Citation: Proch, J.; Orłowska, A.; Niedzielski, P. Elemental and Speciation Analyses of Different Brands of Yerba Mate (*Ilex paraguariensis*). *Foods* **2021**, *10*, 2925. https://doi.org/10.3390/foods10122925

Academic Editor: Amin Mousavi Khaneghah

Received: 27 October 2021
Accepted: 23 November 2021
Published: 26 November 2021

1. Introduction

Yerba mate (*Ilex paraguariensis* St. Hil.) is a native South American tree. It is an important commercial product, consumed in the largest quantities in Brazil and Uruguay, while Argentina is the largest exporter [1]. The consumption of yerba mate has expanded to different countries e.g., Spain, France, Italy, Germany, Korea, Japan, Syria, Russia, United States and Australia [2]. Yerba mate can accumulate both essential trace and potentially toxic elements (PTEs) [1] and their content depends on certain factors, such as soil type, exposure of plants to pollution, even harvest season [3]. High tolerance to metals or metalloids has evolved in a number of plant species. Tolerant plants are often excluders, limiting the entry and translocation, or rarely hyperaccumulators combines extremely high tolerance to, and foliar accumulation of, trace elements [4].

Nowadays (2021), the determination of the total concentration of trace elements in yerba mate or its tea is not enough to evaluate the nutritional or toxic potential of the product. In infusions and decoctions, metals and metalloids may exist as either simple or complexed ions. This fact can affect the bioavailability of elements by humans [5]. What is more, nutritional and toxic potential depends on the element species, therefore a speciation analysis of elements, such as As, Cr, Fe, Se is crucial. The toxicity of elements forms is significantly different, and the greatest obstacle to the efficient determination of these forms is the ease of converting from one form to another [6,7]. In opposite to arsenic, iron (Fe) is an essential trace and the fourth most abundant element in the Earth's crust. Two main species, Fe(II) and Fe(III), are thermodynamically stable and kinetically reactive, however the role and the demand of these forms in living organisms are different [8]. Due to ambiguous classification of this material in the literature (as tea [9], laboratory plant [10] or wild–growing plant [11]), yerba mate *(Ilex paraguariensis)* is widely used by

authors as an application material for new analytical methods [1,5,12–17]. It is surprising that the content of essential trace and potentially toxic elements in yerba mate have been obtained by ICP OES [18], ICP MS [1,19] or both ICP OES and ICP MS [11,20], excluding any speciation studies. Admittedly, some methods for determining the species of selenium [14], arsenic [12], iron [13], as well as iron and arsenic [17] in several samples of yerba mate have already been presented. However, speciation studies have not yet been carried out on a larger number of samples.

In this study, to investigate the speciation of arsenic and iron in yerba mate *(Ilex paraguariensis)*, 58 samples were collected from the Polish market. Additionally, the determination of selected essential trace and potentially toxic elements (PTEs), i.e., Al, As, Cd, Co, Cr, Cu, Fe, Hg, Li, Mn, Mo, Ni, Pb, Sb, Se and Zn, was performed using ICP OES. The determination of As(III), As(V) and DMA as well as Fe(II) and Fe(III) in yerba mate is a novel, although it is an enlargement of the preliminary studies, conducted for the first usage of HPLC–HG–ICP OES with MSIS as an interface [12], the first comparison of HPLC–MIP OES and HPLC–ICP OES [13], and the first combination of two HPLC systems with ICP OES through MSIS (2 HPLC-MSIS-ICP OES) [17].

2. Materials and Methods

2.1. Samples Collecting

Fifty–eight samples of forty–nine yerba mate products from thirteen brands were bought from legal stores located in Poland. Samples were originated from Argentina (n = 15), Brazil (n = 23), and Paraguay (n = 18), however most of samples (n = 33) were repackaged in Poland (and distributed under a Polish trademark). According to kind (type), 30 samples were "con palo" (a mixture of 70% leaves and 30% stalks) and 26 samples were "despalada" (a mixture of 90% leaves and 10% stalks). According to composition (purity), 34 samples contained some additives (Table 1) and 24 samples were pure yerba mate. Additionally, nine products (A1, B5, B7, D1, D2, D3, D4, F3, H1) were collected twice (as a 50 g test sample and a 500 g pack). Full details were shown in Table 1.

Table 1. Details of samples' characteristics.

Sample No.	Product Code	Country of Origin	Type (Kind)	Additives	Packing Type (Weight)
1	A1	Argentina	Con palo	–	a pack (500 g)
2	A1	Argentina	Con palo	–	a test sample (50 g)
3	A2	Argentina	Con palo	–	a test sample (50 g)
4	A3	Argentina	Despalada	–	a pack (500 g)
5	A4	Argentina	Con palo	–	a pack (500 g)
6	A5	Argentina	Despalada	–	a pack (500 g)
7	B1	Paraguay *	Con palo	–	a test sample (50 g)
8	B2	Paraguay *	Con palo	–	a test sample (50 g)
9	B3	Paraguay *	Con palo	aromas	a test sample (50 g)
10	B4	Paraguay *	Despalada	–	a test sample (50 g)
11	B5	Paraguay *	Con palo	aromas	a pack (500 g)
12	B5	Paraguay *	Con palo	aromas	a test sample (50 g)
13	B6	Paraguay *	Con palo	herbs	a test sample (50 g)
14	B7	Paraguay *	Con palo	herbs	a pack (500 g)
15	B7	Paraguay *	Con palo	herbs	a test sample (50 g)
16	C1	Brazil *	Despalada	–	a test sample (50 g)
17	C2	Brazil *	Despalada	fruits, aromas	a test sample (50 g)
18	C3	Brazil *	Despalada	fruits, herbs, aromas	a test sample (50 g)
19	C4	Brazil *	Despalada	fruits, flowers, herbs	a test sample (50 g)
20	C5	Brazil *	Despalada	herbs, fruits, aromas	a test sample (50 g)
21	C6	Brazil *	Despalada	flowers, herbs, seeds, aromas	a test sample (50 g)
22	C7	Brazil *	Despalada	fruits, flowers, aromas	a test sample (50 g)
23	C8	Brazil *	Despalada	fruits, aromas	a test sample (50 g)
24	C9	Brazil *	Despalada	herbs, fruits, aromas	a test sample (50 g)
25	C10	Brazil *	Despalada	herbs, fruit skin, aromas	a test sample (50 g)
26	C11	Brazil *	Despalada	fruit skin, herbs, aromas	a test sample (50 g)
27	C12	Brazil *	Despalada	fruits, flowers, aromas	a test sample (50 g)
28	D1	Paraguay	Con palo	–	a pack (500 g)
29	D1	Paraguay	Con palo	–	a test sample (50 g)
30	D2	Paraguay	Con palo	–	a pack (500 g)

Table 1. *Cont.*

Sample No.	Product Code	Country of Origin	Type (Kind)	Additives	Packing Type (Weight)
31	D2	Paraguay	Con palo	–	a test sample (50 g)
32	D3	Paraguay	Con palo	aromas	a pack (500 g)
33	D3	Paraguay	Con palo	aromas	a test sample (50 g)
34	D4	Paraguay	Con palo	herbs	a pack (500 g)
35	D4	Paraguay	Con palo	herbs	a test sample (50 g)
36	E1	Brazil *	Despalada	–	a test sample (50 g)
37	E2	Brazil *	Despalada	fruits, herbs, flowers, aromas	a test sample (50 g)
38	E3	Brazil *	Despalada	herbs, fruit skin, aromas	a test sample (50 g)
39	E4	Brazil *	Despalada	fruits, aromas	a test sample (50 g)
40	E5	Brazil *	Despalada	herbs, fruits, aromas	a test sample (50 g)
41	E6	Brazil *	Despalada	fruits, herbs, aromas	a test sample (50 g)
42	E7	Brazil *	Despalada	fruit skin, aromas	a test sample (50 g)
43	E8	Brazil *	Despalada	fruits, herbs, flowers, aromas	a test sample (50 g)
44	E9	Brazil *	Despalada	fruits, flowers, aromas	a test sample (50 g)
45	E10	Brazil *	Despalada	herbs, flowers, aromas	a test sample (50 g)
46	F1	Argentina	Con palo	–	a pack (500 g)
47	F2	Argentina	Con palo	–	a pack (500 g)
48	F3	Argentina	Con palo	–	a pack (500 g)
49	F3	Argentina	Con palo	–	a test sample (50 g)
50	G1	Argentina	Con palo	–	a test sample (50 g)
51	H1	Argentina	Con palo	–	a test sample (50 g)
52	H1	Argentina	Con palo	–	a pack (500 g)
53	H2	Argentina	Con palo	aromas	a test sample (50 g)
54	I1	Paraguay	Con palo	–	a test sample (50 g)
55	J1	N/D *	N/D	fruits, flowers, herbs	a weighted pack (100 g)
56	K1	Brazil	Despalada	–	a test sample (50 g)
57	L1	Argentina	Con palo	herbs, aromas	a pack (500 g)
58	M1	N/D *	N/D	fruit skin, fruits	a weighted pack (100 g)

The Latin letter means the brand (A–M), and the following Arabic number means the same product; * means repacked in Poland and distributed as the Polish trademark; N/D means no data.

2.2. Gases and Reagents

High-pure argon (N—5.0, purity 99.999%), obtained from Linde, Poland, was employed as a plasma gas. All solutions were prepared using deionized water (≥18 MΩ cm resistivity, water purification system Milli-Q (Merck Millipore, Darmstadt, Germany)). Standard solutions were prepared from commercially available ICP calibration standards (Romil, Cambridge, UK). Disodium hydroarsenate hepahydrate, sodium arsenite and cacodylic acid were collected from Sigma-Aldrich (Saint Louis, MO, USA). Ferric ammonium sulfate dodecahydrate and ferrous ammonium sulfate hexahydrate were obtained from Acros-Thermo Fisher Scientific (Geel, Belgium). Standard solutions of iron and arsenic (1000 mg L^{-1}) were prepared by dissolving appropriate amounts of chemical compound in water. Less concentrated standard solutions obtained by dilution of the stock solutions were prepared daily. 1 mol L^{-1} orthophosphoric acid was prepared from 85% H_3PO_4 (POCH™, Avantor®, Gliwice, Poland). 65% nitric acid (HNO_3) was obtained from Merck.

A phosphate buffer was prepared by mixing disodium hydrophosphate (Na_2HPO_4) and potassium dihydrophosphate ($KH_2PO_4 \cdot 2H_2O$) obtained from Merck. Appropriate amounts of powder reagents were dissolved and mixed to obtain the mobile phase solution, 25 mmol L^{-1} $KH_2PO_4 \cdot 2H_2O$ and 2.5 mmol L^{-1} Na_2HPO_4 (pH adjusted to 6.0 ± 0.2). 1.0% (w/v) sodium tetrahydroborate ($NaBH_4$), was prepared daily, by dissolving appropriate amounts of powdered $NaBH_4$ (Sigma-Aldrich) in water and stabilized with 0.1% (w/v) NaOH (Merck). 5 mol L^{-1} hydrochloric acid was prepared from 30% HCl (Suprapur®, Merck). A PDCA eluent was prepared by mixing appropriate volumes of pyridine-2,6-dicarboxylic acid (PDCA) and formic acid (HCOOH) (Sigma-Aldrich), then appropriate amounts of potassium hydroxide (KOH) and potassium sulfate (K_2SO_4) (Merck) were dissolved in deionized water. Molar concentrations of PDCA, K_2SO_4 KOH, and HCOOH were 7.0, 5.6, 66 and 74 mmol L^{-1} respectively (pH 4.2 ± 0.2). 100 mmol L^{-1} sodium sulfite (Merck) was obtained by dissolving appropriate amounts of powder (Na_2SO_3) in water and the solution was used to the periodic column conditioning.

2.3. Sample Preparation

Samples were homogenized using agate laboratory grinder (Pulverisette, Fritsch GmbH, Idar-Oberstein, Germany). The procedure of ultrasound-assisted extraction was repeated after previous studies [12,13,17]. Accurately weighted 1.00 (±0.01) g dry samples were placed in a polyethylene test tube. Then 8.0 mL of 1 mol L^{-1} orthophosphoric acid (H_3PO_4) was added and the ultrasound-assisted extraction was conducted for 30 min at ambient temperature. Then samples were filtered through a paper filter, washed previously by 200 mL of water and 20 mL of phosphate buffer. Sample solutions were neutralized with a few drops of 15 mol L^{-1} NaOH to obtain pH value in the range of 6.0 to 6.5 and filled up to the final volume of 10 mL. Prepared extracts were tested using ICP OES (extractable content), HPLC-HG-ICP OES (arsenic speciation analysis) and HPLC-ICP OES (iron speciation analysis). Samples were analyzed daily or stored at −30 °C in the laboratory (no longer than a week). Additionally, accurately weighted, 0.500 (± 0.001) g of dry samples, were digested with 5.0 mL of 65% HNO_3 in closed Teflon® containers (55 mL) using the microwave digestion system, Mars 6 (CEM, Matthews, NC, USA). The process was carried out in three stage: (1) ramping the temperature (20 min), (2) holding at 180 °C (20 min), (3) cooling (20 min). After digestion, samples were diluted with deionized water to a final volume of 10 mL. Digested samples were analyzed using ICP OES (total content of elements).

2.4. Arsenic Speciation Studies Using HPLC-HG-ICP OES

The hyphenated technique, HPLC-HG-ICP OES with multi-mode sample introduction system (MSIS, Agilent, Santa Clara, CA, USA) as an interface was previously described in details [12] and it was used to determine As(III), As(V) and DMA. Full experimental conditions of HPLC-HG-ICP OES were summarized in Table 2. The HPLC system was constructed from a HPLC pump, Shimadzu LC-10AT (Shimadzu, Kyoto, Japan) and an anion-exchange HPLC column, Supelco LC-SAX1, 250 mm × 4.6 mm i.d., resin particle size 5 µm (Supelco, Bellefonte, PA, USA). The outlet of the HPLC column was directly connected (avoiding the peristaltic pump) with the tube which supplied HCl using T-shape connecter. The hydride generation is possible due to inlets located vertically in the center of the MSIS unit. The upper inlet was used to provide $NaBH_4$ solution. The lower inlet provided an eluent with sample solution and HCl, HG reagents were mixed at the top of the inlets, volatile hydrides were formed and transported into ICP torch by argon (introduced by nebulizer gas inlet). A nebulizer sample inlet stayed blocked. The excess liquid was carried from the chamber using a peristaltic pump. The detector of the hyphenated technique was Agilent 5110 ICP-OES (Agilent). The sample was analyzed three times (n = 3). Instrument detection limits (DLs) were calculated using the background equivalent concentration (BEC) and the signal-to-background ratio (SBR). The BEC was calculated as BEC = $C_{standard}$/SBR, where $C_{standard}$ is the concentration of reference standard solution; SBR = ($I_{standard} - I_{blank}$) / I_{blank}; and I_{blank} and $I_{standard}$ are the emission intensities [cps] for the blank and the reference standard solution. The DL was calculated (DL = 3 × RSD_{blank} × BEC/100), RSD_{blank} is the relative standard deviation of multiple (n = 10) blank measurements. Instrument quantification limits (QLs, calculated as 3.3 × DL), were presented in Table 3 with the method quantification limits, which include a sample preparation. The standard addition method was used for traceability measurements. Recoveries were in the acceptable range (80–120%) and full results were presented in Supplementary Materials (Table S1). The uncertainty estimated for complete analytical process (with sample preparation step) was below 20%

Table 2. Operating conditions of HPLC-HG-ICP OES (arsenic speciation analysis), HPLC-ICP OES (iron speciation analysis) and ICP OES (total and extractable content).

	HPLC-HG-ICP OES	HPLC-ICP OES	ICP OES
HPLC conditions			
Pump	Shimadzu LC-10AT	Shimadzu LC-10AT	N/A
Column	Supelco LC-SAX 1 (250 mm × 4.6 mm i.d., 5 µm)	Dionex IonPac CS5A (250 mm × 4.0 mm i.d., 5 µm)	N/A
Mobile phase	Phosphate buffer	PDCA eluent	N/A
composition	2.5 mmol L^{-1} disodium hydrophosphate (Na_2HPO_4), 25 mmol L^{-1} potassium dihydrophosphate (KH_2PO_4 $2H_2O$)	7.0 mmol L^{-1} pyridine-2,6-dicarboxylic acid (PDCA), 66 mmol L^{-1} potassium hydroxide (KOH), 5.6 mmol L^{-1} potassium sulfate (K_2SO_4), 74 mmol L^{-1} formic acid (HCOOH)	N/A
pH	6.0 ± 0.2	4.2 ± 0.2	N/A
flow rate [mL min^{-1}]	2.0	2.0	N/A
Injection volume [mL]	0.2	0.2	N/A
Spray chamber type	MSIS (Agilent)	MSIS (Agilent)	Double-pass cyclonic (Agilent)
Work mode	HG	Nebulization	Nebulization
Sample channel	Lower inlet	Nebulizer (OneNeb, Agilent)	Nebulizer (OneNeb, Agilent)
HG parameters			
$NaBH_4$ concentration [%, *w/v*]	1.0	N/A	N/A
NaOH concentration [%, *v/v*]	0.1	N/A	N/A
HCl concentration [mol L^{-1}]	5.0	N/A	N/A
$NaBH_4$ flow rate [mL min^{-1}]	1.0	N/A	N/A
HCl flow rate [mL min^{-1}]	1.0	N/A	N/A
ICP OES conditions			
Spectrometer	ICP 5110 Dual-View	ICP 5110 Dual-View	ICP 5110 Dual-View
RF power [kW]	1.45	1.20	1.20
Nebulizer gas flow [L min^{-1}]	0.7	0.7	0.7
Plasma gas flow [L min^{-1}]	12	12	12
Auxiliary gas flow [L min^{-1}]	1.0	1.0	1.0
Torch view	axial	SVDV	SVDV
Analytical wavelengths [nm]	As 188.980	Fe 238.204	Al 396.152, As 188.980, Cd 214.439, Cr 267.716, Co 238.892, Cu 327.395, Fe 238.204, Hg 194.164, Li 670.783, Mn 257.610, Mo 202.032, Ni 231.604, Pb 220.353, Sb 206.834, Se 196.026, Zn 213.857.

MSIS—Multi-mode Sample Introduction System; HG—Hydride generation; SVDV—synchronous vertical dual view.

Table 3. Instrument and method quantification limits (including a sample preparation procedure).

	Al [a]	As [a]	As(III) [b]	As(V) [b]	DMA [b]	Cd [a]	Co [a]	Cr [a]	Cu [a]	Fe [a]	Fe(II) [c]	Fe(III) [c]	Hg [a]	Li [a]	Mn [a]	Mo [a]	Ni [a]	Pb [a]	Sb [a]	Se [a]	Zn [a]
QL [µg L^{-1}]	9.3	18	6.2	21	19	0.5	0.7	0.6	0.5	6.7	36	30	4.0	0.3	5.8	1.5	5.0	12	17	7.0	1.6
QL(ext) [mg kg^{-1}]	0.093	0.180	0.062	0.210	0.190	0.005	0.007	*	0.005	0.067	0.360	0.300	0.040	0.003	0.058	0.015	0.050	0.120	0.170	0.070	0.016
QL(total) [mg kg^{-1}]	0.190	0.360	x	x	x	0.010	0.014	0.012	0.010	0.134	x	x	0.080	0.006	0.116	0.030	0.100	0.240	0.340	0.140	0.032

[a]—determined by ICP OES; [b]—determined by HPLC-HG-ICP OES; [c]—determined by HPLC-ICP OES; QL—quantification limit (as 10 standard deviation of the blank); QL(total)—method quantification limit (including microwave-assisted digestion); QL(ext)—method quantification limit (including ultrasound-assisted extraction); x—not determined; *—not determined (due to interferences, details in text).

2.5. Iron Speciation Studies Using HPLC-ICP OES

The hyphenated technique, HPLC-ICP OES was previously described in details [13] and it was used to determine Fe(II) and Fe(III). The HPLC system was made up of a Shimadzu LC-10AT HPLC pump and a Dionex IonPac CS5A cation-exchange HPLC column (250 mm × 4.0 mm i.d., resin particle size 5 µm, Thermo Fisher Scientific, Waltham, MA, USA). The outlet of the cation-exchange HPLC column was directly connected (avoiding the peristaltic pump) with the nebulizer sample inlets. Peristaltic pump of ICP-OES system was used to drain the waste only. MSIS was applied as a conventional cyclonic spray chamber with OneNeb nebulizer (both Agilent). The detector of the hyphenated technique was Agilent 5110 ICP-OES (Agilent). The operating conditions were placed in Table 2. The sample was analyzed 3 times (n = 3). All DLs and QLs were calculated as described in the Section 2.4 and the results were presented in Table 3. The standard addition method was used for accuracy studies. Recoveries were in the acceptable range (80–120%) and full results were presented in Supplementary Materials (Table S1). The uncertainty for the complete analytical process (including a sample preparation) was at the level of 20%.

2.6. ICP OES Determination of Selected Elements Content

An inductively coupled plasma optical emission spectrometer (Agilent 5110 ICP-OES) was used to determine selected elements (Al, As, Cd, Co, Cr, Cu, Fe, Hg, Li, Mn, Mo, Ni, Pb, Sb, Se, Zn) in acid digests (total content) and extracts (extractable content). Synchronous vertical dual view (SVDV), which allows the axial and radial view analysis simultaneously, was used (viewing height for radial plasma observation was 8 mm). Grading fixed optic was thermostated at 35 °C and a detector, VistaChip II with the charge coupled device (CCD) was cooled to −40 °C using a triple Peltier system. The signal accusation time was 5 s for three replicates. The operating conditions were summarized in Table 2. The sample was analyzed three times (n = 3). All DLs and QLs were calculated as described in the Section 2.4 and the results are presented in Table 3. The standard addition method was used for traceability measurements. Recoveries were in the acceptable range (80–120%) and full results were presented in Supplementary Materials (Tables S1 and S2). The uncertainty for the complete analytical process with sample preparation step was estimated at the level of 20%.

2.7. Statistical Analysis

Statistical analyses were performed using computer software Statistica 13.3 (StatSoft, TIBCO Software Inc., Palo Alto, CA, USA). The distribution of the data was studied by the Kolmogorov-Smirnov, Lilliefors and Shapiro-Wilk tests. Given that the data did not follow a normal distribution, the Spearman's rank correlation coefficient, which is a nonparametric test, was used. The multidimensional statistical analysis (principal components analysis, PCA) was provided for the results of ICP OES analysis to indicate the individual differences in the elemental composition of the yerba mate samples. The probability value, p = 0.05, was applied for all statistical tests.

3. Results and Discussion

3.1. As and Fe Speciation Studies

When examining the composition of yerba mate in terms of the content of selected forms of arsenic and iron, two methods of sample preparation were used prior to the ICP OES analysis: microwave-assisted digestion to determine As(total) and Fe(total), and ultrasound-assisted extraction to determine As and Fe extractable with phosphoric acid, i.e., As(ext) and Fe(ext). Then extracted samples were analyzed parallel by HPLC-HG-ICP OES determining the content of As(III), As(V) and DMA and HPLC-ICP OES determining the content of Fe(II) and Fe(III). The differences between the extractable content and the sum of arsenic or iron species were described as undefined As or Fe extractable forms, i.e., As(und-ext) and Fe(und-ext). Moreover, the differences between the total content and the extractable content were described as a non-extractable fraction of As and Fe, i.e.,

As(non-ext) and Fe(non-ext). Results of arsenic and iron speciation studies were presented in Figure 1 as (a) the content of each fraction (mg kg^{-1}) and (b) the percentage of each fraction in total content (as 100%).

Arsenic was determined below the quantification limit (BQL) in 38 of the yerba mate samples. As(total) and As(ext) were found above quantification limit (AQL) in 20 and eight samples, respectively. As(ext) was determined BQL in 12 of 20 samples, therefore the content As(non-ext) was equal to As(total). In turn, As(III), As(V) and DMA were detected AQL only in two, four and four samples, respectively. Three arsenic species were only found AQL in one sample (no. 4), which was pure despalada from Argentina. As(III) was found at the similar level, 0.09 and 0.08 mg kg^{-1}, in samples nos. 4 and 8, respectively. These samples also contained inorganic As (the sum of As(III) and As(V)) at the highest level, i.e., 0.36 mg kg^{-1}. The As(V) content was in the narrow range, from 0.21 (no. 44) to 0.28 mg kg^{-1} (no. 8). The content of DMA was found in the range from 0.21 (no. 58) to 0.47 mg kg^{-1} (no. 12) and it was the highest of the three arsenic species. On one hand, the sum of three arsenic species represented the majority (80–98%) of As(ext), except samples nos. 13 and 18, containing only undefined As extractable forms (As(und-ext)) at relatively low levels, 0.28 and 0.24 mg kg^{-1}, respectively. On the other hand, the content of As(ext) was 29% (as median) of As(total).

The content of As(total) and As(ext) exceeded the recommended limit (0.60 mg kg^{-1}), established by legislation [21], in 16 and two samples (nos. 4 and 53), respectively. Surprisingly, the mean value of As(total) (1.35 mg kg^{-1}) was 26 [20], 28 [11,19] and 34 times higher [1,22] than in the literature, however it was also found BQL in 38 samples. Additionally, it is difficult to clearly indicate whether the ultrasound-assisted extraction in 1 mol L^{-1} H_3PO_4 (at room temperature) allows to extract its higher content than a traditional extraction in hot water (80 ± 10 °C). Opinions are divided in the literature and the following percentage of total content were found in hot water, 18% [22], 48% [20] and 49% [10]. Therefore, the risk of exceeding the recommended level cannot be directly assessed. The determination of three As species has not been performed on yerba mate samples yet, except the introduction as an application material for HPLC-HG-ICP OES [12] and 2 HPLC-MSIS-ICP OES [17], therefore no comparable data are available in the literature. In the first work, As(III), As(V) and DMA were found at lower ranges in six samples: 0.012–0.032 mg kg^{-1}, 0.046–0.108 mg kg^{-1} and 0.044–0.097 mg kg^{-1}, respectively [12]. In the second work, only As(V) was determined in three samples (0.31–0.33 mg kg^{-1}), while As(III) and DMA were found BQL in all samples (n = 8) [17]. Although results were rather comparable with those obtained in previous studies, occurring As and its species in yerba mate as well as occasionally the high content, are accidental rather than related to studied factors, i.e., country of origin and packing, kind or purity.

Fe(total) and Fe(ext) were found in the following ranges: 51.1–1059 mg kg^{-1} and 2.92–62.8 mg kg^{-1}, respectively, in the whole sample population (n = 58). In the case of Fe, it is difficult to clearly indicate whether the ultrasound-assisted extraction in 1 mol L^{-1} H_3PO_4 (at room temperature) allows one to extract a higher amount than a traditional extraction in hot water (80 ± 10 °C). Opinions on this in the literature are divided and the following percentages of total content were found in hot water: 1.3% [23], 2% [22], 3% [10] and 15% [20]. However, the percentage of extraction by cold water (1.1%) was similar to hot water (1.3%) [23], therefore a higher percentage of extraction may be obtained with the method proposed in this study, 8% (as median). Ionic Fe(II) and Fe(III) were determined AQL in 26 and 31 samples respectively. The content of Fe(II) and Fe(III) was ranging, 0.61–15.4 mg kg^{-1} and 0.66–43.1 mg kg^{-1}, respectively. Although the Fe(III)/Fe(II) ratio was found in wide range (0.3–33), the dominance of Fe(III) was observed (median = 2.7). Higher content of Fe(II) was determined in four samples (nos. 6, 29, 37, 39). The highest content of Fe(II) and Fe(III) was detected in samples nos. 11 and 9, respectively, which were both Paraguayan yerba mate con palo with additives (aromas) and distributed under the same Polish brand (Table 1).

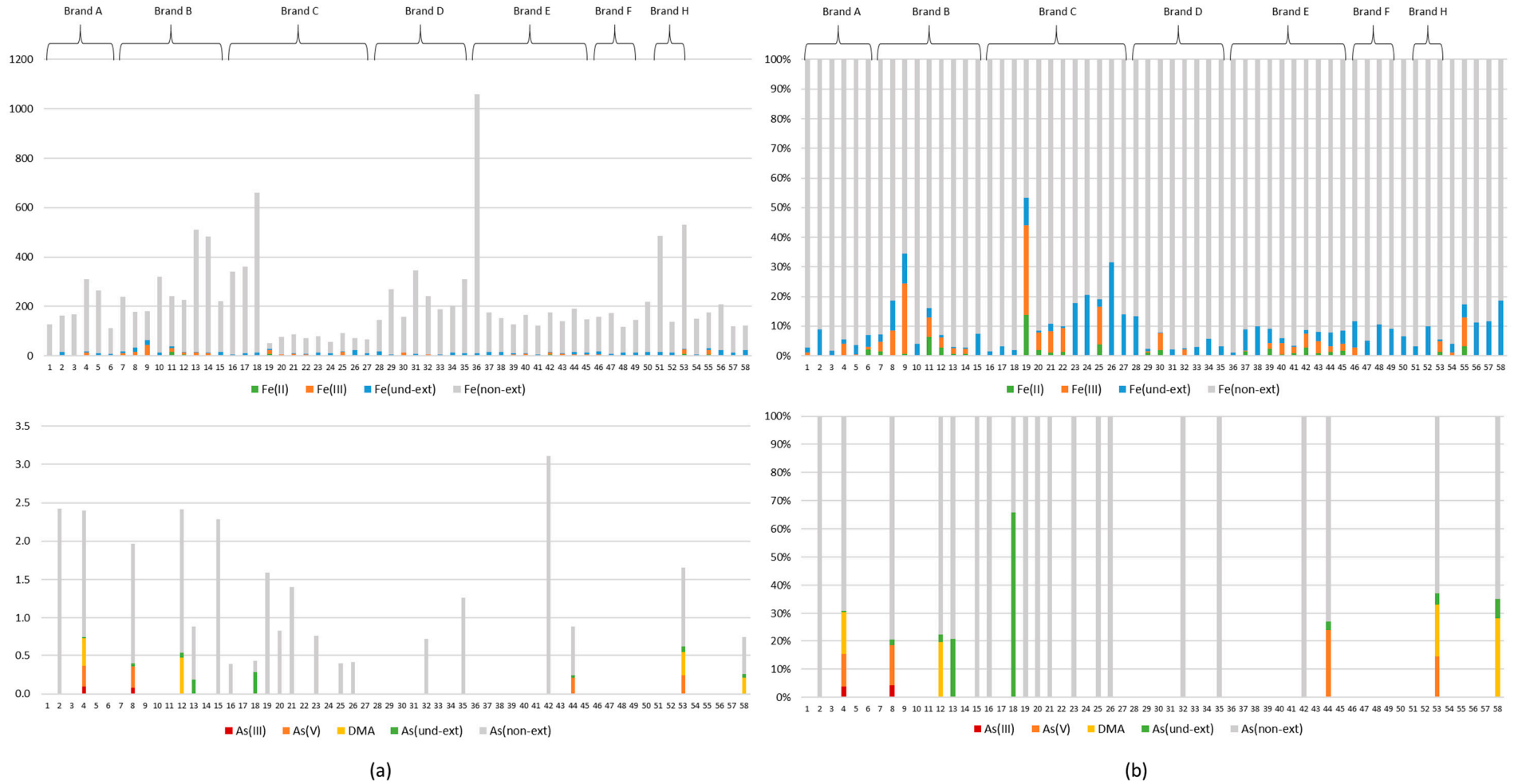

Figure 1. Results of iron and arsenic speciation analysis of yerba mate: (**a**) the concentration of each fraction in total content (as a sum, mg kg^{-1}) and (**b**) the percentage of each fraction in total content (as 100%). Captions: As(und-ext), Fe(und-ext)—undefined extractable fraction of arsenic and iron (i.e., the difference between extractable content and the sum of species content); As(non-ext), Fe(non-ext)—non-extractable fraction of arsenic or iron (i.e., the difference between total and extractable content).

The determination of two Fe species has not been performed on yerba mate samples yet, except the introduction as an application material for HPLC-ICP OES and HPLC-MIP OES [13] and 2 HPLC-MSIS-ICP OES [17], therefore no comparable data are found in the literature. In the first work, higher content of Fe(II) and Fe(III) were found in 2 (15–31 mg kg^{-1}) and three samples (16–43 mg kg^{-1}) respectively [13]. In the second study, Fe(III) was found in the range from 1.33 to 19.1 mg kg^{-1} in all samples (n = 8), while Fe(II) was determined in four samples (3.07–7.05 mg kg^{-1}) [17]. The dominance of Fe(III) was observed in mentioned studies what may indicate the implication of the oxidizing conditions of the production process of yerba mate (e.g., roasting) [24]. Based on data from preliminary studies [13,17], it was expected that the content of ionic Fe(II) and Fe(III) in yerba mate is widespread. Surprisingly, only Fe(und-ext) was detected in 27 samples. On the one hand, this may indicate the presence of certain extractable iron complex compounds in yerba mate, which remain stable despite the use of ultrasound-assisted extraction and are inert towards cation-exchange column. On the other hand, these complexes could also be formed with any compounds extractable under these conditions from the sample matrix. Nevertheless, in order to confirm or reject this hypothesis, it would be advisable to continue speciation studies on yerba mate, including by increasing the number of samples as well as analytes.

3.2. Total and Extractable Content of Selected Elements

The samples were considered as a whole (n = 58) and three groups, depending on the country of origin (Argentina, Brazil or Paraguay), kind (con palo or despalada) or composition (pure yerba mate or those with additives) (Table 1). The total content of selected essential trace and potentially toxic elements in yerba mate *(Ilex paraguariensis)* was presented in Table 4. The Kolmogorov-Smirnov, Lilliefors and Shapiro-Wilk tests indicated that the data did not follow a normal distribution (except Cu, what may be related with using Cu containing chemical products to control fungal diseases). According to this, the Spearman's rank correlation coefficient was used and results are discussed in Section 3.3.

Nine elements (Al, Cd, Co, Cr, Cu, Fe, Mn, Ni and Zn) were found AQL in all samples. Among the trace elements in yerba mate, the manganese content is indisputably the highest. Generally, the following order of total concentration (as median): Mn > Al > Fe > Zn > Cu > Ni > other elements, was observed in the whole population and every group which was reported before in several studies [11,20,22,23]. The only difference was Fe > Al in Paraguayan samples (Table 4). Other elements, which were found in the whole population (n = 58), were arranged in the following order: Cr > Co > Cd. Moreover, the same order was also observed for despalada, yerba mate with additives or those originating from Brazil and Paraguay. However, the different order (Cr > Cd > Co) was found in con palo and pure yerba mate. The order Cr > Cd > Co was also reported in the literature [11,20]. The order Co > Cr > Cd was observed in the case of Argentinian samples (n = 15). Seven elements, As, Hg, Li, Mo, Pb, Sb and Se, were found AQL in 20, 27, 42, 54, 15, 50 and 38 samples respectively (Table 5). The order As > Sb > Se > Pb was observed in the whole population and con palo samples. Moreover, the order Sb > Se > As > Pb was found in the case of despalada and Brazilian samples while it was different for Argentinian (As > Sb > Se > Pb), Paraguayan (Sb > As > Se > Pb) samples and pure yerba mate (As > Pb > Sb > Se). Moreover, Pb > Se distinguished pure and Brazilian samples. The content of Hg, Li and Mo was similarly low and the order Hg > Mo > Li was observed in each subgroup and the whole population. It is worth mentioning that the same order, containing all of 16 elements (in total content), was observed in two subgroups (despalada and Brazilian samples). The above compliance is due to the fact that all Brazilian samples (n = 23) are despalada (n = 26).

Table 4. Total content (mg kg^{-1}) of selected essential trace and potentially toxic elements in yerba mate *(Ilex paraguariensis)* in accordance with the whole population, origin, kind (type) and composition (purity).

	Origin			Kind (Type)		Composition (Purity)		Whole Population
	Argentina (*n* = 15)	**Brazil (*n* = 23)**	**Paraguay (*n* = 18)**	**Con Palo (*n* = 30)**	**Despalada (*n* = 26)**	**Pure Mate (*n* = 24)**	**With Additives (*n* = 34)**	**(*n* = 58)**
Elements	**Median {Range} (AQL)**	**Median {Range} (AQL)**	**Median {Range} (AQL)**	**Median {Range} (AQL)**	**Median {Range} (AQL)**	**Median {Range} (AQL)**	**Median {Range} (AQL)**	**Median {Range} (AQL)**
Al	210 {86–337} (15)	220 {97–366} (23)	208 {128–371} (18)	210 {86–371} (30)	220 {97–366} (26)	226 {128–366} (24)	207 {86–371} (34)	215 {86–371} (58)
As	2.40 {1.66–2.43} (3)	0.79 {0.39–3.11} (10)	1.61 {0.71–2.42} (6)	1.81 {0.71–2.43} (8)	0.83 {0.39–3.11} (11)	2.18 {0.39–2.43} (4)	0.89 {0.40–3.11} (16)	1.08 {0.39–3.11} (20)
Cd	0.30 {0.16–0.52} (15)	0.41 {0.25–0.68} (23)	0.43 {0.26–0.64} (18)	0.41 {0.16–0.64} (30)	0.40 {0.24–0.68} (26)	0.41 {0.16–0.62} (24)	0.40 {0.24–0.72} (34)	0.41 {0.16–0.72} (58)
Co	0.79 {0.16–1.68} (15)	0.34 {0.02–0.94} (23)	0.33 {0.17–0.60} (18)	0.41 {0.16–1.68} (30)	0.37 {0.02–0.94} (26)	0.47 {0.16–1.68} (24)	0.34 {0.02–0.94} (34)	0.39 {0.02–1.68} (58)
Cr	0.64 {0.26–2.11} (15)	0.57 {0.01–1.20} (23)	0.52 {0.35–0.79} (18)	0.53 {0.26–2.11} (30)	0.56 {0.01–1.20} (26)	0.59 {0.30–1.20} (24)	0.53 {0.01–2.11} (34)	0.55 {0.01–2.11} (58)
Cu	5.46 {3.01–9.20} (15)	7.14 {4.45–9.50} (23)	6.32 {4.62–10.6} (18)	6.16 {3.95–10.6} (30)	7.06 {3.01–9.50} (26)	5.60 {3.01–9.50} (24)	6.98 {3.95–10.6} (34)	6.75 {3.01–10.6} (58)
Fe	164 {113–532} (15)	141 {51–1059} (23)	233 {145–510} (18)	196 {118–532} (30)	144 {51–1059} (26)	176 {113–1059} (24)	170 {51–660} (34)	173 {51–1059} (58)
Hg	0.29 {0.09–0.59} (8)	0.26 {0.09–1.34} (10)	0.33 {0.03–0.56} (8)	0.33 {0.03–0.59} (15)	0.22 {0.09–1.34} (11)	0.31 {0.03–0.59} (12)	0.30 {0.09–1.34} (15)	0.30 {0.03–1.34} (27)
Li	0.06 {0.01–0.09} (9)	0.06 {0.01–0.18} (14)	0.10 {0.03–0.21} (18)	0.07 {0.01–0.21} (25)	0.06 {0.01–0.18} (16)	0.07 {0.01–0.21} (19)	0.06 {0.01–0.21} (23)	0.06 {0.01–0.21} (42)
Mn	2717 {986–3461} (15)	1518 {800–2321} (23)	1231 {653–1966} (18)	1396 {653–3461} (30)	1650 {800–3265} (26)	1969 {797–3461} (24)	1448 {653–3257} (34)	1575 {653–3461} (58)
Mo	0.28 {0.06–0.52} (14)	0.15 {0.05–0.94} (21)	0.23 {0.05–0.55} (17)	0.22 {0.05–0.55} (28)	0.18 {0.05–0.94} (24)	0.24 {0.07–0.55} (23)	0.19 {0.05–0.94} (31)	0.21 {0.05–0.94} (54)
Ni	5.79 {3.26–8.60} (15)	4.01 {2.65–11.9} (23)	4.27 {2.57–12.9} (18)	4.82 {2.57–12.9} (30)	4.08 {2.65–11.9} (26)	5.25 {2.57–12.9} (24)	4.11 {2.61–11.9} (34)	4.30 {2.57–12.9} (58)
Pb	0.88 {0.60–1.17} (2)	0.45 {0.27–2.92} (7)	0.59 {0.27–1.24} (5)	0.60 {0.27–1.24} (7)	0.45 {0.27–2.92} (7)	0.90 {0.27–1.25} (5)	0.58 {0.27–2.92} (10)	0.60 {0.27–2.92} (15)
Sb	0.90 {0.29–2.77} (14)	1.04 {0.39–3.10} (17)	1.17 {0.40–2.60} (17)	0.91 {0.40–2.60} (28)	1.21 {0.29–3.10} (20)	0.89 {0.29–2.77} (21)	0.94 {0.39–3.10} (29)	0.92 {0.29–3.10} (50)
Se	0.76 {0.47–2.15} (8)	0.86 {0.15–2.54} (17)	0.71 {0.57–2.25} (11)	0.71 {0.47–2.25} (18)	0.90 {0.15–2.54} (18)	0.73 {0.47–2.15} (12)	0.90 {0.15–2.54} (26)	0.81 {0.15–2.54} (38)
Zn	36.5 {24.3–68.7} (15)	42.5 {31.3–135} (23)	78.5 {55.2–105} (18)	66.9 {27.4–103} (30)	41.7 {24.3–135} (26)	57.5 {24.3–135} (24)	56.3 {27.2–110} (34)	57.2 {24.3–135} (58)

AQL—above method qualification limit (the number of results exceeding AQL in round brackets); Range—as content {min–max}.

Table 5. Extractable content (mg kg^{-1}) of selected essential trace and potentially toxic elements in yerba mate *(Ilex paraguariensis)* in accordance with the whole population (including the percentage of extraction), origin, kind (type) and composition (purity).

	Origin			Kind (Type)		Composition (Purity)		Whole Population (n = 58)	
	Argentina (n = 15)	**Brazil (n = 23)**	**Paraguay (n = 18)**	**Con Palo (n = 30)**	**Despalada (n = 26)**	**Pure Mate (n = 24)**	**With Additives (n = 34)**	**Content (mg kg^{-1})**	**% of Total Content**
Elements	**Median {Range} (AQL)**	**Median {Range} (AQL)**	**Median {Range} (AQL)**	**Median {Range} (AQL)**	**Median {Range} (AQL)**	**Median {Range} (AQL)**	**Median {Range} (AQL)**	**Median {Range} (AQL)**	**Median {Range} (AQL)**
Al	66.2 {8.70–132} (15)	51.1 {16.3–124} (23)	41.6 {12.5–131} (18)	47.6 {8.70–132} (30)	54.4 {16.3–124} (26)	60.1 {8.70–132} (24)	49.2 {20.2–131} (34)	52.9 {8.70–132} (58)	28 {4–80} (58)
As	0.68 {0.62–0.74} (2)	0.26 {0.24–0.28} (2)	0.40 {0.18–0.54} (3)	0.47 {0.18–0.62} (4)	0.28 {0.24–0.74} (3)	0.57 {0.40–0.74} (2)	0.27 {0.18–0.62} (6)	0.34 {0.18–0.74} (8)	29 {20–66} (8)
Cd	0.05 {0.02–0.22} (13)	0.06 {0.02–0.21} (20)	0.11 {0.04–0.35} (13)	0.07 {0.02–0.35} (23)	0.06 {0.02–0.21} (23)	0.05 {0.02–0.35} (21)	0.08 {0.02–0.33} (27)	0.07 {0.02–0.35} (48)	17 {3–86} (48)
Co	0.24 {0.07–0.51} (14)	0.18 {0.03–0.60} (17)	0.16 {0.02–0.44} (15)	0.18 {0.03–0.51} (26)	0.17 {0.02–0.60} (20)	0.16 {0.02–0.51} (22)	0.19 {0.03–0.60} (25)	0.18 {0.02–0.60} (47)	37 {3–99.8} (47)
Cr	x	x	x	x	x	x	x	x	x
Cu	2.22 {0.43–4.52} (15)	2.54 {0.77–4.42} (23)	1.95 {0.56–4.91} (18)	2.10 {0.43–4.91} (30)	2.65 {0.77–4.42} (26)	2.29 {0.43–4.06} (24)	2.50 {0.86–5.79} (34)	2.30 {0.43–5.79} (58)	39 {8–99} (58)
Fe	13.8 {2.92–29.4} (15)	11.5 {4.18–27.3} (23)	13.4 {5.72–62.8} (18)	13.8 {2.92–62.8} (30)	11.9 {4.18–27.3} (26)	12.9 {2.92–33.3} (24)	13.8 {4.18–62.8} (34)	13.2 {2.92–62.8} (58)	8 {1–53} (58)
Hg	0.08 * (1)	BQL	BQL	0.08 * (1)	BQL	BQL	0.08 * (1)	0.08 * (1)	84 * (1)
Li	BQL	BQL	0.03 {0.01–0.04} (2)	0.03 {0.01–0.04} (2)	BQL	BQL	0.03 {0.01–0.04} (2)	0.03 {0.01–0.04} (2)	34 {33–35} (2)
Mn	513 {58.7–1110} (15)	326 {126–860} (23)	239 {29.3–913} (18)	317 {29.3–1110} (30)	342 {126–922} (26)	376 {29.3–1110} (24)	313 {63.9–1085} (34)	343 {29.3–1110} (58)	23 {2–66} (58)
Mo	BQL	0.14 * (1)	0.11 * (1)	0.11 * (1)	0.14 * (1)	0.11 * (1)	0.13 {0.13–0.14} (2)	0.13 {0.11–0.14} (3)	57 {32–60} (3)
Ni	1.60 {0.77–2.67} (14)	1.01 {0.08–2.35} (23)	1.09 {0.29–2.70} (18)	1.39 {0.29–2.70} (29)	1.01 {0.08–2.67} (26)	1.47 {0.29–2.67} (23)	1.02 {0.08–2.70} (34)	1.11 {0.08–2.70} (57)	27 {3–70} (57)
Pb	0.82 * (1)	0.71 {0.11–1.37} (3)	0.44 {0.21–0.59} (3)	0.51 {0.21–0.82} (4)	0.71 {0.11–1.37} (3)	0.76 {0.71–0.82} (2)	0.44 {0.11–1.37} (5)	0.59 {0.11–1.37} (7)	56 {17–75} (7)
Sb	0.44 {0.13–0.80} (13)	0.27 {0.09–0.65} (17)	0.39 {0.08–1.17} (16)	0.42 {0.08–1.17} (27)	0.27 {0.09–0.65} (19)	0.34 {0.08–0.68} (19)	0.42 {0.09–1.17} (29)	0.39 {0.08–1.17} (48)	36 {9–94} (48)
Se	0.70 {0.15–1.25} (2)	0.88 {0.83–0.95} (3)	1.12 * (1)	0.64 {0.15–1.12} (2)	0.91 {0.83–1.25} (4)	0.70 {0.15–1.25} (2)	0.88 {0.18–1.12} (5)	0.88 {0.15–1.25} (7)	61 {19–88} (7)
Zn	16.1 {1.69–36.2} (15)	19.7 {6.79–33.7} (23)	23.9 {5.50–72.2} (18)	19.5 {1.69–72.2} (30)	19.4 {6.79–37.6} (26)	15.4 {1.69–66.3} (24)	21.6 {6.79–72.2} (34)	19.4 {1.69–72.2} (58)	35 {5–99} (58)

AQL—above method qualification limit (the number of results exceeding AQL in round brackets); Range—as content {min–max}; BQL—below quantification limit (if AQL = 0); *—the value (if AQL = 1); x—not determined due to interference, details in text.

The extractable content of selected essential trace and potentially toxic elements in 58 samples of yerba mate *(Ilex paraguariensis)* is presented in Table 5. In contrast to total content, only five elements were found AQL in all samples (Al, Cu, Fe, Mn, and Zn). Moreover, Ni was detected BQL only in one sample (no. 1), which was a pure yerba mate con palo from Argentina. In turn, Cd, Co and Sb were determined in 48, 47 and 48 extracts, respectively. It is worth noting that other studied elements were found AQL only in one (Hg), two (Li), three (Mo), seven (Pb and Se) and eight samples (As). However, Cr extractable content was significantly higher than its total content. The increase in the results was repeatable and it seemed to be caused by unexpected signal interferences related to the selection of the sample preparation method (ultrasonic extraction with diluted phosphoric acid) or a peculiarity of the sample matrix. Nevertheless, this problem would require further clarification, therefore the results for the Cr extractable content was rejected.

The following order of extractable content was observed (as median) in the whole population and each subgroup: Mn > Al > Zn > Fe > Cu > Ni > other elements. Considering only elements, whose results were BQL for <20% of all samples (i.e., Al, Cd, Co, Cu, Fe, Mn, Sb, and Zn), the order for each subgroup as well as the whole population was identical: Mn > Al > Zn > Fe > Cu > Ni > Sb > Co > Cd. In the case of other elements (As, Pb and Se), the order Se > Pb > As was found in the whole population and four subgroups (con palo, despalada, yerba mate with additives and those originating from Brazil). The order Pb >Se > As was observed for pure yerba mate (n = 24).

For the whole sample population (n = 58), the percentages of extraction (as median) were arranged in the ascending order: Fe (8%), Cd (17%), Mn (23%), Ni (27%), Al (28%), As (29%), Li (34%), Zn (35%), Sb (36%), Co (37%), Cu (39%), Pb (56%), Mo (57%), Se (61%), and Hg (84%), however Hg(ext) was only determined AQL in one sample (no. 53, Argentinian yerba mate con palo with additives). Comparing to other studies, where the percentages were obtained after hot water extraction [10,20,22,23,25], the percentages in this study were both lower (Co) and higher (Al and Se). In the case of other elements, it is difficult to clearly indicate whether the ultrasound-assisted extraction in 1 mol L^{-1} H_3PO_4 (at room temperature) allows to extract its higher content than a traditional extraction in hot water (80 ± 10 °C). According to the studies mentioned above, As, Cu, Li, Mn and Ni were usually better extracted using hot water and Cd, Fe, Mo, Pb and Zn were rather better extracted with diluted phosphoric acid [10,20,22,23,25].

In the case of tea or yerba mate, the maximum limits of total concentrations of As, Cd and Pb were established by legislation (0.6, 0.4, and 0.6 mg kg^{-1}, respectively) [21], however, the results for arsenic have already been discussed in Section 3.1. The content of Pb(total) and Pb(ext) exceeded the recommended limit (0.6 mg kg^{-1}) in eight and three samples (nos. 16, 19 and 50), respectively. The mean value of Pb(total) (0.86 mg kg^{-1}) was slight higher than in the literature [10,20,22,23], however samples exceeding the Pb limit were also reported before [1,15,19,26]. Nevertheless, Pb(total) was found BQL in 43 samples. In turn, Cd(total) was determined in all samples (n = 58), while Cd(ext) was found AQL in 48 samples. The content of Cd(total) and Cd(ext) exceeded the recommended limit (0.4 mg kg^{-1}) in 30 and six samples (nos. 4, 8, 43, 46, 50, 53), respectively. Moreover, the mean value of Cd(total) (also the median, 0.41 mg kg^{-1}) exceeded the limit. These results corresponds to several studies which indicate that Cd was frequently found above 0.4 mg kg^{-1} [1,15,19,20,22,23,26,27]. Based on these findings, these concentrations may be considered natural and established limits should be revised, especially for Cd and Pb [26,27].

For easier evaluation of the results obtained in this study, the total content of elements in yerba mate samples was compared with the literature data (Table 6). In addition, the results were also divided into groups (origin, kind and composition), as pure yerba mate samples and those with additives have not been compared previously in terms of the elemental composition.

Table 6. Total content (as mean ± SD, mg kg^{-1}) obtained in this study in comparison to the literature data.

Group		N	Al	As	Cd	Co	Cr	Cu	Fe	Hg	Li	Mn	Mo	Ni	Pb	Sb	Se	Zn	Ref.
Whole population		58	217 ± 67	1.35 ± 0.81	0.41 ± 0.13	0.49 ± 0.37	0.60 ± 0.28	6.69 ± 1.60	221 ± 168	0.33 ± 0.26	0.08 ± 0.05	1727 ± 735	0.26 ± 0.18	4.79 ± 2.00	0.86 ± 0.65	1.18 ± 0.68	0.93 ± 0.52	59.4 ± 24.9	This study
		54	361 ± 108	0.052 ± 0.251	0.410 ± 0.180	0.169 ± 0.956	0.528 ± 0.240	11.9 ± 2.06	205 ± 89.1	ND	0.085 ± 0.079	1078 ± 377	0.066 ± 0.325	2.74 ± 0.945	0.314 ± 0.181	ND	ND	63.6 ± 25.0	[11]
		32	90.4 ± 50.9	ND	0.19 ± 0.12	BQL	0.35 ± 0.13	5.17 ± 2.07	21.6 ± 16.5	ND	3.57 ± 1.94	66.4 ± 30.2	0.60 ± 0.40	1.39 ± 0.44	0.36 ± 0.41	ND	ND	32.5 ± 11.9	[23]
Origin	Argentina	15	214 ± 63	2.16 ± 0.36	0.32 ± 0.13	0.88 ± 0.43	0.73 ± 0.40	5.73 ± 1.57	216 ± 127	0.27 ± 0.16	0.05 ± 0.03	2543 ± 672	0.28 ± 0.14	5.71 ± 1.41	0.88 [b]	1.07 ± 0.60	0.89 ± 0.49	43.1 ± 15.4	This study
		14	347 ± 60	0.04 ± 0.01	0.373 ± 0.167	0.209 ± 0.073	0.689 ± 0.18	12.6 ± 2.0	196 ± 42	ND	66.9 ± 22.4	1368 ± 256	0.051 ± 0.020	2.72 ± 0.718	0.222 ± 0.107	BDL	BDL	79.4 ± 17.7	[20]
		10	ND	ND	0.31 [a]	ND	1.15 [a]	7.72 [a]	200 [a]	ND	ND	1730 [a]	ND	3.96 [a]	0.40 [a]	ND	ND	78.01 [a]	[25]
	Brazil	23	216 ± 73	1.02 ± 0.80	0.44 ± 0.12	0.39 ± 0.28	0.61 ± 0.25	7.38 ± 1.22	203 ± 225	0.37 ± 0.36	0.06 ± 0.04	1525 ± 448	0.22 ± 0.21	4.38 ± 1.98	0.92 ± 0.88	1.28 ± 0.78	0.91 ± 0.54	55.9 ± 27.4	This study
		19	291 ± 56	0.05 ± 0.03	0.491 ± 0.225	0.121 ± 0.094	0.37 ± 0.19	11.4 ± 2.1	154 ± 48	ND	74.5 ± 134	987 ± 352	0.066 ± 0.040	2.38 ± 1.14	0.407 ± 0.230	BDL	BDL	44.2 ± 14.7	[20]
		9	378 ± 113	0.04 ± 0.02	0.40 ± 0.13	0.21 ± 0.09	ND	9.22 ± 0.95	280 ± 221	ND	0.11 ± 0.06	1313 ± 592	0.05 ± 0.05	2.19 ± 0.55	0.28 ± 0.12	ND	0.03 ± 0.02	55 ± 13	[22]
	Paraguay	18	219 ± 63	1.59 ± 0.67	0.45 ± 0.10	0.33 ± 0.11	0.52 ± 0.11	6.44 ± 1.62	257 ± 102	0.34 ± 0.16	0.10 ± 0.05	1224 ± 339	0.28 ± 0.17	4.53 ± 2.25	0.78 ± 0.38	1.23 ± 0.62	0.97 ± 0.55	79.0 ± 12.7	This study
		14	384 ± 62	0.06 ± 0.03	0.295 ± 0.082	0.101 ± 0.084	0.70 ± 0.13	11.1 ± 1.9	226 ± 122	ND	59.1 ± 33.3	730 ± 150	0.089 ± 0.022	2.81 ± 0.720	0.314 ± 0.178	BDL	BDL	77.3 ± 25.4	[20]
		5	ND	ND	0.30 [a]	ND	0.88 [a]	7.28 [a]	130 [a]	ND	ND	680 [a]	ND	3.03 [a]	0.45 [a]	ND	ND	115.05 [a]	[25]
Kind (type)	con palo	30	216 ± 63	1.70 ± 0.64	0.40 ± 0.13	0.56 ± 0.42	0.62 ± 0.31	6.26 ± 1.61	237 ± 118	0.32 ± 0.16	0.08 ± 0.06	1776 ± 836	0.26 ± 0.15	5.06 ± 2.06	0.81 ± 0.36	1.09 ± 0.50	0.87 ± 0.46	63.7 ± 20.3	This study
		10	ND	ND	0.33 [a]	ND	0.95 [a]	7.35 [a]	150 [a]	ND	ND	1070 [a]	ND	3.27 [a]	0.39 [a]	ND	ND	96.49 [a]	[25]
	despalada	26	217 ± 72	1.15 ± 0.86	0.43 ± 0.12	0.43 ± 0.29	0.61 ± 0.23	7.07 ± 1.49	208 ± 215	0.35 ± 0.36	0.06 ± 0.03	1615 ± 541	0.25 ± 0.22	4.47 ± 1.93	0.92 ± 0.88	1.36 ± 0.85	0.97 ± 0.60	55.5 ± 28.7	This study
		5	ND	ND	0.28 [a]	ND	1.29 [a]	8.03 [a]	220 [a]	ND	ND	1990 [a]	ND	4.41 [a]	0.52 [a]	ND	ND	78.10 [a]	[25]
Composition (purity)	pure mate	24	235 ± 69	1.79 ± 0.83	0.38 ± 0.14	0.65 ± 0.44	0.62 ± 0.19	6.15 ± 1.59	250 ± 191	0.29 ± 0.13	0.07 ± 0.05	2037 ± 837	0.27 ± 0.15	5.38 ± 2.18	0.84 ± 0.36	1.11 ± 0.61	0.83 ± 0.42	58.2 ± 27.4	This study
	with additives	34	205 ± 62	1.24 ± 0.77	0.43 ± 0.13	0.38 ± 0.26	0.59 ± 0.33	7.06 ± 1.50	201 ± 146	0.37 ± 0.32	0.08 ± 0.05	1509 ± 558	0.24 ± 0.20	4.37 ± 1.74	0.88 ± 0.76	1.24 ± 0.71	0.97 ± 0.56	60.3 ± 22.9	This study

N—number of samples; BQL—below quantification limit; BDL—below detection limit; SD—standard deviation; ND—not determined; [a]—mean (if SD was not reported); [b]—median (if $n < 3$).

According to the latest literature, the total content of all selected elements was variable, however the results were generally in the same order of magnitude, except for As and Li (Table 6). Generally, most of determined elements had slightly higher contents than in the literature and the exceptions were Cu and Li. Significant excess levels of selected elements in comparison with the literature may be caused by dust residue deposition, which increased Fe, Ti, As, Pb, Li, Mo, and V concentrations of foliar tissue, what was confirmed in the washing process [26]. As samples were not washed prior to their homogenization, it explains higher content of As, Fe, Mn, Pb, Mo, Ni and Sb found in our study than in the literature (Table 6). It was reported that field handling, transportation, and loading procedures were likely routes of soil contamination of commercial products [26].

Nevertheless, some observations in accordance with studied groups were similar to the literature data. According to kind (con palo or despalada), obtained results for total content of Cu, Ni, Pb and Zn corresponded to those obtained by Baran et al. [25], however the results for Cd, Fe and Mn showed an opposite trend. Authors similarly reported the higher content of Cr and Zn and lower of Mn in Paraguayan yerba mate than those originating from Argentina [25]. According to origin, the highest content of Mn and Co in Argentinean samples, the lowest content of Mn and Co in Paraguayan samples and the lowest content of Fe, Ni and Zn in Brazilian samples were reported by Pozebon et al. [20]. According to the composition, samples of pure yerba mate contained higher content of Mn, Fe, Al, Ni, As, Co and Mo than yerba mate with additives (n = 34), which contained more Zn, Cu, Sb, Se, Pb and Hg. Nevertheless, no significant data have been found in the literature evaluating the influence of additives on the elemental composition of yerba mate. It is worth adding that the results of the total elemental content in the context of the whole population of yerba mate samples were similar to those in the literature, except for the aforementioned exceptions [11,23].

3.3. Spearman's Rank Correlation Test

The Spearman's rank correlation coefficient (r_s) was used to describe the pairwise associations between total and extractable content of elements in yerba mate samples. The plot of the Spearman's correlation matrix of elements was presented in Figure S1.

For total content of 16 elements, there were no strong positive ($r_s \geq 0.7$) nor strong negative correlations ($r_s \leq -0.7$). Moderate positive correlations ($0.4 \leq r_s < 0.7$) were observed between Zn/Cd, Mn/Co, Zn/Fe, Li/Al, Ni/Mn, Pb/Cu, Cu/Al, Pb/Al, Pb/Li, Mn/Cr, Ni/Co, Li/Fe, Zn/Li and Fe/Al. Other positive correlations, which were statistically significant ($p < 0.05$), were weak ($r_s < 0.4$). In turn, moderate negative correlation ($-0.7 \leq r_s < -0.4$) was observed between the pairs: Li/Co, Cu/Co, Pb/Co, Co/Al and Mn/Li. Other negative correlations, which were statistically significant, were weak ($r_s > -0.4$). In the literature, positive correlations were also reported for Ni/Mn (0.78), Pb/Cu (0.71) [25] and Al/Pb (0.55) [26]. For extractable content of 15 elements (without Cr), there were two pairs of elements almost fully positive correlated ($r_s \geq 0.9$): Mn/Al and Cu/Al. Strong positive correlations ($0.7 \leq r_s < 0.9$) were observed between Fe/Cu, Ni/Al, Ni/Mn, Fe/Al, Ni/Fe, Ni/Cu, Mn/Cu, Fe/Cd and Zn/Fe, while moderate positive correlations ($0.4 \leq r_s < 0.7$) were observed between the following pairs: Mn/Fe, Cu/Cd, Zn/Cu, Zn/Cd, Cd/Al, Ni/Cd, Zn/Ni, Zn/Al, Zn/Mn and Mn/Cd. All statistically significant negative correlations (Li/Co and Pb/Mn) were weak ($r_s > -0.4$). The r_s coefficient was also calculated between total and extractable content, however there were no strong positive ($r_s \geq 0.7$) nor strong and moderate negative correlations ($r_s \leq -0.4$). Moderate positive correlations ($0.4 \leq r_s < 0.7$) were observed for total and extractable of Pb, As, Sb, Mn, Co and Ni (r_s = 0.39). Moreover, positive correlation for total and water extractable content of Mn, Ni and Co were also reported [22]. It is presumed that the higher concentrations as well as significant correlations of the total and extracted content, are related to the origin of these elements, which is dust residue deposition. It was confirmed that the higher contents of some elements in foliar tissue of yerba mate *(Ilex paraguariensis)* came from surface deposition of soil dust [26]. In the case of other elements, the r_s coefficient was not significant statistically

($p < 0.05$) between their total and extractable content. In turn, moderate positive correlation was also observed in the following pairs: Mn(ext)/Ni(total), Ni(ext)/Mn(total) and Zn(ext)/Cd(total), while weak positive correlation for Co(ext)/Cr(total), Al(ext)/Mn(total), Fe(ext)/As(total), As(ext)/Fe(total), Al(ext)/Ni(total), Sb(ext)/Mn(total), Sb(ext)/Cd(total), Co(ext)/Mn(total), Cd(ext)/Se(total), Li(ext)/Se(total), Cu(ext)/Mn(total), As(ext)/Sb(total). There were also observed weak negative correlations between the pairs: Mn(ext)/Li(total), Mn(ext)/Zn(total), Pb(ext)/Mn(total), and Cu(ext)/Li(total) (Figure S1). Significantly high correlations between Zn and Cd may be associated with their chemical similarities [23], while other correlations (e.g., Fe/As) may indicate that these elements came from the common source (e.g., soil dust) [26].

3.4. Principal Component Analysis (PCA)

The results, obtained in the ICP OES analysis, were subjected to analysis by principal component analysis (PCA). Two components described 99.6% variability of the results of total concentration of 16 elements (n = 928 of single results for 58 digested samples of yerba mate) and 99.8% variability of the results of extractable concentration of 15 elements (n = 870 of single results for 58 samples of yerba mate extracted with H_3PO_4 solution). In both cases, all samples were cumulated in one group (at the point +1.0 of the PC1 axis and it was distributed along the PC2 axis, from −0.2 to 0.3). According to this, it is clearly indicated that samples were similar in the elemental composition (both in accordance with total and extractable content). In the case of total content of 16 elements, 11 samples could be distinguished from the group, nos. 7, 14, 19, 29, 32, 33, 35, 36, 39, 43, 53, and most of them were paired as followed: 29 + 35, 32 + 33 (both pairs were Brand D), 39 + 43 (both samples were Brand E) and 7 + 53. What is more, samples nos. 32 and 33 were the same product (D3), collected both as a 500 g pack (no. 32) and a 50 g test sample (no. 33). The differentiation in terms of the total content of elements may be due to the additives (except samples nos. 7, 29 and 36 were pure yerba mate). Moreover, half of the Brand D samples (nos. 29, 32, 33 and 35) is also distinct. In the case of extractable content of 15 elements, only five samples could be distinguished from the group, nos. 9, 19, 29, 34, 35. The only pair (34 + 35) was the same product (D4), collected both as a 500 g pack (no. 34) and a 50 g test sample (no. 35). As in the case of the total content, differentiations may be related to the additives (except sample no. 29). Only samples nos. 19, 29 and 35 were differed from the group in both contents, however their only common factor is being test samples.

The PCA for total and extractable content did not show any significant individual differences between the studied samples. Due to this, the percentages of extraction were additionally subjected to analysis by the PCA, however the data were reduced to nine elements only (n = 490 of single results for 58 samples), whose results were BQL for <20% of all samples. Reduced data represented 93.9% of all results. The 70.4% variability of results was described by two components (Figure 2). For easy identification, samples were colored and divided in accordance with origin, type, composition and brand.

Two groups of samples could be formed (Figure 2). According to the country of origin, the Argentinian samples were distributed mainly in group 1, however samples nos. 3, 47, 50, 52 and 53 were in group 2. A substantial similarity between samples was visible for two brands: Brand A (except for sample no. 3) and Brand F (except for sample no. 47). In turn, the Brazilian samples were distributed between both groups (7 and 11 samples in group 1 and 2, respectively), however two samples (nos. 19 and 26) were significantly separated. A substantial difference between the two brands was visible in the case of the Brazilian yerba mate. Brand E samples were on the positive part of the PC2 axis (except for sample no. 36), while the Brand C samples were usually on the negative part of the PC2 axis (except for samples nos. 19 and 26). The Paraguayan samples were generally in group 2, however samples nos. 7, 10, 11 were out of the group. Moreover, the Brand D samples were on the negative part of the PC2 axis (except for sample no. 28, which was separated).

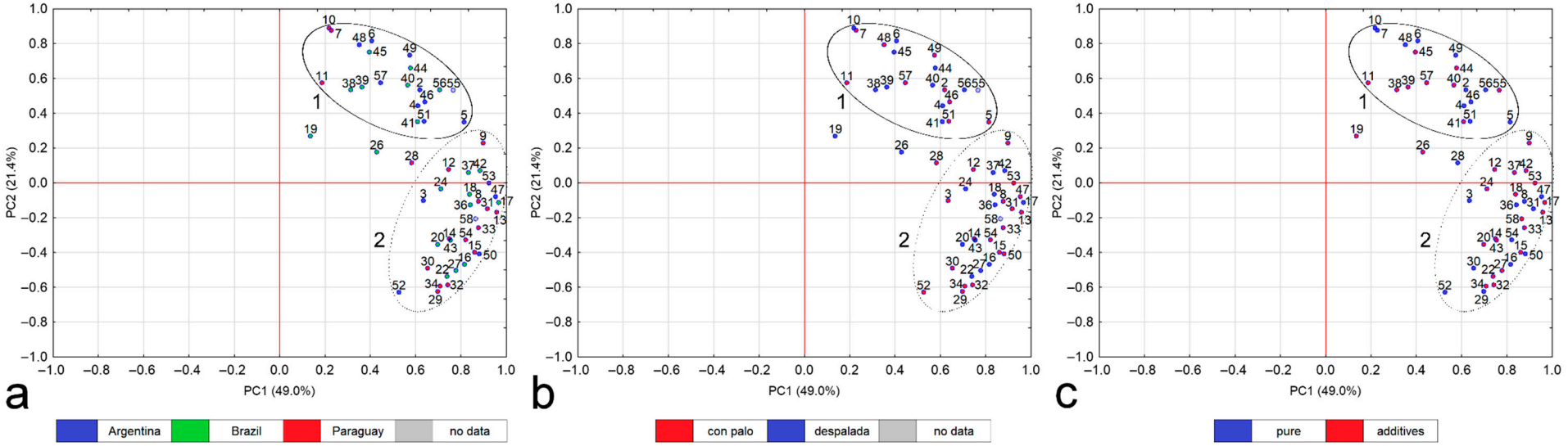

Figure 2. Results of Principle Components Analysis for the extractable percentages of selected elements (Al, Cd, Co, Cu, Fe, Mn, Ni, Sb, Zn) in yerba mate samples (n = 58) in accordance with (**a**) origin, (**b**) kind, and (**c**) composition. The 70.4% variability of the results was described by two components (PC1, PC2).

According to the kind of yerba mate, the con palo samples were distributed between both groups in the ratio 1:2 (9 and 18 samples in group 1 and 2, respectively) while despalada samples were distributed proportionally between both groups (10 and 11 samples in group 1 and 2, respectively). According to the composition (purity), samples were also distributed between both groups. Pure yerba mate samples were distributed proportionally between both groups, with 11 and 10 samples in group 1 and 2, respectively. In turn, nine and 20 samples of yerba mate with additives were distributed in group 1 and 2, respectively. Therefore, the PCA for the extraction percentages did not indicate any significant order in terms of the type (type) or composition (purity) of the yerba mate samples. Nevertheless, selected products, which were collected twice (a 500 g pack and a 50 g test samples), were generally distributed in the same group, except samples of B5 (nos. 11 and 12), and H1 (nos. 51 and 52).

The PCA results, such as the lack of a clear grouping of samples according to the country of origin, type (kind) or composition (purity), are partially confirmed by the latest literature data. Although the difference in elemental composition of yerba mate, indicated by the multidimensional statistical analysis, was defined as a geographical factor [20,22,28], it should be linked with the soil parent material where plants were cultivated [26]. This observation was also reported when the Brazilian samples from three different states were studied [22].

4. Conclusions

New methods of single-element speciation analysis have been applied for the first time to 58 commercial samples of yerba mate. As expected, the results of arsenic and iron species were comparable with those obtained for several samples in our preliminary studies [12,13,17]. By comparing the content of selected essential trace and potentially toxic elements obtained with two different procedures of sample preparation (digestion, extraction), it was shown that non-extractable content predominated in yerba mate, especially for iron (approx. 92%). According to this, the determination of the arsenic and iron species as well as extractable content must be assessed in the context of the total content of these elements since the elements were built into the plant tissues during the growth stage. The occurrence of selected As and Fe species in yerba mate as well as occasionally the high content, are accidental rather than related to studied factors, i.e., country of origin, kind, composition or packing. What is more, no significant differences were noticed between the yerba mate products packaged in Poland and those packaged in South American countries. Probably the soil which was used for the cultivation of *Ilex paraguariensis*, is the main factor influencing the elemental composition, and not the country of origin as previously thought. In the future perspective, new methods of multi-element speciation analysis as well as an appropriate preparation procedure of this sample matrix should be developed to obtain more information about the origin, type and composition of yerba mate.

Supplementary Materials: The following are available online at https://www.mdpi.com/article/10.3390/foods10122925/s1, Table S1. Results of spiked recovery in standard addition method (two sample solutions, P1 and P2, obtained in ultrasound-assisted extraction were spiked with two concentrations of mixed standard solution); Table S2. Results of spiked recovery in standard addition method (two sample solutions, P1 and P2, obtained in microwave-assisted digestion were spiked: Figure S1. The Spearman's correlation matrix of studied elements for total content and extractable content (without Cr, details in text). Statistically significant coefficients ($p < 0.05$) are bolded and marked by asterisks.

Author Contributions: Conceptualization J.P. and P.N.; methodology P.N.; validation J.P; investigation J.P and A.O.; data curation J.P.; writing—original draft J.P. and A.O.; writing—review & editing P.N.; funding acquisition J.P. All authors have read and agreed to the published version of the manuscript.

Funding: This research was funded by the European Social Fund under the Operational Program Knowledge Education Development grant number POWR.03.02.00-00-I026/16.

Data Availability Statement: All data presented in the article are available from the corresponding author.

Conflicts of Interest: The authors declare no conflict of interest.

References

1. Pardinho, R.; Vecchia, P.D.; Mendes, A.; Bizzi, C.; Mello, P.; Duarte, F.; Flores, E. Determination of toxic elements in yerba mate by ICP-MS after diluted acid digestion under O_2 pressure. *Food Chem.* **2018**, *263*, 37–41. [CrossRef] [PubMed]
2. Cardozo, E., Jr.; Morand, C. Interest of mate (Ilex paraguariensis A. St.–Hil.) as a new natural functional food to preserve human cardiovascular health—A review. *J. Funct. Foods* **2016**, *21*, 440–454. [CrossRef]
3. Bastos, M.C.; Cherobim, V.; Reissmann, C.; Kaseker, J.F.; Gaiad, S. Yerba mate: Nutrient levels and quality of the beverage depending on the harvest season. *J. Food Compost. Anal.* **2018**, *69*, 1–6. [CrossRef]
4. Verbruggen, N.; Hermans, C.; Schat, H. Mechanisms to cope with arsenic or cadmium excess in plants. *Curr. Opin. Plant Biol.* **2009**, *12*, 364–372. [CrossRef]
5. Schmite, B.; Bitobrovec, A.; Hacke, A.; Pereira, R.; Weinert, P.; dos Anjos, V. In vitro bioaccessibility of Al, Cu, Cd, and Pb following simulated gastro–intestinal digestion and total content of these metals in different Brazilian brands of yerba mate tea. *Food Chem.* **2019**, *281*, 285–293. [CrossRef]
6. Carelton, J. *Final Report: Biogeochemistry of Arsenic in Contaminated Soils of Superfund Sites*; Environmental Protection Agency: Washington, DC, USA, 2007.
7. Wolle, M.; Conklin, S.; Wittenberg, J. Matrix–Induced transformation of arsenic species in seafoods. *Anal. Chim. Acta* **2019**, *1060*, 53–63. [CrossRef] [PubMed]
8. Sánchez, M.; Sabio, L.; Gálvez, N.; Capdevila, M.; Dominguez-Vera, J. Iron chemistry at the service of life. *IUBMB Life* **2017**, *69*, 382–388. [CrossRef]
9. Podwika, W.; Kleszcz, K.; Krośniak, M.; Zagrodzki, P. Copper, Manganese, Zinc, and Cadmium in Tea Leaves of Different Types and Origin. *Biol. Trace Elem. Res.* **2017**, *183*, 389–395. [CrossRef] [PubMed]
10. Barbosa, J.; Motta, A.; Consalter, R.; Poggere, G.; Santin, D.; Wendling, I. Plant growth, nutrients and potentially toxic elements in leaves of yerba mate clones in response to phosphorus in acid soils. *An. Acad. Bras. Cienc.* **2018**, *90*, 557–571. [CrossRef]
11. Marcelo, M.; Martins, C.; Pozebon, D.; Dressler, V.; Ferrão, M. Classification of yerba mate (Ilex paraguariensis) according to the country of origin based on element concentrations. *Microchem. J.* **2014**, *117*, 164–171. [CrossRef]
12. Proch, J.; Niedzielski, P. In–spray chamber hydride generation by multi–mode sample introduction system (MSIS) as an interface in the hyphenated system of high performance liquid chromatography and inductivity coupled plasma optical emission spectrometry (HPLC/HG-ICP-OES) in arsenic species determination. *Talanta* **2019**, *208*, 120395. [CrossRef]
13. Proch, J.; Niedzielski, P. Iron species determination by high performance liquid chromatography with plasma based optical emission detectors: HPLC-MIP OES and HPLC-ICP OES. *Talanta* **2021**, *231*, 122403. [CrossRef]
14. Escudero, L.; Pacheco, P.; Gasquez, J.; Salonia, J. Development of a FI-HG-ICP-OES solid phase preconcentration system for inorganic selenium speciation in Argentinean beverages. *Food Chem.* **2015**, *169*, 73–79. [CrossRef]
15. Pereira, C.; Souza, A.; Oreste, E.; Cidade, M.; Cadore, S.; Ribeiro, A.; Vieira, M. Acid Decomposition of Yerba Mate (Ilex paraguariensis) Using a Reflux System for the Evaluation of Al, Ca, Cd, Cr, Cu, Fe, K, Mg, Mn, Na, Pb and Zn Contents by Atomic Spectrometric Techniques. *J. Braz. Chem. Soc.* **2016**, *27*, 685–693. [CrossRef]
16. Borges, A.; Bazanella, D.; Duarte, Á.; Zmozinski, A.; Vale, M.; Welz, B. Development of a method for the sequential determination of cadmium and chromium from the same sample aliquot of yerba mate using high–resolution continuum source graphite furnace atomic absorption spectrometry. *Microchem. J.* **2017**, *130*, 116–121. [CrossRef]
17. Proch, J.; Niedzielski, P. Multi–mode Sample Introduction System (MSIS) as an interface in the hyphenated system 2 HPLC-MSIS-ICP–OES in simultaneous determination of metals and metalloids species. *Anal. Chim. Acta* **2021**, *1147*, 1–14. [CrossRef]
18. Schunk, P.; Kalil, I.; Pimentel–Schmitt, E.; Lenz, D.; de Andrade, T.; Ribeiro, J.; Endringer, D. ICP-OES and Micronucleus Test to Evaluate Heavy Metal Contamination in Commercially Available Brazilian Herbal Teas. *Biol. Trace Elem. Res.* **2015**, *172*, 258–265. [CrossRef]
19. Santos, L.; Neto, S.V.; Iozzi, G.; Jacob, S. Arsenic, cadmium and lead concentrations in Yerba mate commercialized in Southern Brazil by inductively coupled plasma mass spectrometry. *Cienc. Rural* **2017**, *47*. [CrossRef]
20. Pozebon, D.; Dressler, V.; Marcelo, M.; de Oliveira, T.; Ferrão, M. Toxic and nutrient elements in yerba mate (Ilex paraguariensis). *Food Addit. Contam. B* **2015**, *8*, 215–220. [CrossRef]
21. ANVISA. *Regulamento Técnico Mercosul Sobre Limites Máximos de Contaminantes Inorgânicos em Alimentos (REVOGAÇÃO DAS RES. GMC N° 102/94 e N°35/96)*; Mercosul, Ed.; Agência Nacional de Vigilância Sanitária: Brasília, Brazil, 2013; pp. 1–18.
22. Ulbrich, N.; do Prado, L.; Barbosa, J.; Araujo, E.; Poggere, G.; Motta, A.; Prior, S.; Magri, E.; Young, S.; Broadley, M. Multi–elemental Analysis and Health Risk Assessment of Commercial Yerba Mate from Brazil. *Biol. Trace Elem. Res.* **2021**, 1–9. [CrossRef]
23. Olivari, I.; Paz, S.; Gutiérrez, Á.; González–Weller, D.; Hardisson, A.; Sagratini, G.; Rubio, C. Macroelement, trace element, and toxic metal levels in leaves and infusions of yerba mate (Ilex paraguariensis). *Environ. Sci. Pollut. Res.* **2020**, *27*, 21341–21352. [CrossRef] [PubMed]

24. Da Costa, A.G.; Nogami, E.; Visentainer, J.; de Souza, N.; Garcia, E. Fractionation of Aluminum in Commercial Green and Roasted Yerba Mate Samples (Ilex paraguariensis St. Hil.) and in Their Infusions. *J. Agric. Food Chem.* **2009**, *57*, 196–200. [CrossRef] [PubMed]
25. Baran, A.; Gruszecka–Kosowska, A.; Kołton, A.; Jasiewicz, C.; Piwowar, P. Content and health risk assessment of selected elements in the Yerba mate (Ilex paraguariensis, St. hillaire). *Hum. Ecol. Risk Assess. Int. J.* **2017**, *24*, 1092–1114. [CrossRef]
26. Motta, A.; Barbosa, J.; Magri, E.; Pedreira, G.; Santin, D.; Prior, S.; Consalter, R.; Young, S.; Broadley, M.; Benedetti, E. Elemental composition of yerba mate (Ilex paraguariensis A.St.–Hil.) under low input systems of southern Brazil. *Sci. Total Environ.* **2020**, *736*, 139637. [CrossRef]
27. Magri, E.; Valduga, A.; Gonçalves, I.; Barbosa, J.; Rabel, D.; Menezes, I.; Nascimento, P.; Oliveira, A.; Corrêa, R.; Motta, A. Cadmium and lead concentrations in yerba mate leaves from agroforestry and plantation systems: An international survey in South America. *J. Food Compost. Anal.* **2021**, *96*, 103702. [CrossRef]
28. Bragança, V.; Melnikov, P.; Zanoni, L. Trace Elements in Different Brands of Yerba Mate Tea. *Biol. Trace Elem. Res.* **2011**, *144*, 1197–1204. [CrossRef] [PubMed]

UNIWERSYTET IM. ADAMA MICKIEWICZA W POZNANIU
Wydział Chemii
Zakład Chemii Analitycznej

Poznań, dnia 06.12.2021 r.

OŚWIADCZENIE

Oświadczam, że w pracy:
Proch, J., Niedzielski, P. (2020). In–spray chamber hydride generation by multi–mode sample introduction system (MSIS) as an interface in the hyphenated system of high performance liquid chromatography and inductivity coupled plasma optical emission spectrometry (HPLC/HG–ICP–OES) in arsenic species determination. Talanta, 208, 120395. doi: 10.1016/j.talanta.2019.120395 mój udział polegał na konsultacji idei badań, nadzoru i pomocy w ich realizacji i tworzeniu metodyki oraz pomocy przy edytowaniu tekstu artykułu. Swój udział szacuję na 30%. Oświadczam, iż rola Pana mgr. Jędrzeja Procha była w tej pracy wiodąca.

prof. dr hab. Przemysław Niedzielski

ul. Uniwersytetu Poznańskiego 8, Collegium Chemicum, 61-614 Poznań
NIP 777 00 06 350, REGON 000001293
tel. +48 61 829 15 74; fax. +48 61 829 15 55
pnied@amu.edu.pl
www.chemia.amu.edu.pl

UNIWERSYTET IM. ADAMA MICKIEWICZA W POZNANIU
Wydział Chemii
Zakład Chemii Analitycznej

Poznań, dnia 06.12.2021 r.

OŚWIADCZENIE

Oświadczam, że w pracy:
Proch, J., Niedzielski, P. (2021). Iron species determination by high performance liquid chromatography with plasma based optical emission detectors: HPLC–MIP OES and HPLC–ICP OES. Talanta, 231, 122403. doi: 10.1016/j.talanta.2021.122403 mój udział polegał na konsultacji idei badań, nadzoru i pomocy w ich realizacji i tworzeniu metodyki oraz pomocy przy edytowaniu tekstu artykułu. Swój udział szacuję na 30%. Oświadczam, iż rola Pana mgr. Jędrzeja Procha była w tej pracy wiodąca.

prof. dr hab. Przemysław Niedzielski

ul. Uniwersytetu Poznańskiego 8, Collegium Chemicum, 61-614 Poznań
NIP 777 00 06 350, REGON 000001293
tel. +48 61 829 15 74; fax. +48 61 829 15 55
pnied@amu.edu.pl
www.chemia.amu.edu.pl

UNIWERSYTET IM. ADAMA MICKIEWICZA W POZNANIU
Wydział Chemii
Zakład Chemii Analitycznej

Poznań, dnia 06.12.2021 r.

OŚWIADCZENIE

Oświadczam, że w pracy:
Proch, J., & Niedzielski, P. (2021). Multi–mode Sample Introduction System (MSIS) as an interface in the hyphenated system 2 HPLC–MSIS–ICP–OES in simultaneous determination of metals and metalloids species. Analytica Chimica Acta, 1147, 1-14. doi: 10.1016/j.aca.2020.12.047 mój udział polegał na konsultacji idei badań, nadzoru i pomocy w ich realizacji i tworzeniu metodyki oraz pomocy przy edytowaniu tekstu artykułu. Oświadczam, iż rola Pana mgr. Jędrzeja Procha była w tej pracy wiodąca.

prof. dr hab. Przemysław Niedzielski

ul. Uniwersytetu Poznańskiego 8, Collegium Chemicum, 61-614 Poznań
NIP 777 00 06 350, REGON 000001293
tel. +48 61 829 15 74; fax. +48 61 829 15 55
pnied@amu.edu.pl
www.chemia.amu.edu.pl

UNIWERSYTET IM. ADAMA MICKIEWICZA W POZNANIU
Wydział Chemii
Zakład Chemii Analitycznej

Poznań, dnia 06.12.2021 r.

OŚWIADCZENIE

Oświadczam, że w pracy:
Proch, J. Orłowska, A., Niedzielski, P. (2021). Elemental and Speciation Analyses of Different Brands of Yerba Mate (Ilex paraguariensis). Foods 10(12), 2925; doi: 10.3390/foods10122925 mój udział polegał na konsultacji idei badań, nadzoru i pomocy w ich realizacji i tworzeniu metodyki oraz pomocy przy edytowaniu recenzowanej wersji tekstu artykułu. Swój udział szacuję na 20%. Oświadczam, iż rola Pana mgr. Jędrzeja Procha była w tej pracy wiodąca.

prof. dr hab. Przemysław Niedzielski

Przemysław Niedzielski

Oświadczam, że w pracy:
Proch, J. Orłowska, A., Niedzielski, P. (2021). Elemental and Speciation Analyses of Different Brands of Yerba Mate (Ilex paraguariensis). Foods 10(12), 2925; doi: 10.3390/foods10122925 mój udział polegał na pomocy przy wykonywaniu części analiz oraz pomocy przy edytowaniu tekstu artykułu. Swój udział szacuję na 10%. Oświadczam, iż rola Pana mgr. Jędrzeja Procha była w tej pracy wiodąca.

mgr Aleksandra Orłowska

Aleksandra Orłowska

ul. Uniwersytetu Poznańskiego 8, Collegium Chemicum, 61-614 Poznań
NIP 777 00 06 350, REGON 000001293
tel. +48 61 829 15 74; fax. +48 61 829 15 55
pnied@amu.edu.pl
www.chemia.amu.edu.pl